Neurohydrodynamics: an engineering perspective

Bryn Martin, Ph.D.
mail@neurohydrodynamics.com
Neurohydrodynamics and Medical Technology Laboratory and
Laboratory of Hemodynamics and Cardiovascular Technology at the
Swiss Federal Institute of Technology, EPFL
Friday, August 12, 2011

ÉCOLE POLYTECHNIQUE
FÉDÉRALE DE LAUSANNE

CSF at EPFL

You are invited to come visit at EPFL anytime!

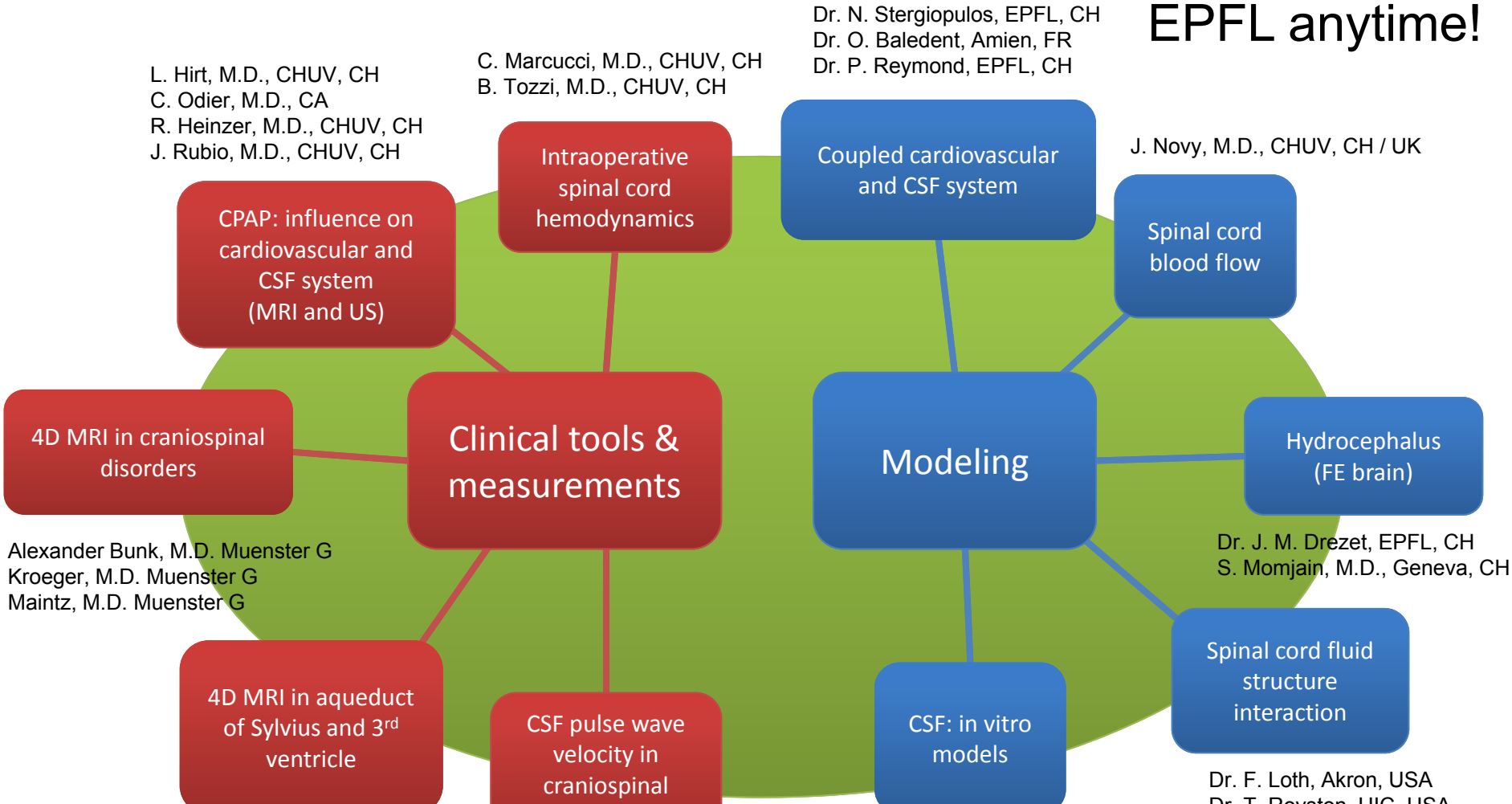

Outline

- Motivation
- Neurohydrodynamics: anatomy & physiology
  - Intracranial space (CSF, blood & brain)
  - Blood vessels
  - Brain and spinal cord
- Current concepts in craniospinal pathologies
- Current diagnostic and imaging trends in neurohydrodynamics

Motivation

- neurohydrodynamics play a role in craniospinal pathologies (and cerebrovascular)

Craniospinal disorder	Prevalence (USA)
Hydrocephalus	1 in 500
Chiari malformation	1 in 1,000
Spina bifida	1 in 1,500
Tethered cord	1 in 4,000
Syringomyelia	1 in 8,000
Spinal cord tumor	3,200 / yr. diagnosed
Brain tumor	195,000 / year diagnosed

ninds.nih.gov/disorders/

Neurohydrodynamics research

Goals

1. Identify mechanical forces that could play a role in craniospinal disorders.
2. Provide quantitative tools for craniospinal disorder assessment.

The big picture

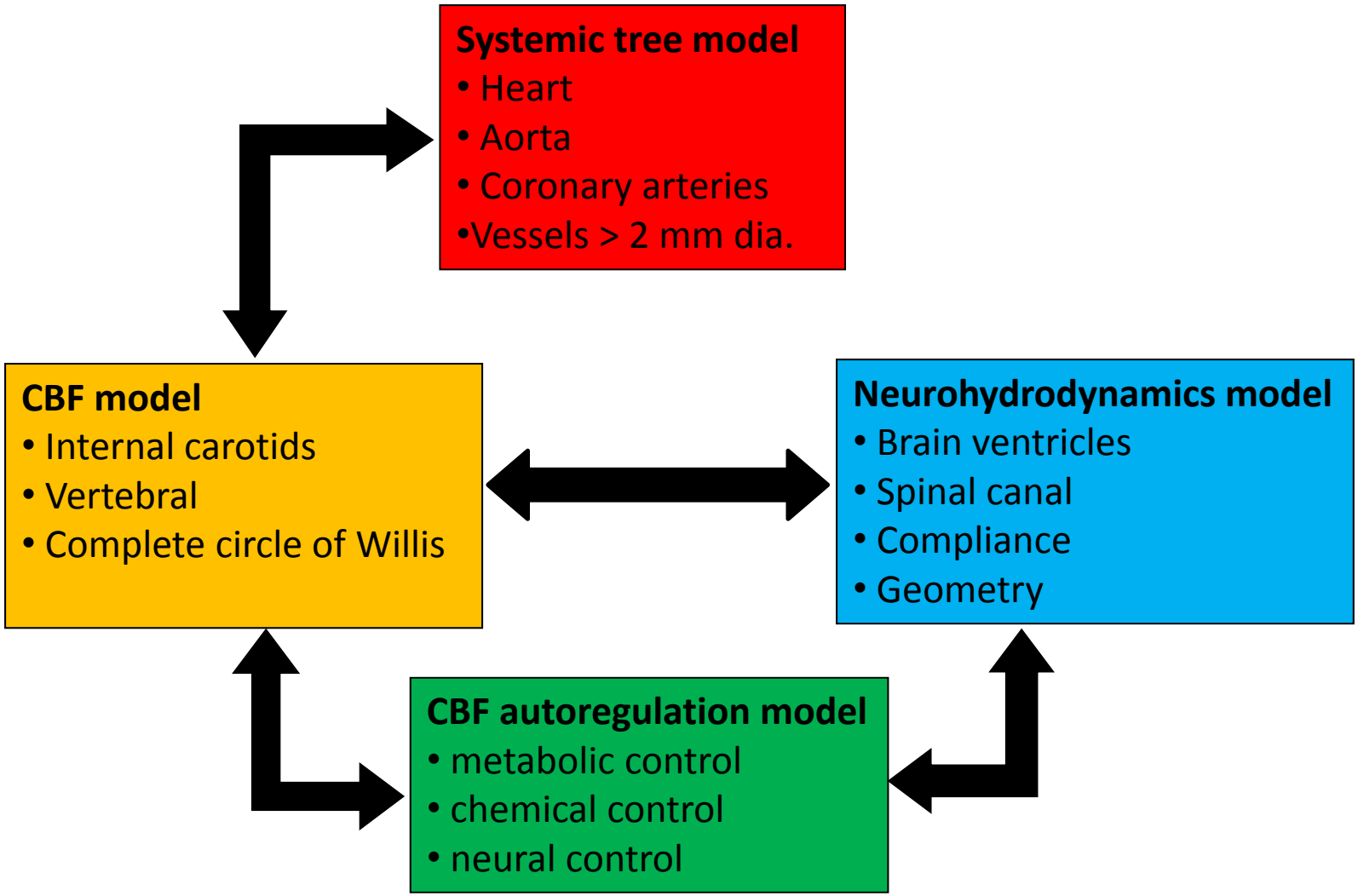

Systemic Tree model

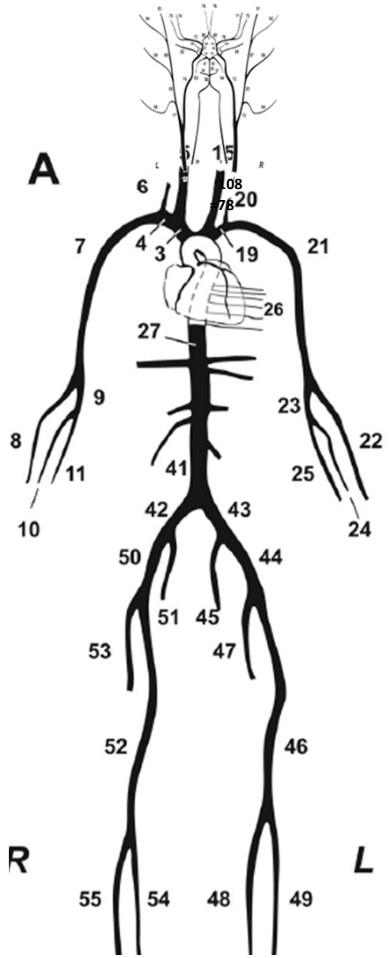

Cerebrospinal Fluid model

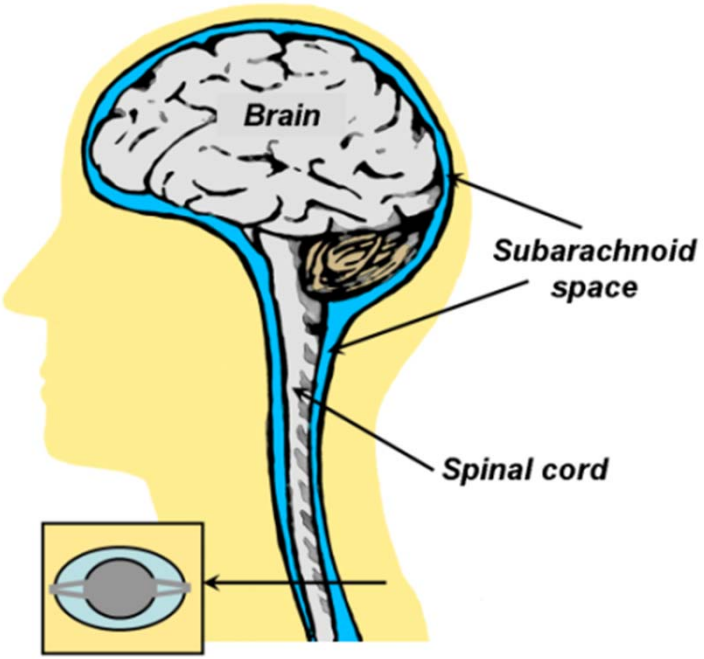

Mechanical perspective of CSF and cardiovascular system

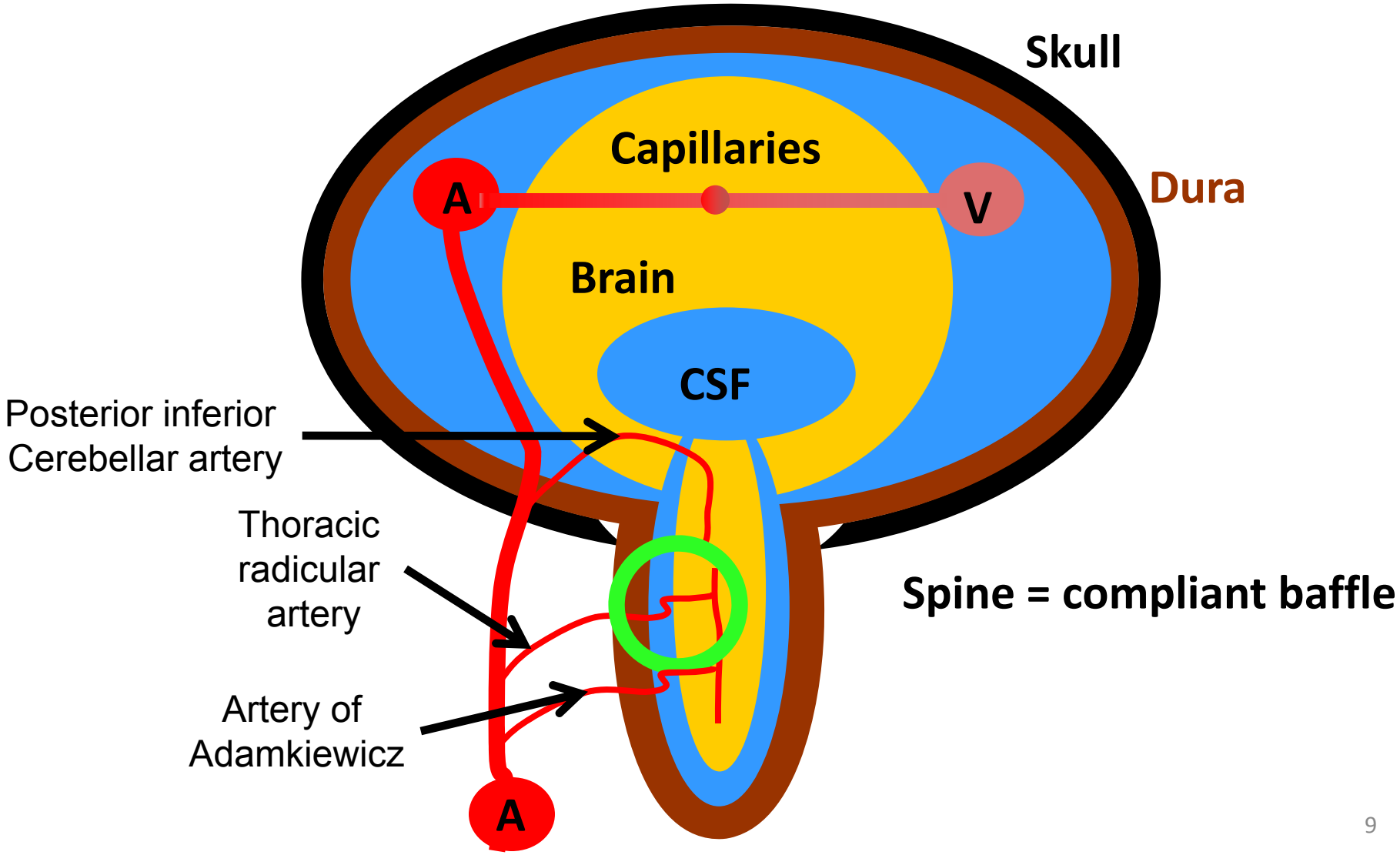

The intracranial space (CSF, blood & brain)

- A 1700 ml “control volume” (Monroe-Kelly)

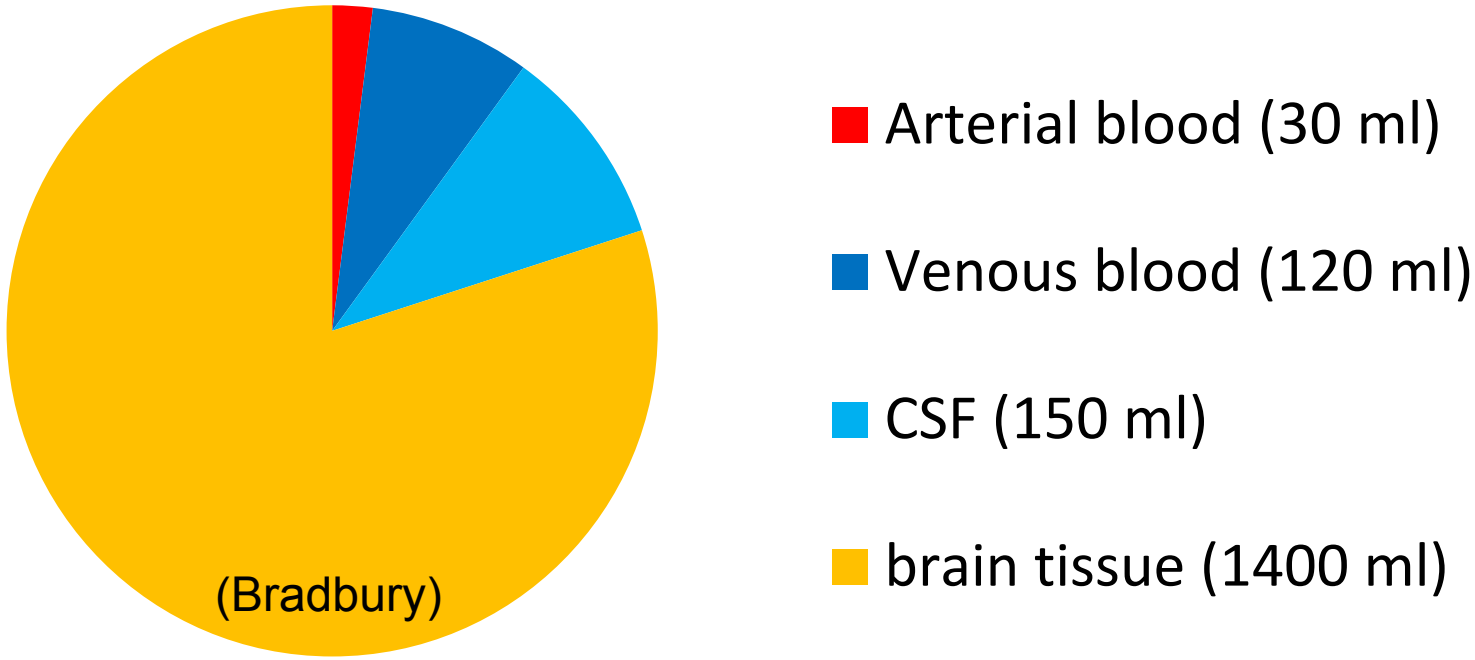

Kelly, G. (1824). "An account of the appearances observed in the dikssection of two of three individuals presumed to have perished in the storm of the 3rd, and whose bodies were deiscovered in the vicinity of the Leith on the morning of the 4th of November 1821, with some reflections on the pathology of the brain." Trans Med Chir Sci Edinb **1:**: 84–169.
Monroe, A. (1783). "Observations on the structure and function of the nervous system." Edinburgh: Creech & Johnson.
Bradbury, M. W. B. (1979). The concept of a blood-brain barrier. Chichester ; New York, Wiley.

Cerebrospinal fluid: CSF

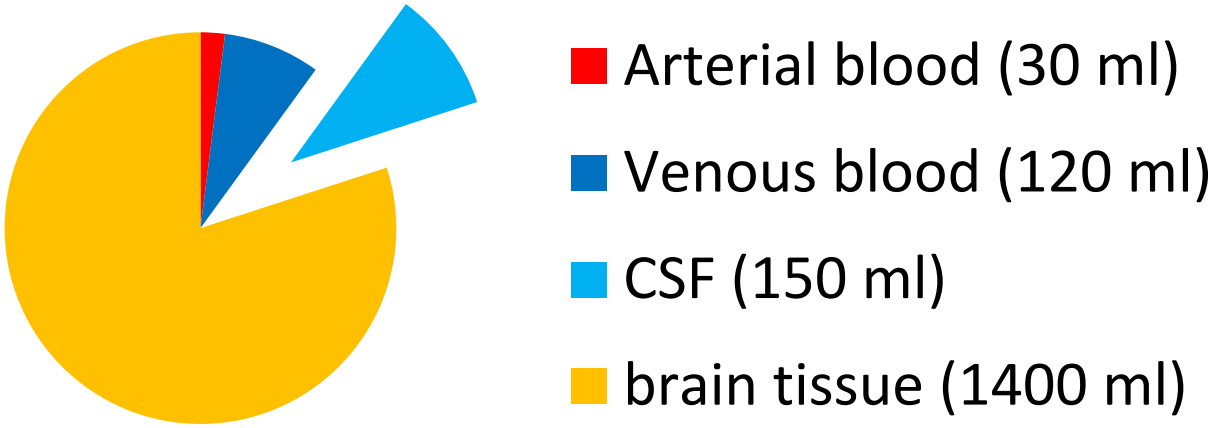

Volumetric distribution of CSF

- μ = 0.01 g/cm*s, ρ = 1.0 g/cm, plasma (Blmfld)
- Provides buoyancy to brain

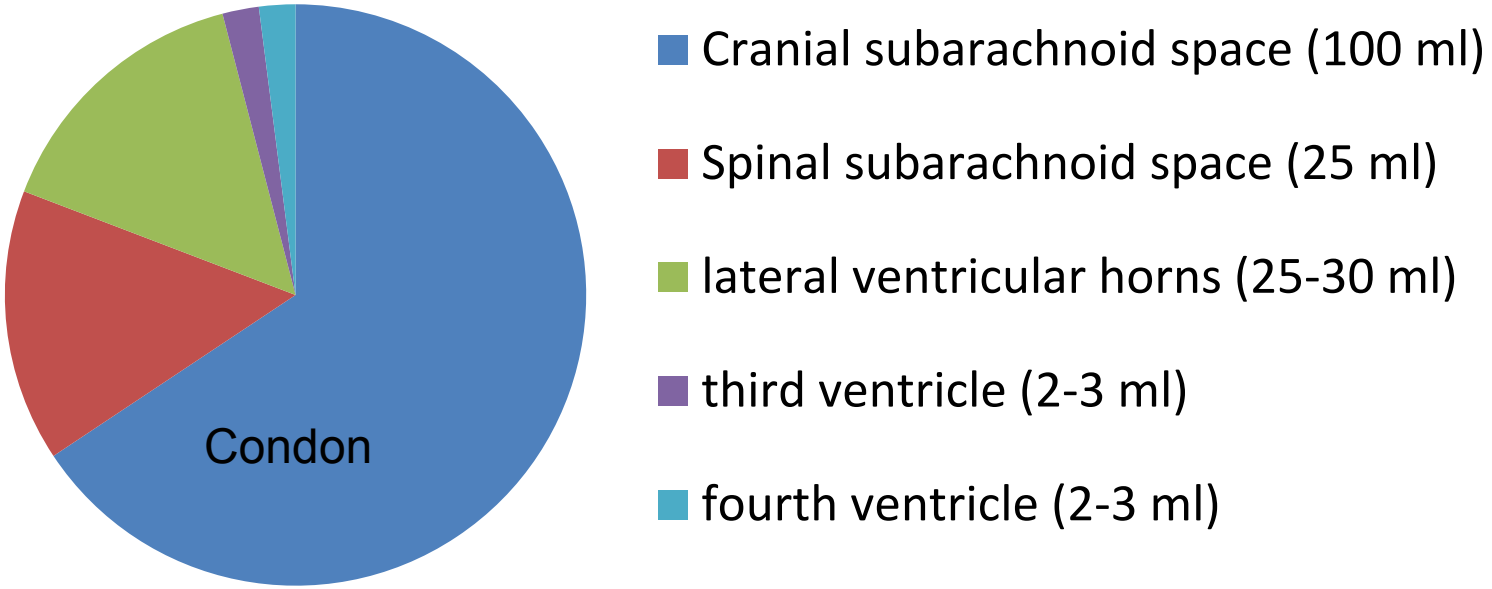

Condon, B., J. Patterson, et al. (1986). "Use of magnetic resonance imaging to measure intracranial cerebrospinal fluid volume." Lancet **1**(8494): 1355-7.
Bloomfield, I. G., I. H. Johnston, et al. (1998). "Effects of proteins, blood cells and glucose on the viscosity of cerebrospinal fluid." Pediatr Neurosurg **28**(5): 246-51.

Production and absorption of CSF

Production

- Choroid plexus 0.3-0.7 ml/min (Guyton)
- Replaced about 3-4 times each day

Absorption

- arachnoid granulations (AG) at SSS (Gray).
- # of AG varies with age
- (50 at 0-9 / 250 at 60 / <10 at 90 yrs.) (Ikshm)

Gray, H., P. L. Williams, et al. (1995). Gray's anatomy : the anatomical basis of medicine and surgery. New York, Churchill Livingstone.
Guyton, A. C. and J. E. Hall (2006). Textbook of medical physiology. Philadelphia, Elsevier Saunders.
Ikushima, I., Y. Korogi, et al. (1999). "MRI of arachnoid granulations within the dural sinuses using a FLAIR pulse sequence." Br J Radiol **72**(863): 1046-51.

Ependymal cells produce CSF

- Cell wall thickness ~10-20 um
- Ependymal cells have a column or cube shape

Choroid plexus

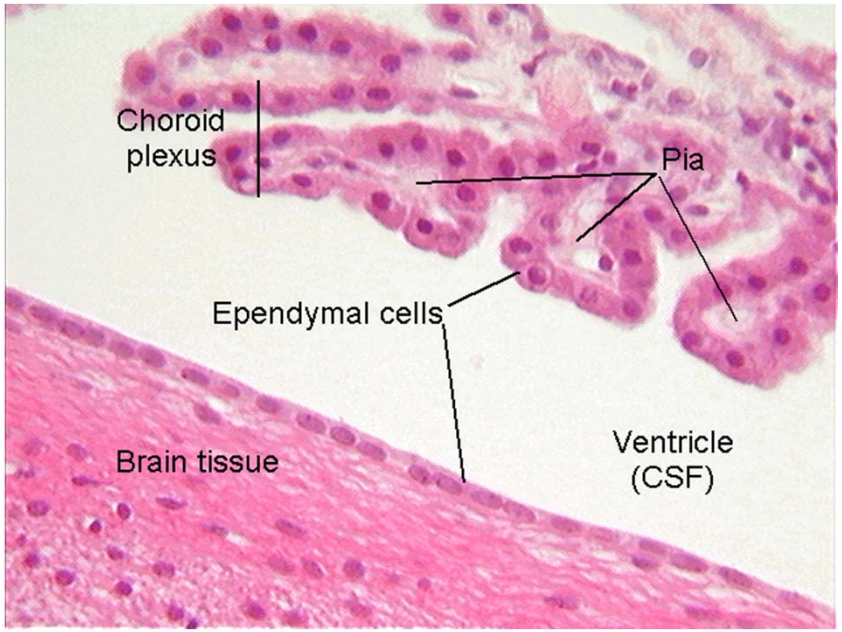

Central canal

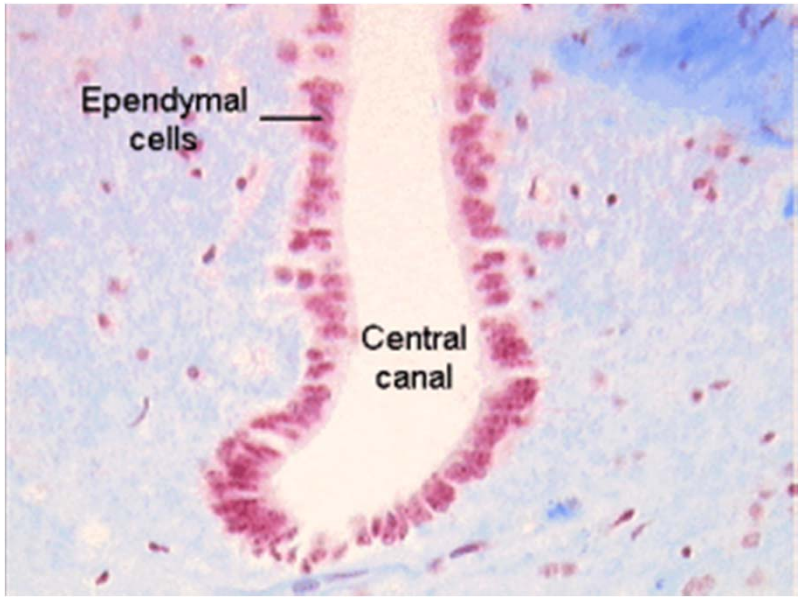

More about ependymal cells

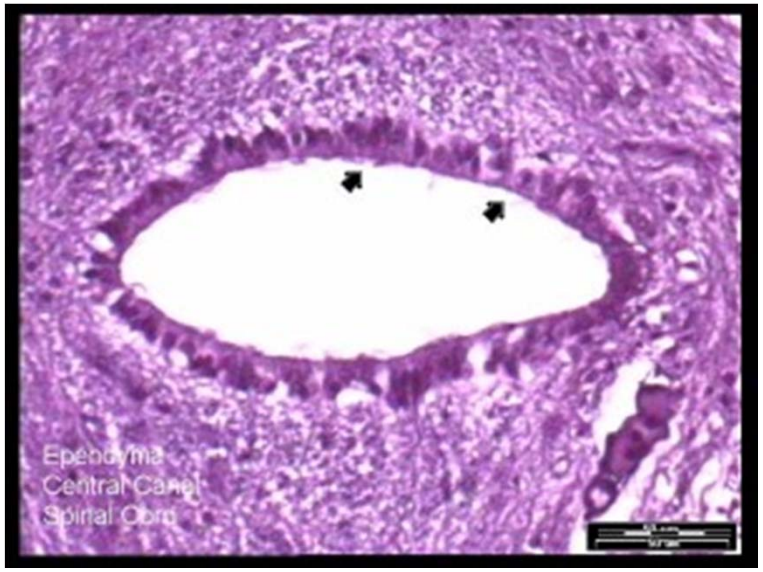

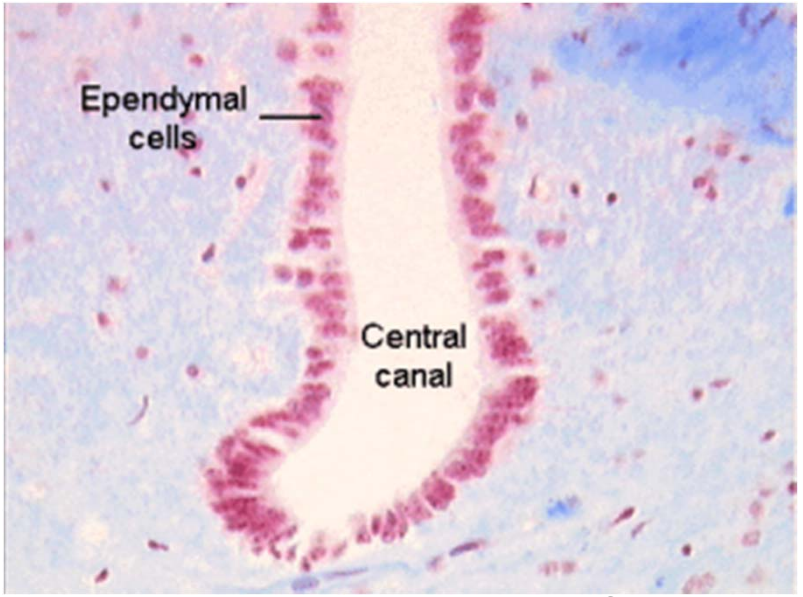

These cells have cilia (like little arms/tails) that help to move the spinal fluid. These cells tend to have a cube or column shape.

Scientists still aren't sure as to all of the functions of the ependymal cell. They do know for sure that it creates and directs spinal fluid, but they still believe more functions are undiscovered.

CSF is absorbed through the arachnoid granulations

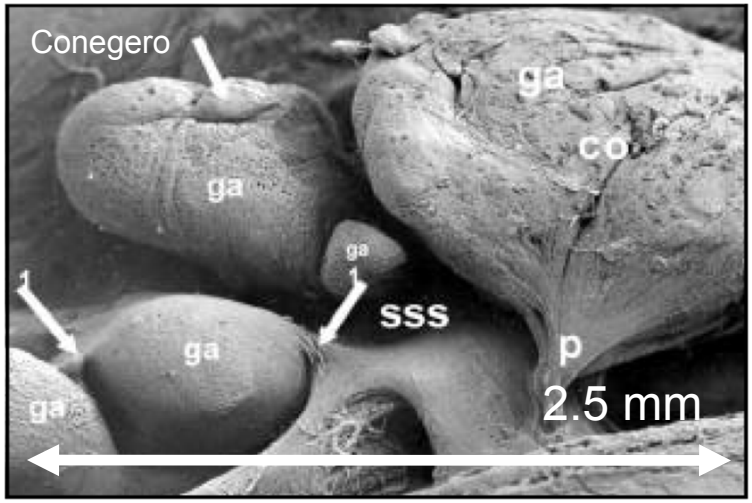

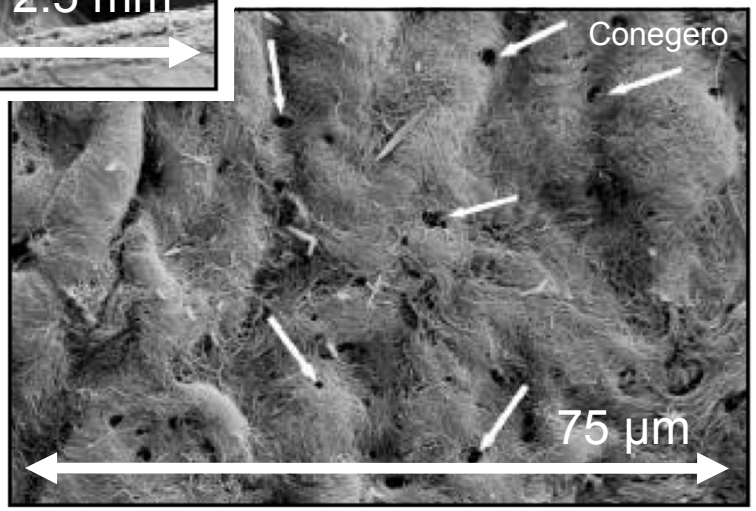

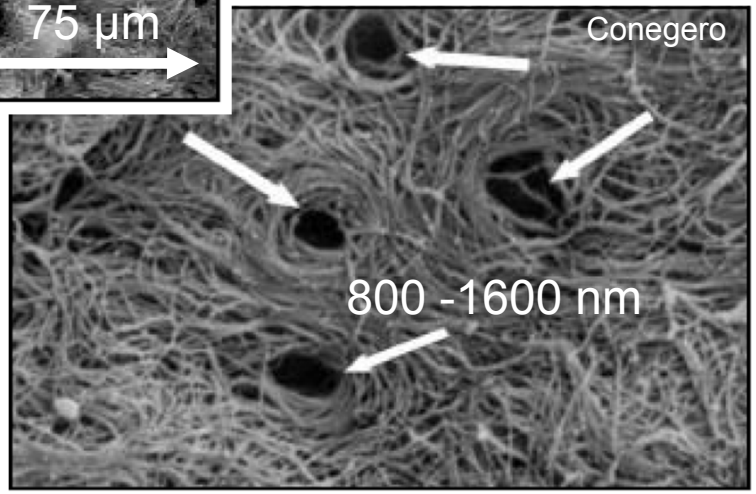

Conegero, C. I. and R. P. Chopard (2003). "Tridimensional architecture of the collagen element in the arachnoid granulations in humans: a study on scanning electron microscopy." Arq Neuropsiquiatr **61**(3A): 561-5.

Lateral, 3rd, and 4th Ventricles

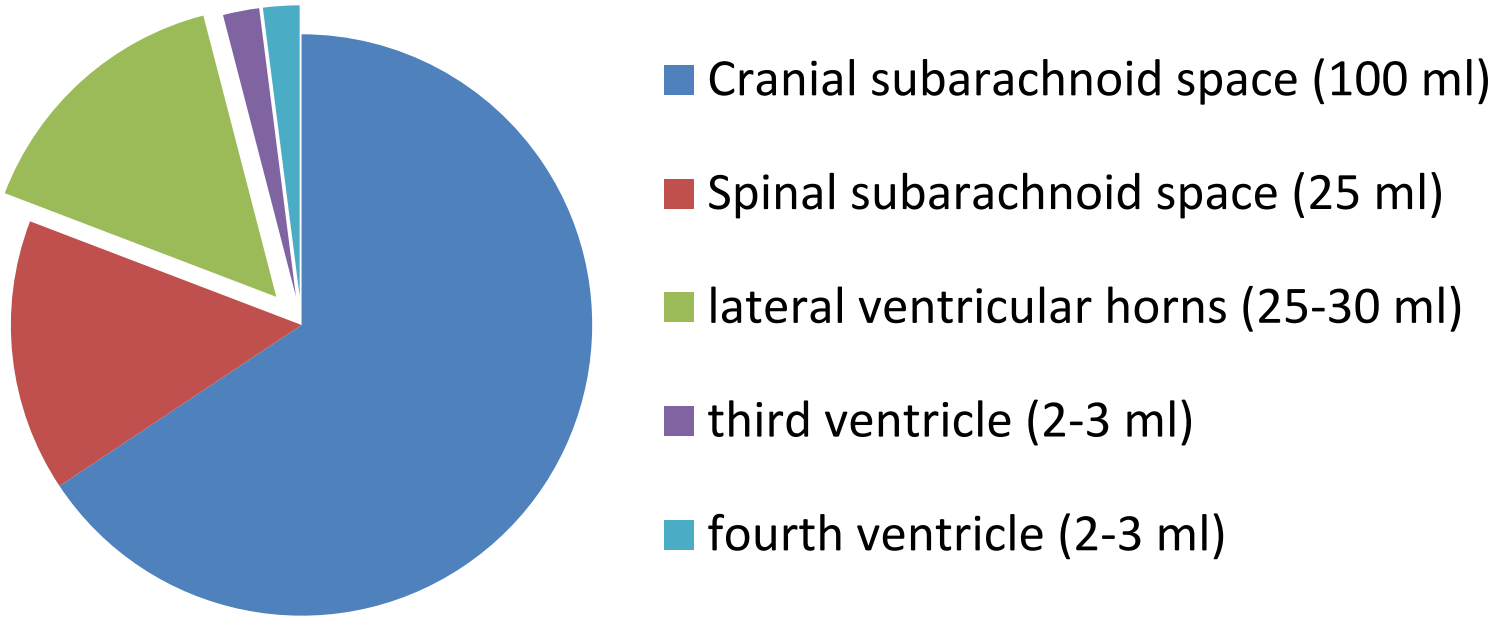

Ventricle geometry

- aqueduct of Sylvius provides greatest hydraulic resistance to CSF flow

3D ventricle reconstruction

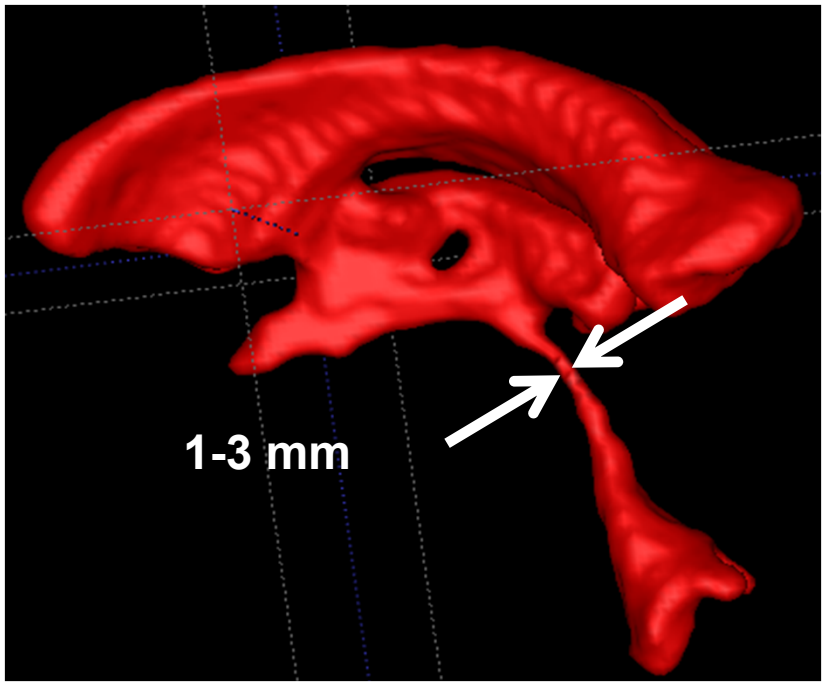

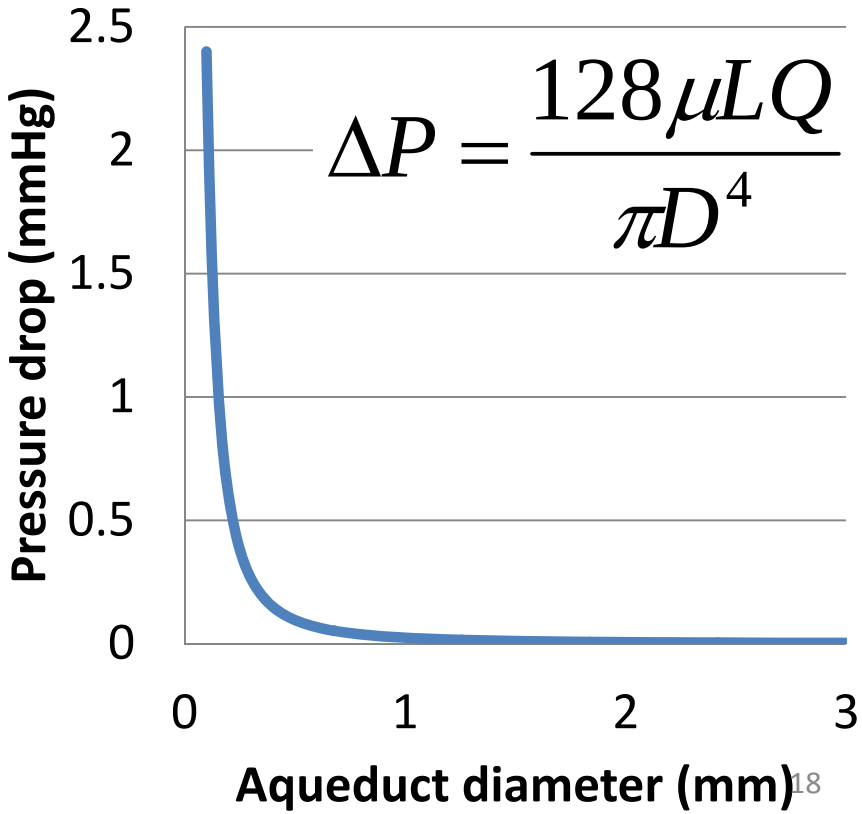

Cranial subarachnoid space

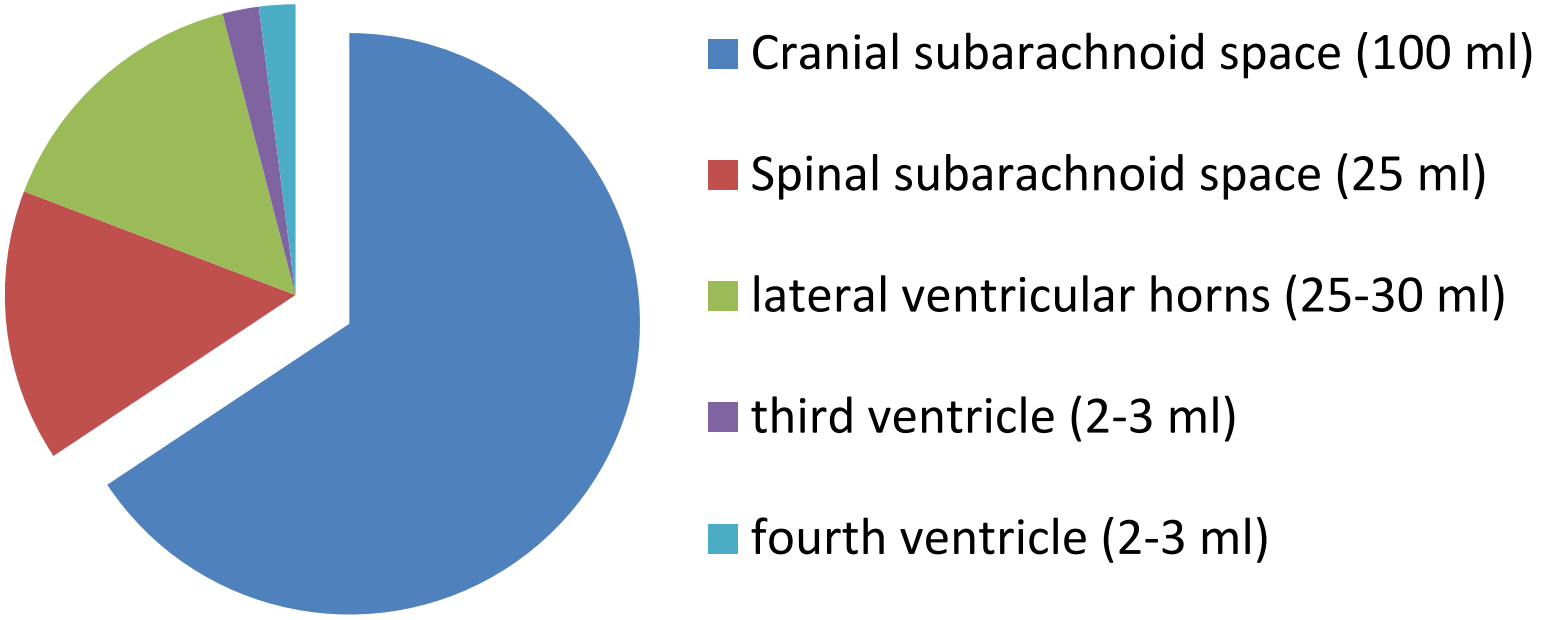

Cranial subarachnoid space

- 100 ml total volume
- 2-9 mm space separates pia/arachnoid mater

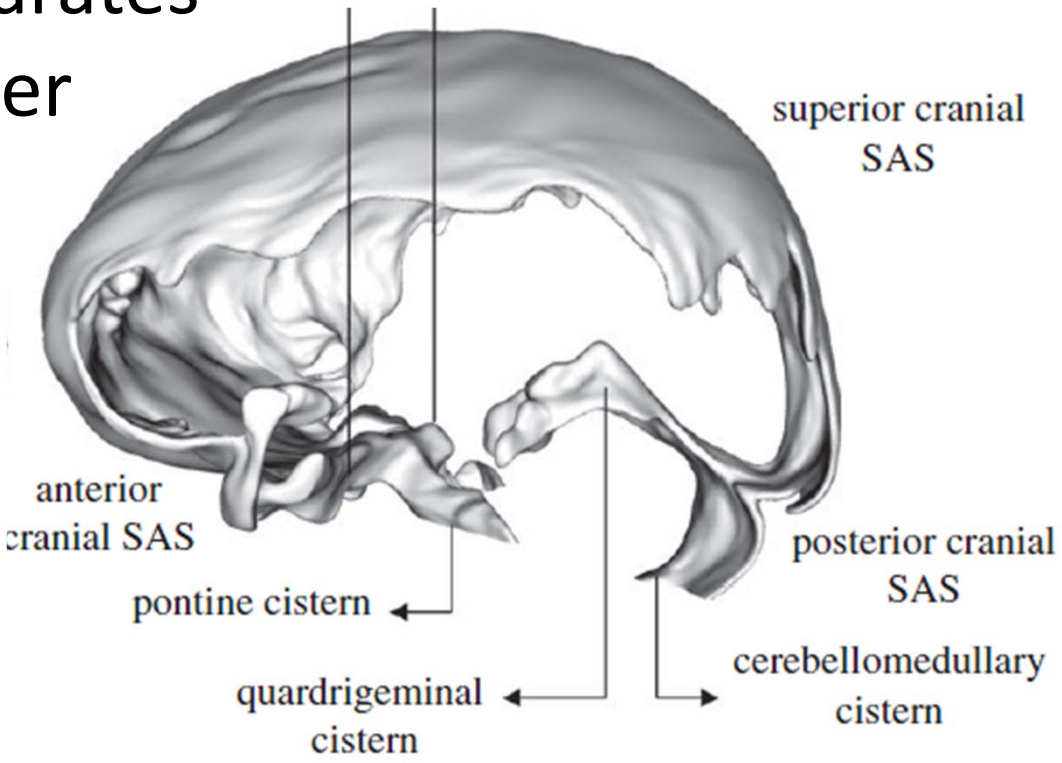

Gupta, S., M. Soellinger, et al. "Cerebrospinal fluid dynamics in the human cranial subarachnoid space: an overlooked mediator of cerebral disease. I. Computational model." J R Soc Interface **7**(49): 1195-204.

Spinal subarachnoid space

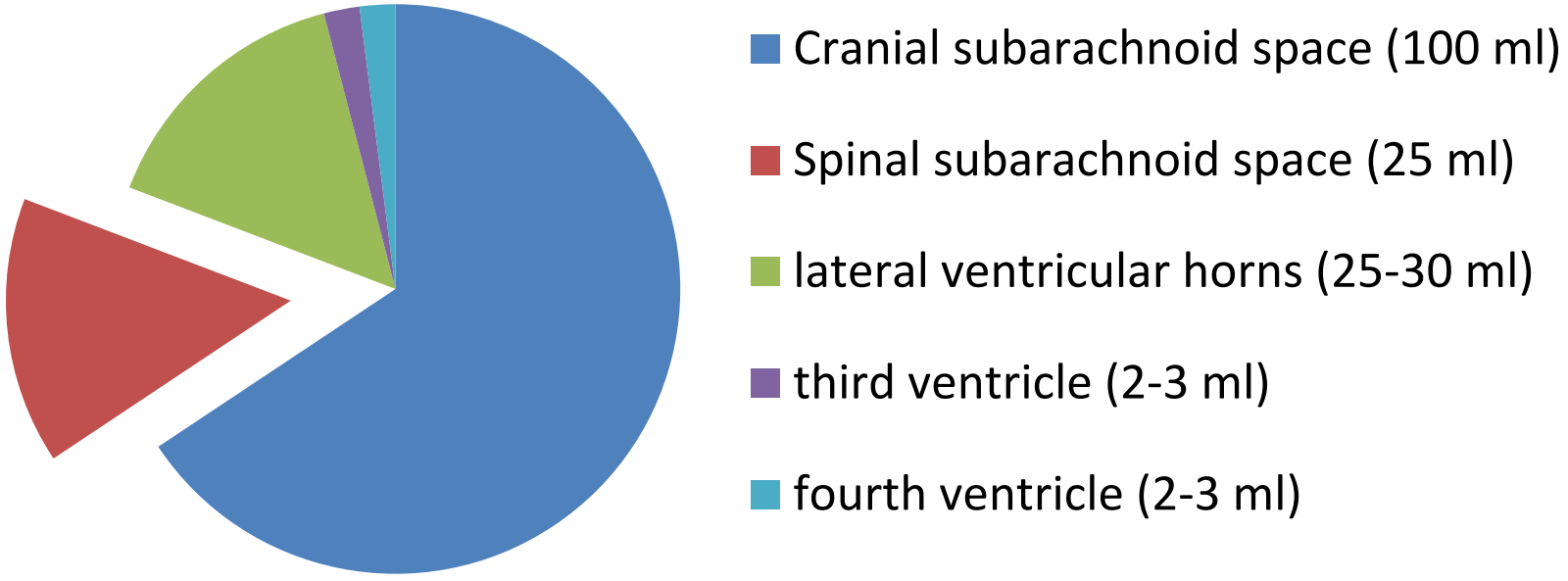

Spinal subarachnoid space

- 25 ml total volume
- 3 mm “doughnut” of space

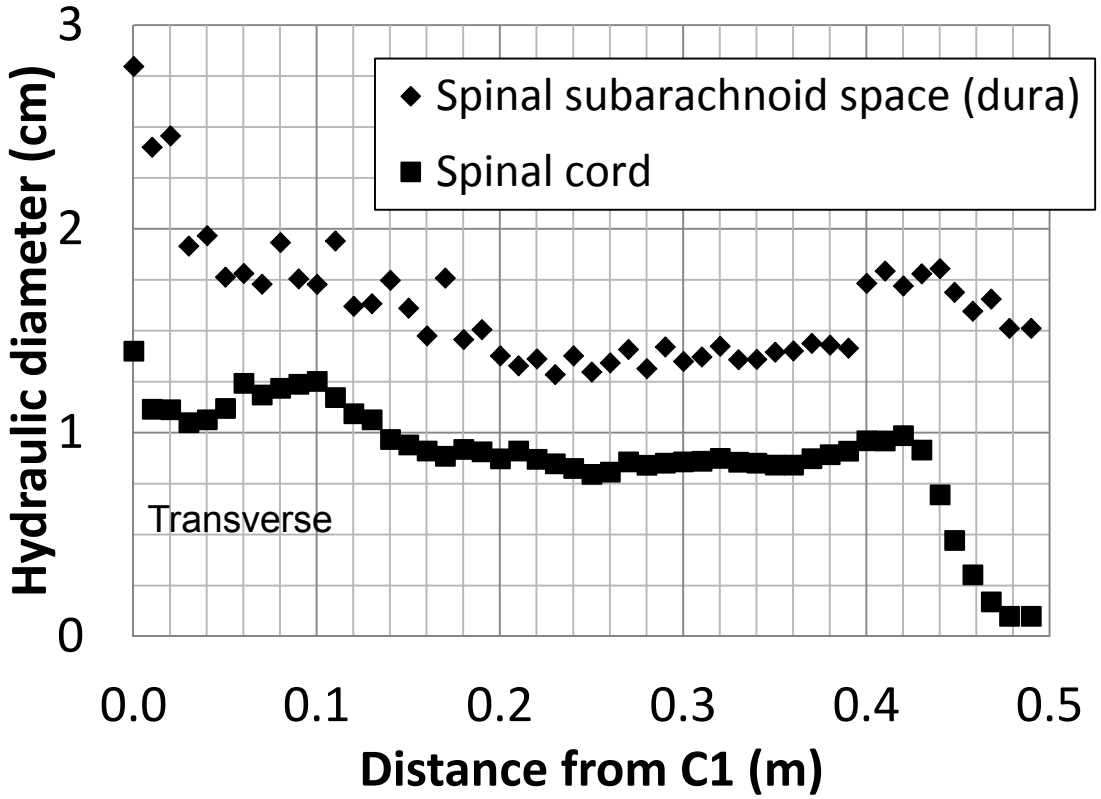

3D reconstruction of spinal SAS

The subarachnoid space is porous

- Arachnoid trebeculae have 30 µm dia. (Gupta)
- Anisotropic porosity (void fraction?)

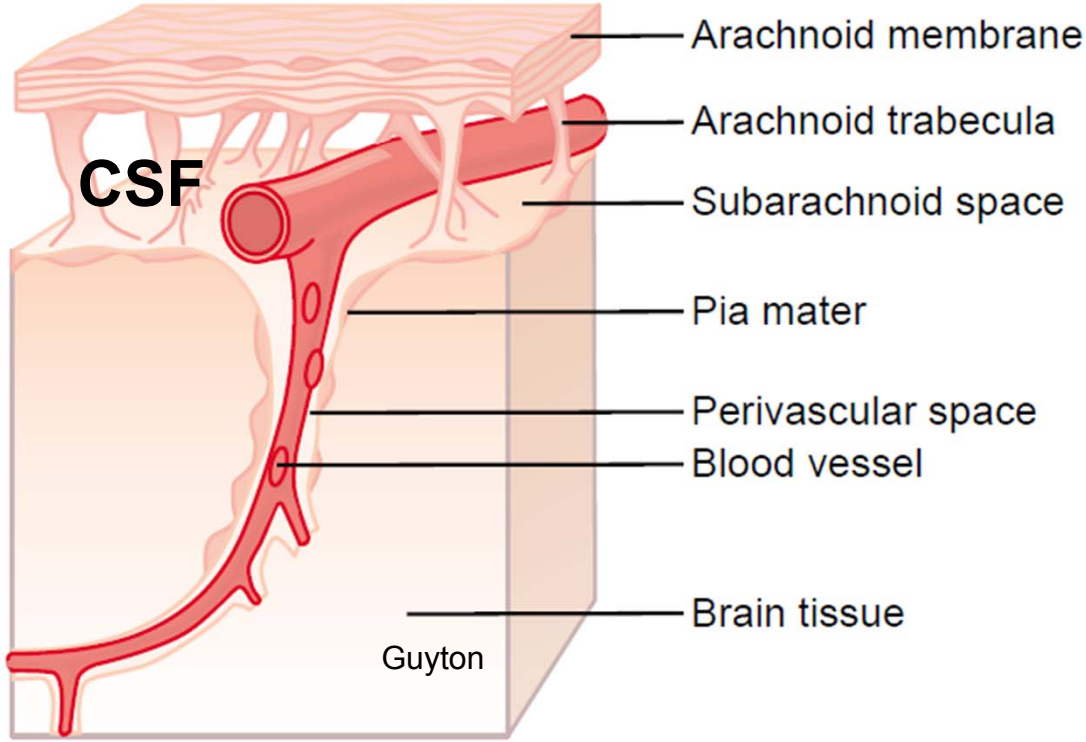

Gupta, S., M. Soellinger, et al. (2009). "Three-dimensional computational modeling of subject-specific cerebrospinal fluid flow in the subarachnoid space." J Biomech Eng **131**(2): 021010.
Guyton, A. C. and J. E. Hall (2006). Textbook of medical physiology. Philadelphia, Elsevier Saunders.

Arachnoid trabeculae

(2) Spinal meninges and subarachnoid space. A view of the cut end of the spinal cord **(SPC)** shows the pia mater **(PM)** lying directly upon the surface of the cord. Arachnoid trabeculae **(AT),** continuous with the pia, extend to the arachnoid mater **(AM)** and to an artery **(A)** above. The separation of the arachnoid mater from the thick dura mater **(DM)** is an artifact of preparation. The subarachnoid space **(SAS)** separates the arachnoid from the pia. *x* 140.

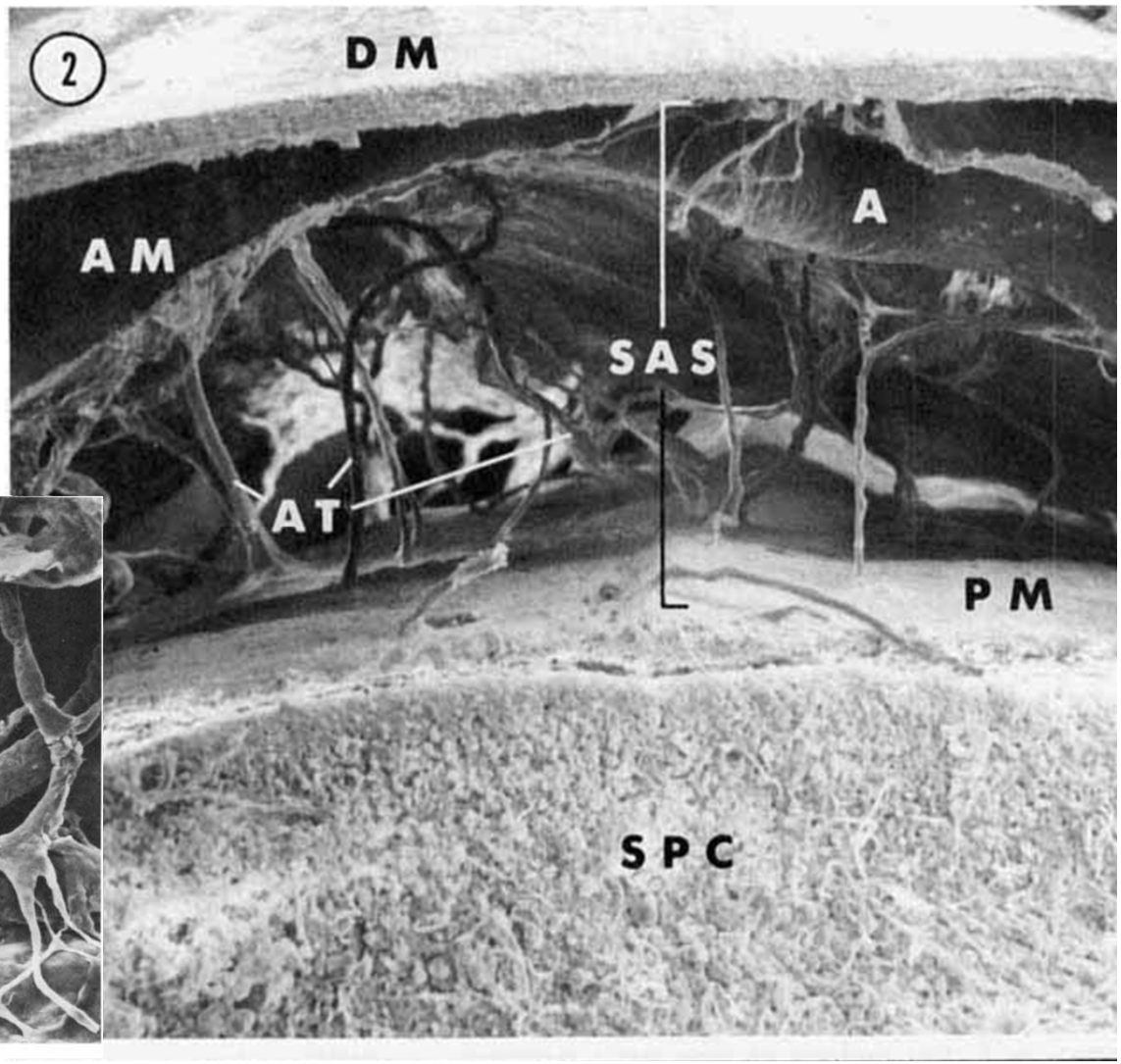

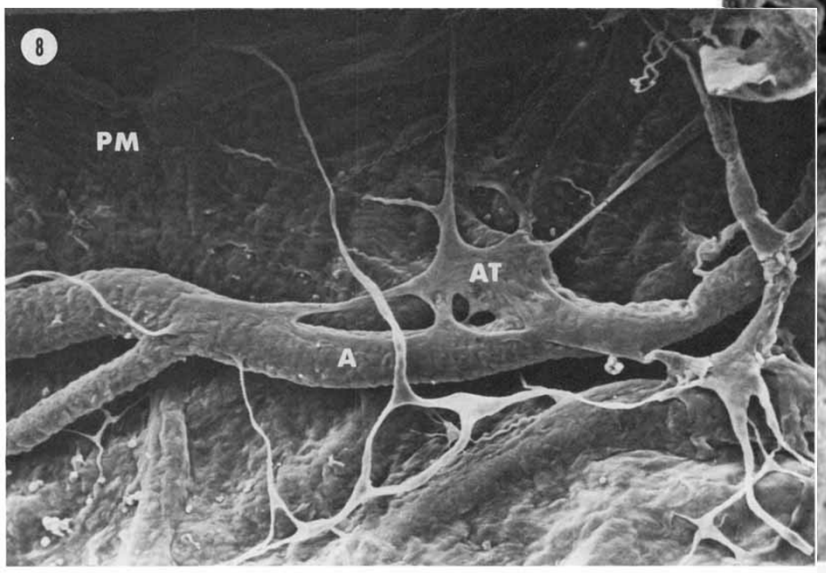

(1) Allen, D. J. and F. N. Low (1975). "Scanning electron microscopy of the subarachnoid space in the dog. III. Cranial levels." The Journal of comparative neurology **161**(4): 515-539.

(2) Cloyd, M. W. and F. N. Low (1974). "Scanning electron microscopy of the subarachnoid space in the dog. I. Spinal cord levels." The Journal of comparative neurology **153**(4): 325-368.

Trabeculae microstructure

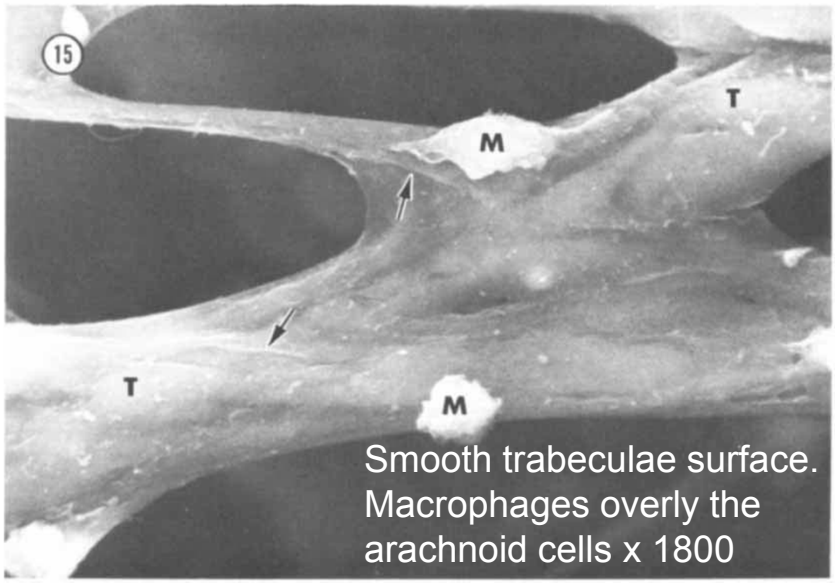

Smooth trabeculae surface. Macrophages overly the arachnoid cells x 1800

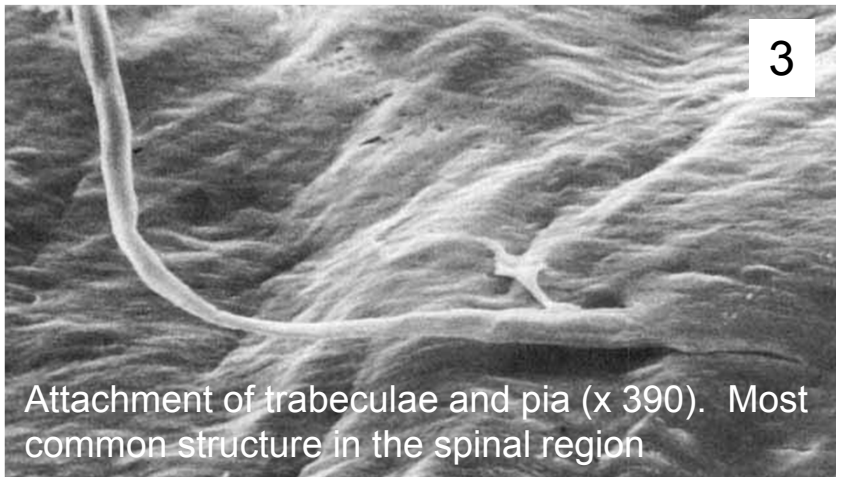

Attachment of trabeculae and pia (x 390). Most common structure in the spinal region

Arachnoid trabeculae formed between closely apposed structures (X120).

(15) Malloy, J. J. and F. N. Low (1974). "Scanning electron microscopy of the subarachnoid space in the dog. II. Spinal nerve exits." The Journal of comparative neurology **157**(1): 87-107.
(36,3) Cloyd, M. W. and F. N. Low (1974). "Scanning electron microscopy of the subarachnoid space in the dog. I. Spinal cord levels." The Journal of comparative neurology **153**(4): 325-368.

Analytical expression for porosity

- Westhuizen and DuPlessis analytical expression for longitudinal and transverse permeability
- For trabecular fiber radius, *r*
- Subarachoind space porosity *ε* (*in vivo* = ????

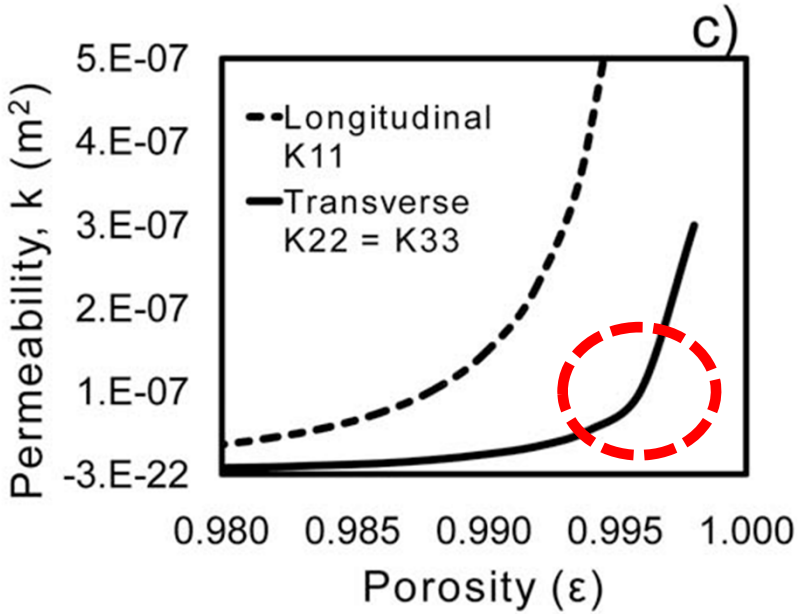

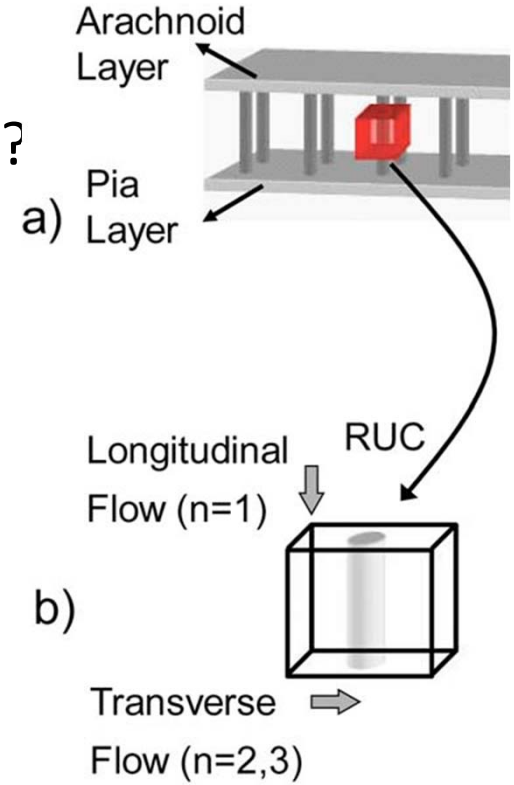

Transverse

$$\frac{k_{11}}{r^2} = \frac{\varepsilon^2 \cdot (\pi + 2.157 \cdot (1-\varepsilon))}{48 \cdot (1-\varepsilon)^2},$$

Longitudinal

$$\frac{k_{22}}{r^2} = \frac{k_{33}}{r^2} = \frac{\pi \cdot \varepsilon \cdot (1-\sqrt{1-\varepsilon})^2}{24 \cdot (1-\varepsilon)^{3/2}}$$

Gupta, S., M. Soellinger, et al. (2009). "Three-dimensional computational modeling of subject-specific cerebrospinal fluid flow in the subarachnoid space." J Biomech Eng **131**(2): 021010.

CSF pressure
(steady state and pulsatile components)

Steady state CSF pressure

- ICP is 7-15 mmHg in supine (Ghajar, Czsnk.)
- 0-10 mmHg in vertical position (Ghjar, Czsnk.)
- Only small pressure gradients exist (<<1 mmHg)

Ghajar, J. (2000). "Traumatic brain injury." Lancet **356**(9233): 923-9.
Czosnyka, M., Z. Czosnyka, et al. (2004). "Cerebrospinal fluid dynamics." Physiol Meas **25**(5): R51-76.
Czosnyka, M. and J. D. Pickard (2004). "Monitoring and interpretation of intracranial pressure." J Neurol Neurosurg Psychiatry **75**(6): 813-21.

CSF pressure during coughing

- High spikes in CSF pressure are possible
- ~ 55 mmHg!
- Higher in patients with syringomyelia (Sansur)

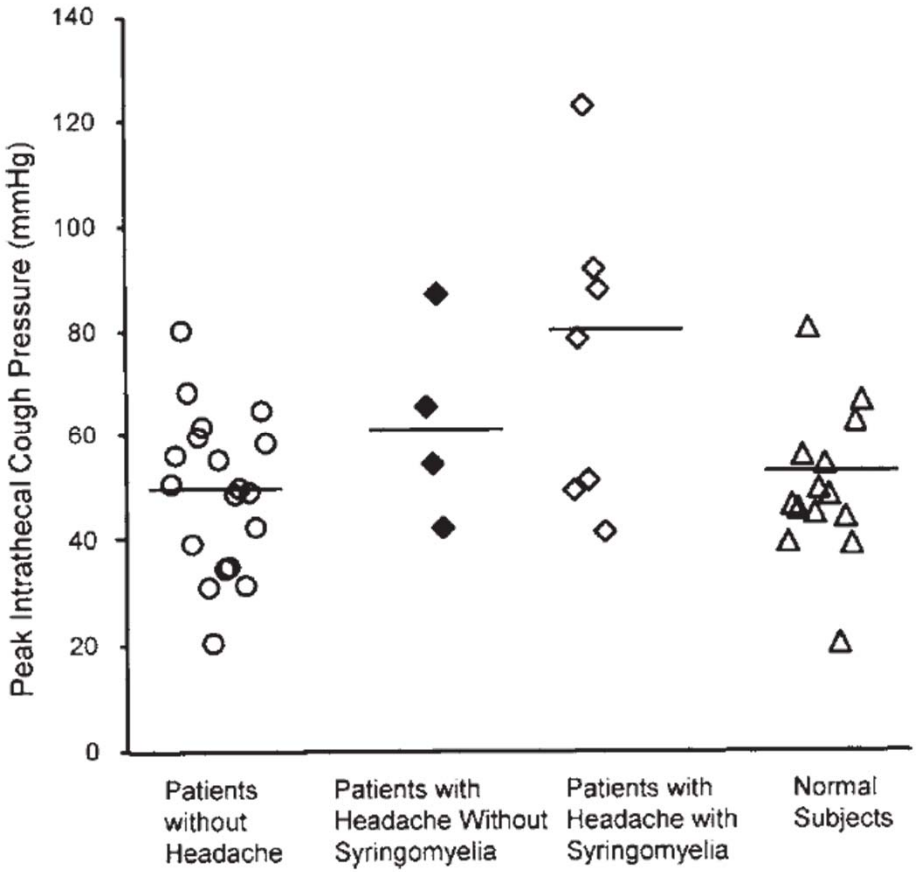

Sansur, C. A., J. D. Heiss, et al. (2003). "Pathophysiology of headache associated with cough in patients with Chiari I malformation." J Neurosurg **98**(3): 453-8.

CSF pressure and flow pulsations are in the ventricular system and subarachnoid space

- ~ 0.5-1 mmHg in healthy adult

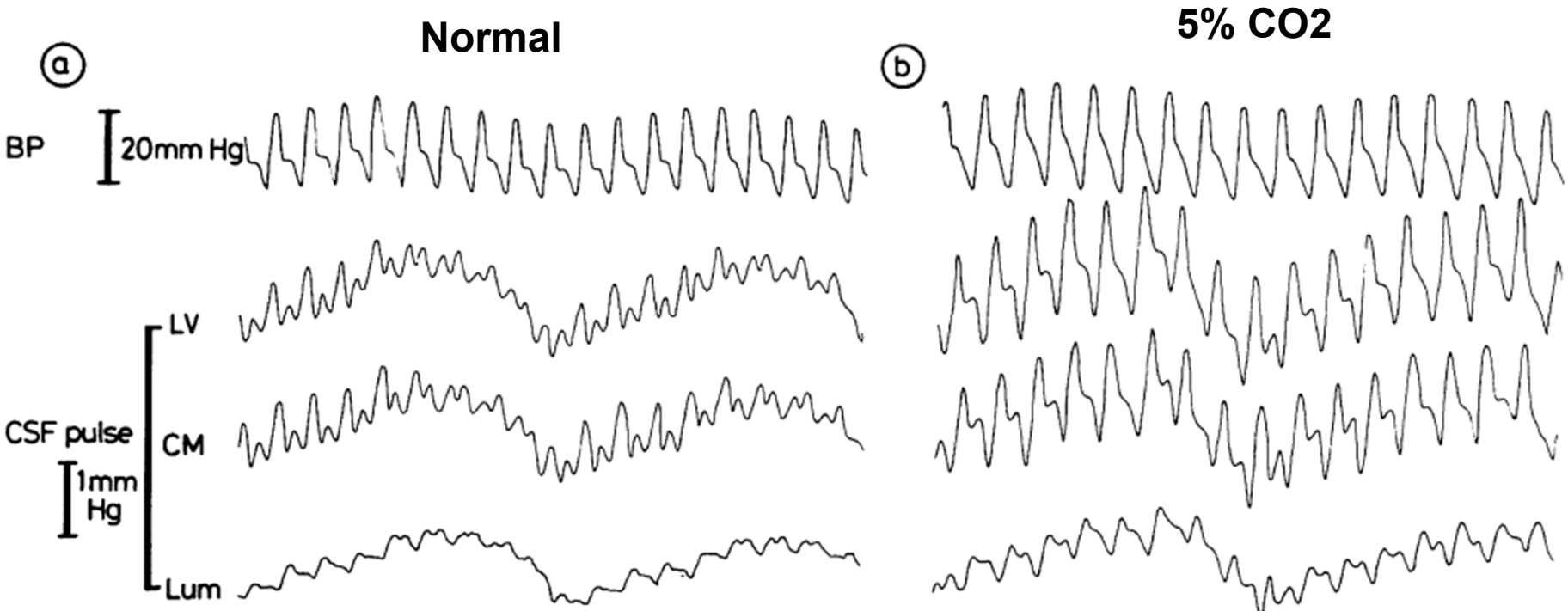

LV = lateral ventricle
CM = cisterna magna
Lum = lumbar sss

Takizawa, H., T. Gabra-Sanders, et al. (1986). "Spectral analysis of the CSF pulse wave at different locations in the craniospinal axis." J Neurol Neurosurg Psychiatry **49**(10): 1135-41.

CSF pulse comes from the brain

- PWV from figure = 2.5 m/s [0.5/(1/5)]

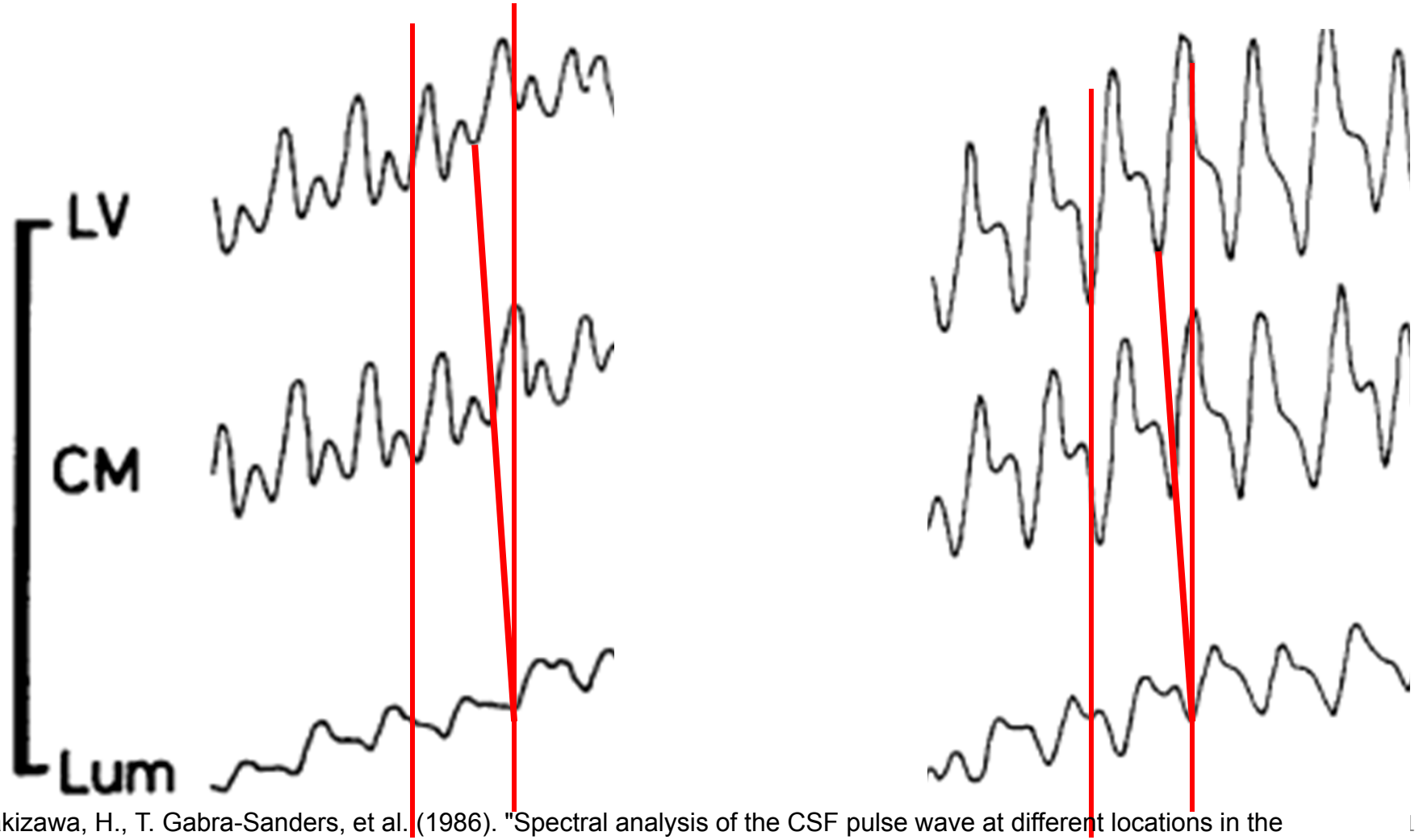

Takizawa, H., T. Gabra-Sanders, et al. (1986). "Spectral analysis of the CSF pulse wave at different locations in the craniospinal axis." J Neurol Neurosurg Psychiatry **49**(10): 1135-41.

CSF pressure pulsation amplitude is dependent on craniospinal compliance

- C=dV/dP
- (Arterial compliance is 1-5 ml/mmHg)

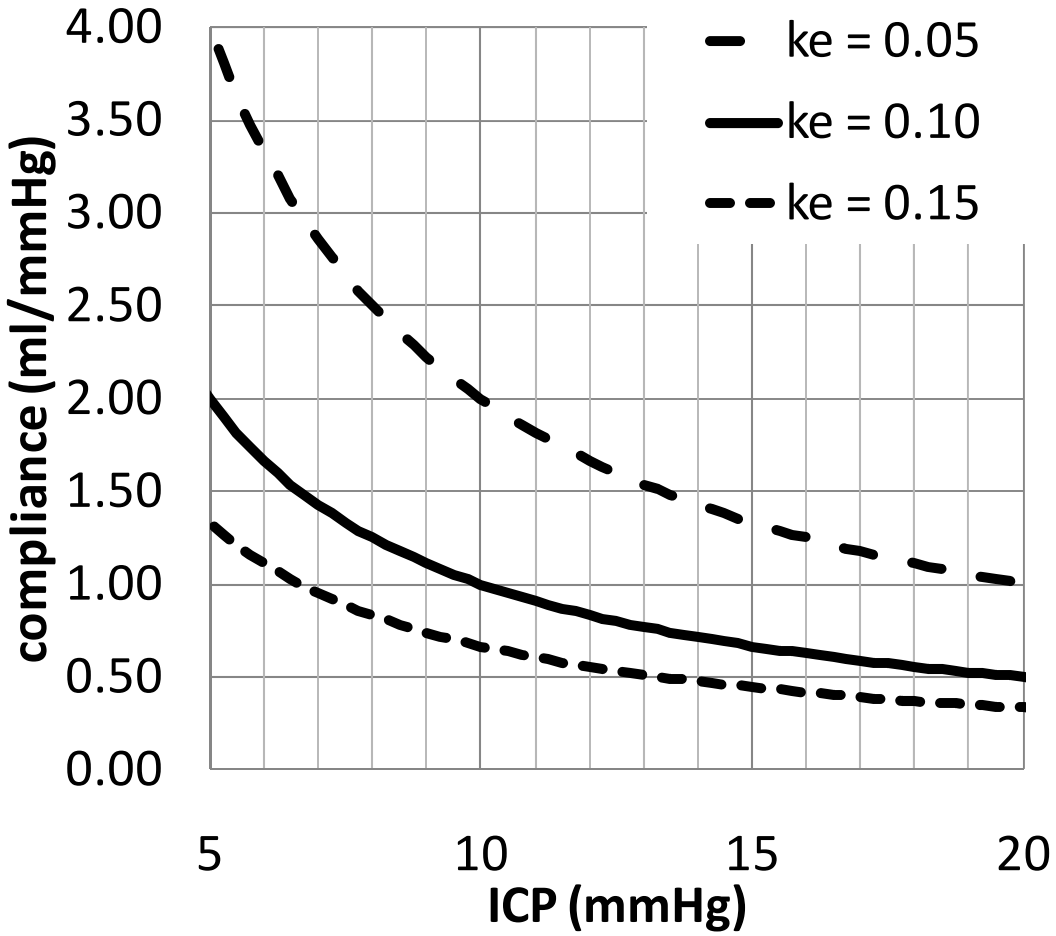

$$C_{ic} = 1/(k_e P_{ic})$$

Ursino M: A mathematical study of human intracranial hydrodynamics. Part 1--The cerebrospinal fluid pulse pressure. *Ann Biomed Eng* 1988, 16:379-401.

CSF flow pulsations

CSF flow pulsations come from cerebral blood flow pulsations

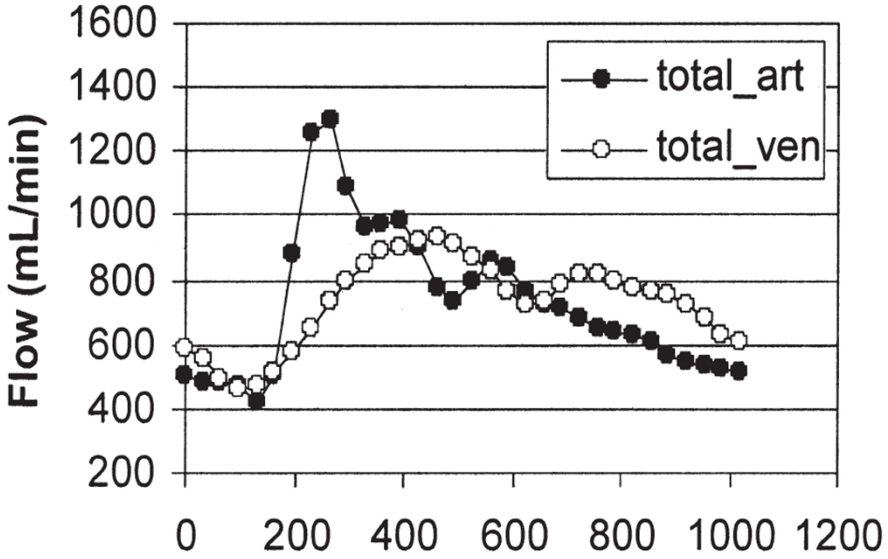

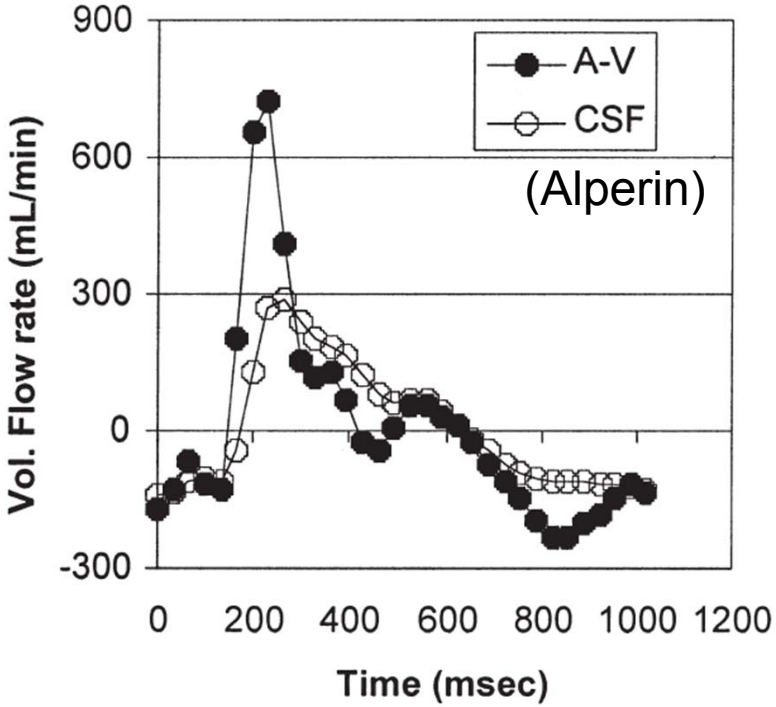

Alperin, N., A. Sivaramakrishnan, et al. (2005). "Magnetic resonance imaging-based measurements of cerebrospinal fluid and blood flow as indicators of intracranial compliance in patients with Chiari malformation." J Neurosurg **103**(1): 46-52.
Baledent, O., C. Gondry-Jouet, et al. (2004). "Relationship between cerebrospinal fluid and blood dynamics in healthy volunteers and patients with communicating hydrocephalus." Invest Radiol **39**(1): 45-55.
Baledent, O., M. C. Henry-Feugeas, et al. (2001). "Cerebrospinal fluid dynamics and relation with blood flow: a magnetic resonance study with semiautomated cerebrospinal fluid segmentation." Invest Radiol **36**(7): 368-77.

CSF pulsations are present throughout the subarachnoid space

- ~ Zero net flow

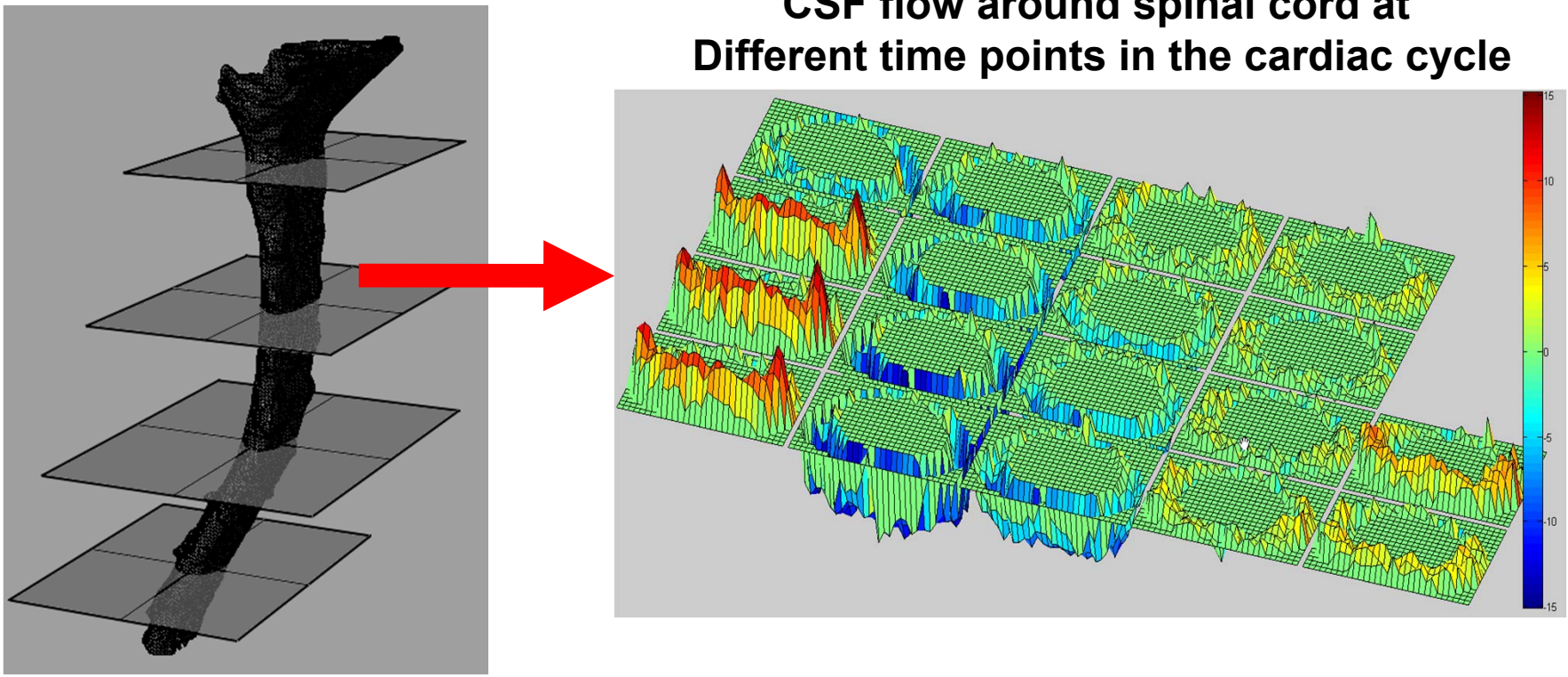

The spinal CSF pulsation decreases in the caudal direction

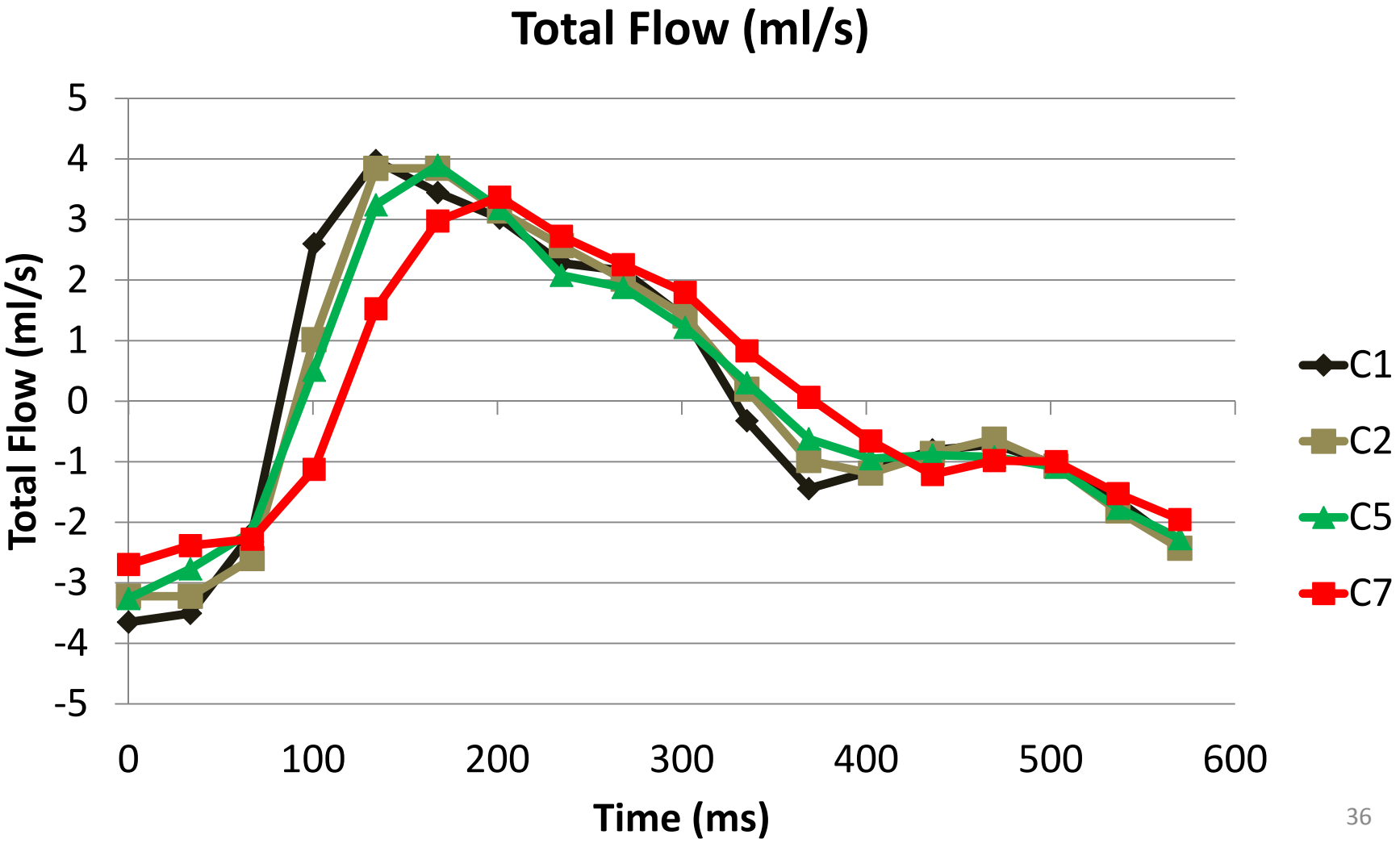

The CSF pulse travels down the spinal subarachnoid space

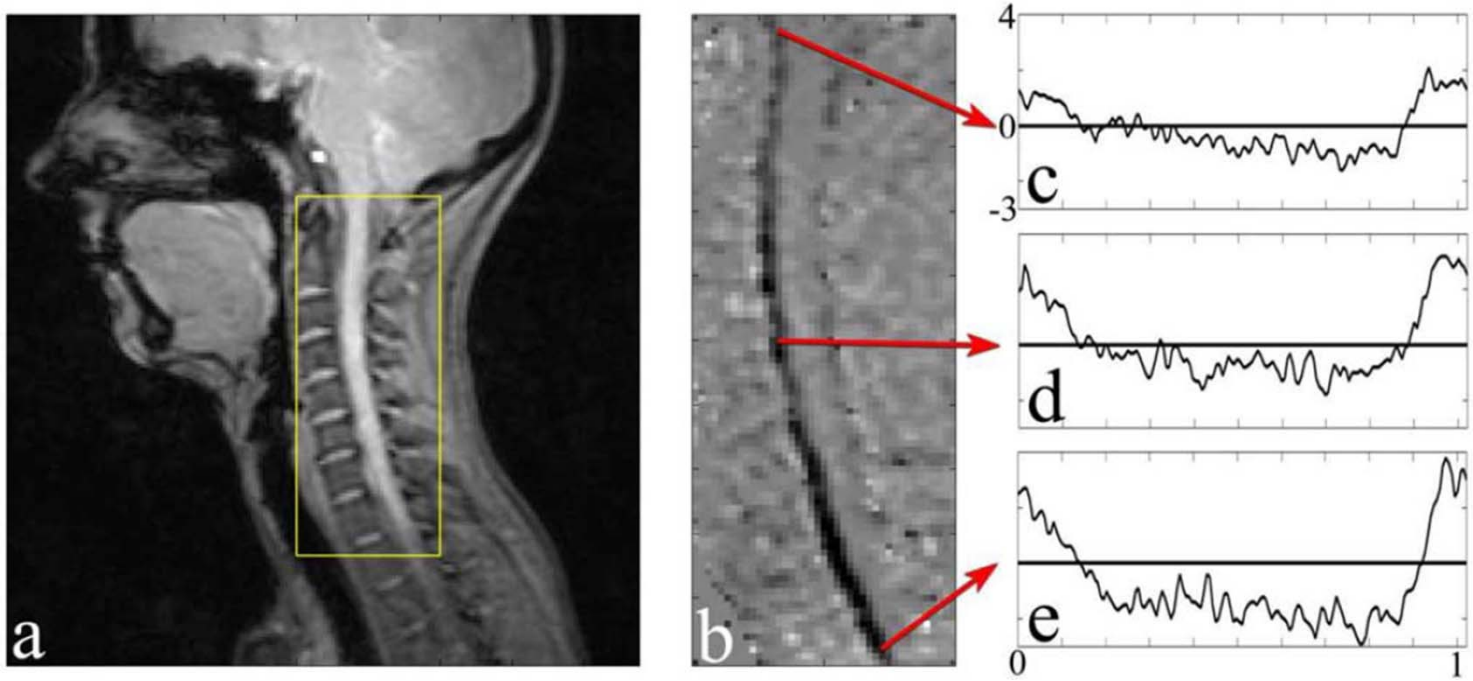

- Wave propagation velocity of ~ 4.6 m/s
- Related to craniospinal compliance

Kalata, W., B. Martin, et al. (2009). "MR Measurement of Cerebrospinal Fluid Velocity Wave Speed in the Spinal Canal." IEEE Trans Biomed Eng.

The largest CSF velocities occur in the aqueduct of Sylvius

- 5-40 mm/s

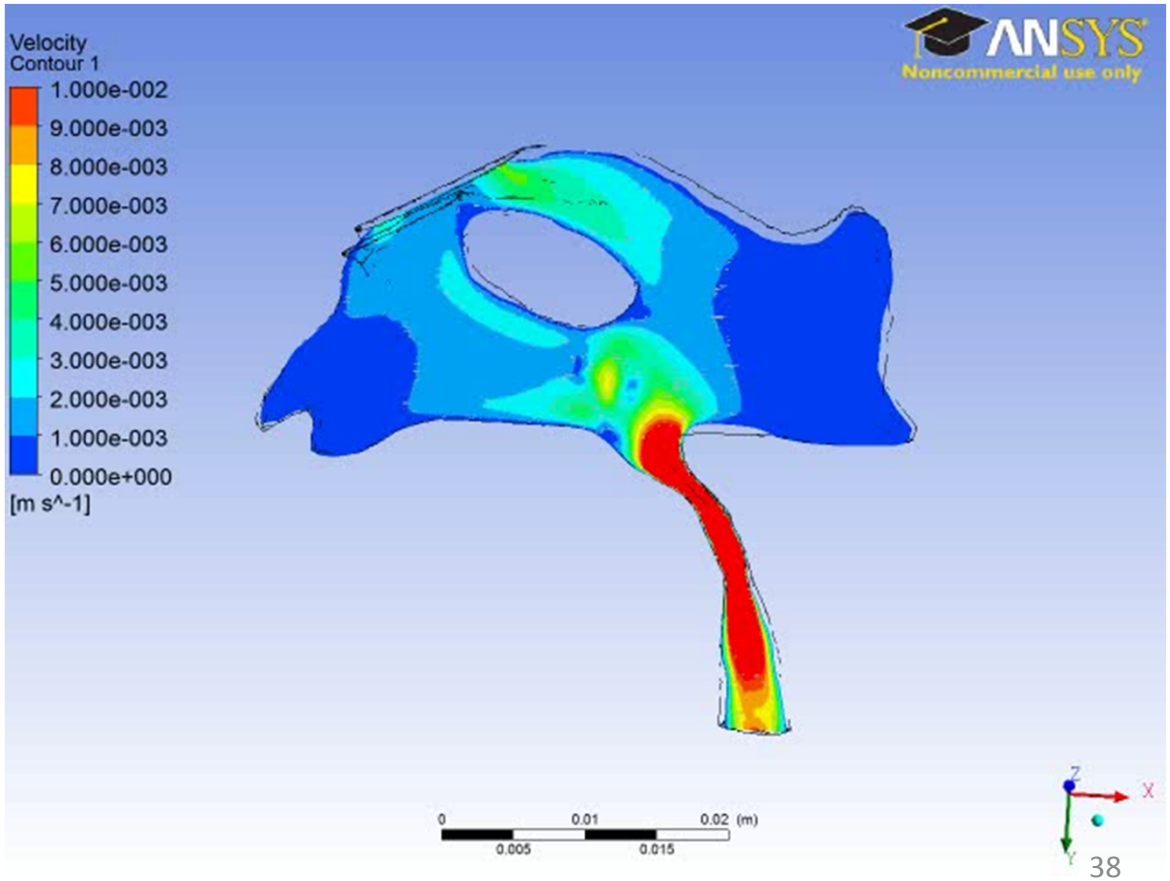

Blood
(cerebral and spinal cord)

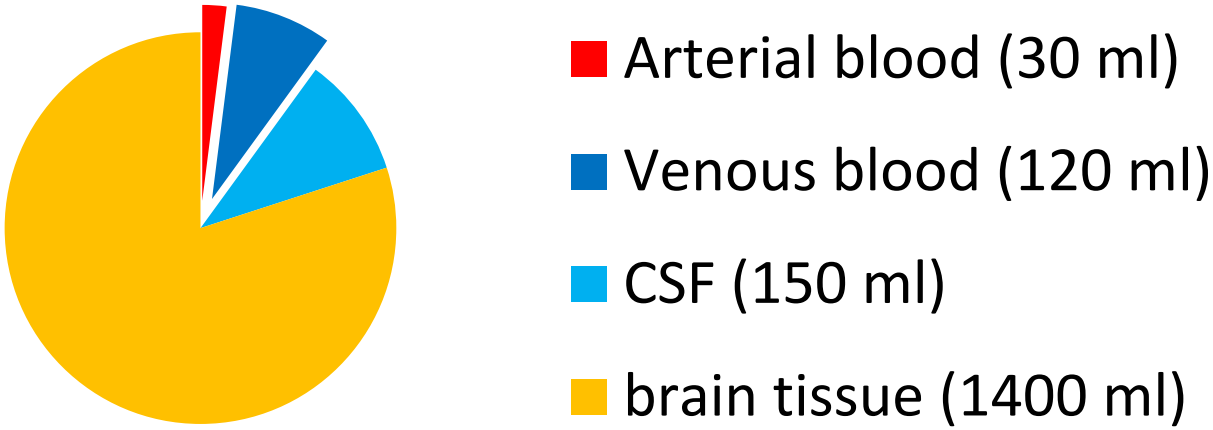

Total cerebral blood volume

TABLE 1. *Cerebral blood volume in man**

Reference	No. of Patients	Cerebral Blood Volume Range, ml
Nylin et al., 1956 (265)	11	46–100
1960 (268)	12	72–240
1961 (266)	10	70–140
1961 (267)	13	83–183
Gallyas et al., 1967 (101)	12	99–167

* From Gallon (100).

Betz, E., 1972, "Cerebral blood flow: its measurement and regulation," Physiol Rev, 52(3), pp. 595-630.

Cerebral blood flow is modified by the CSF system

- Transmural pressure acts on vessels from CSF
- Perfusion pressure is related to venous pressure (and abdominal pressure)
- ICP = 1.5mmHg + venousP
- 50 ml/min of blood

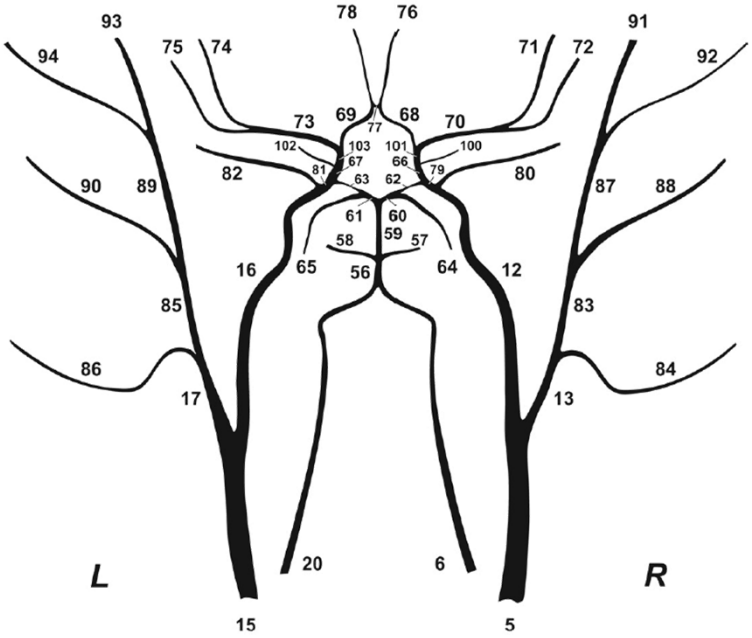

Reymond, P., F. Merenda, et al. (2009). "Validation of a one-dimensional model of the systemic arterial tree." Am J Physiol Heart Circ Physiol **297**(1): H208-22.

Role of CSF in CBF?

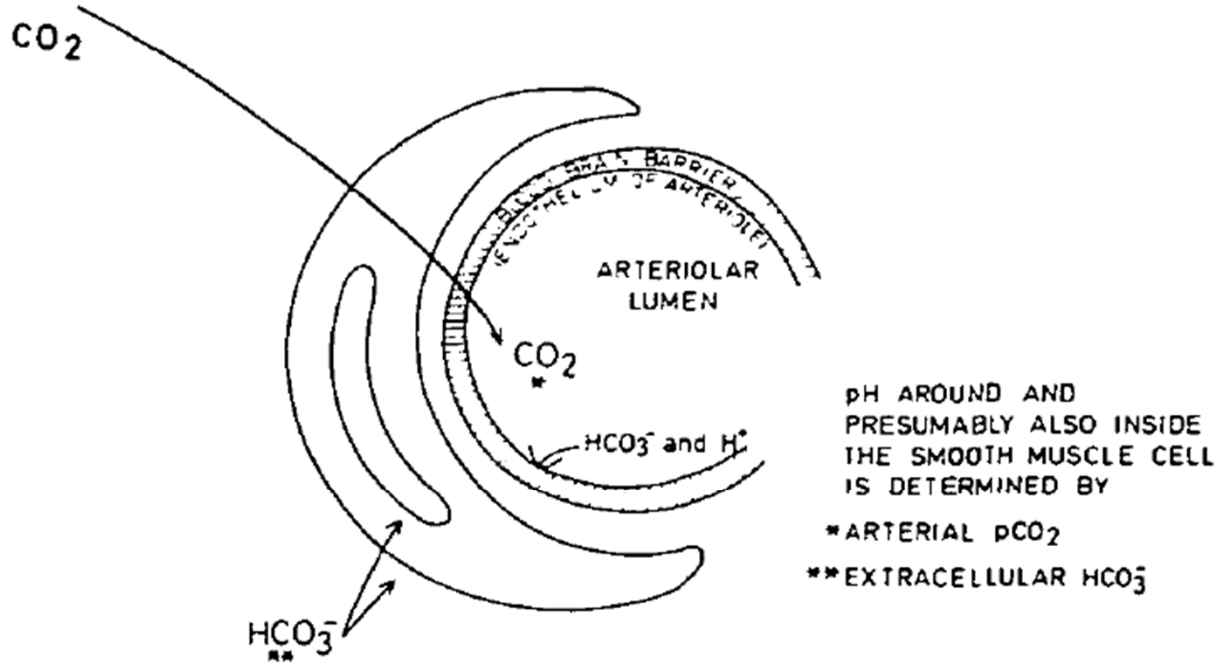

FIGURE 2

Cerebrospinal fluid pH is the main factor controlling cerebral blood flow: it is apparently responsible for the chemical control of cerebral blood flow (CBF) (CO_2 and O_2), the adaptation of CBF, and probably also the metabolic control of CBF.

Lassen, N. A., 1974, "Control of cerebral circulation in health and disease," Circulation Research, 34(6), pp. 749-760.

CBF autoregulation (human)

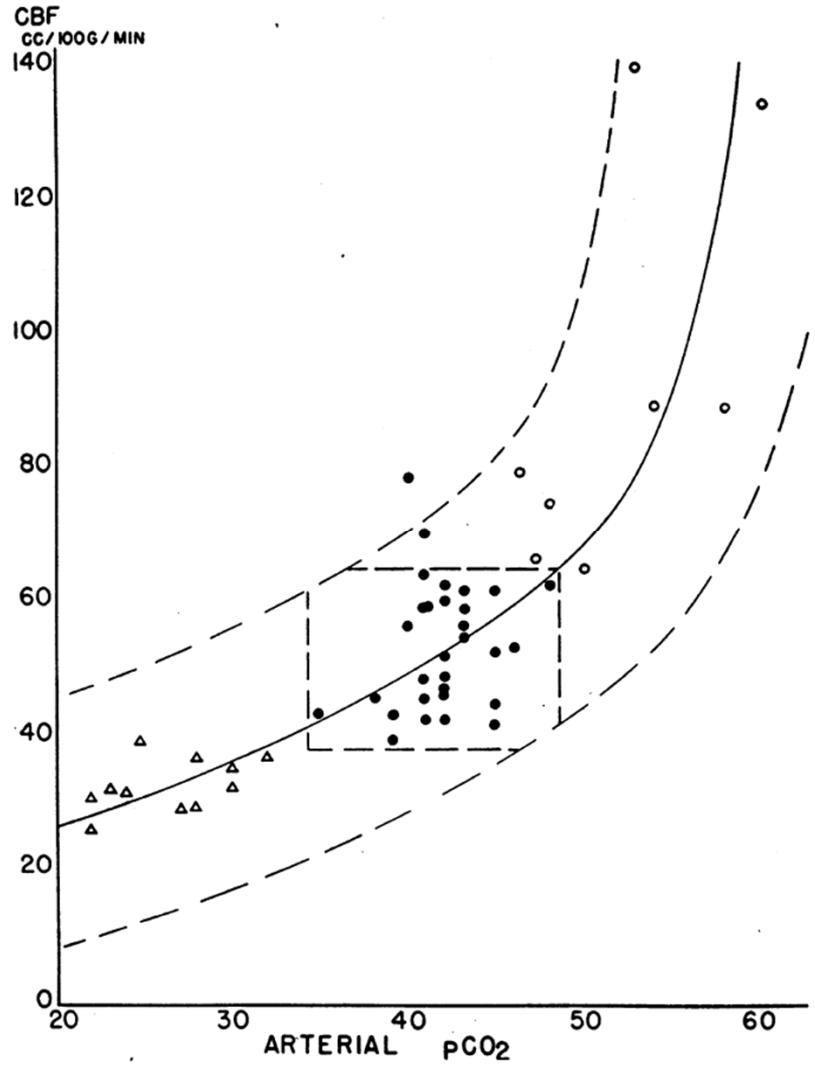

Kety, S. S., and Schmidt, C. F., 1948, "The effects of altered arterial tensions of carbon dioxide and oxygen on cerebral blood flow and cerebral oxygen consumption of normal young men," J Clin Invest, 27(4), pp. 484-492.

MCA velocity and PCO2 (human)

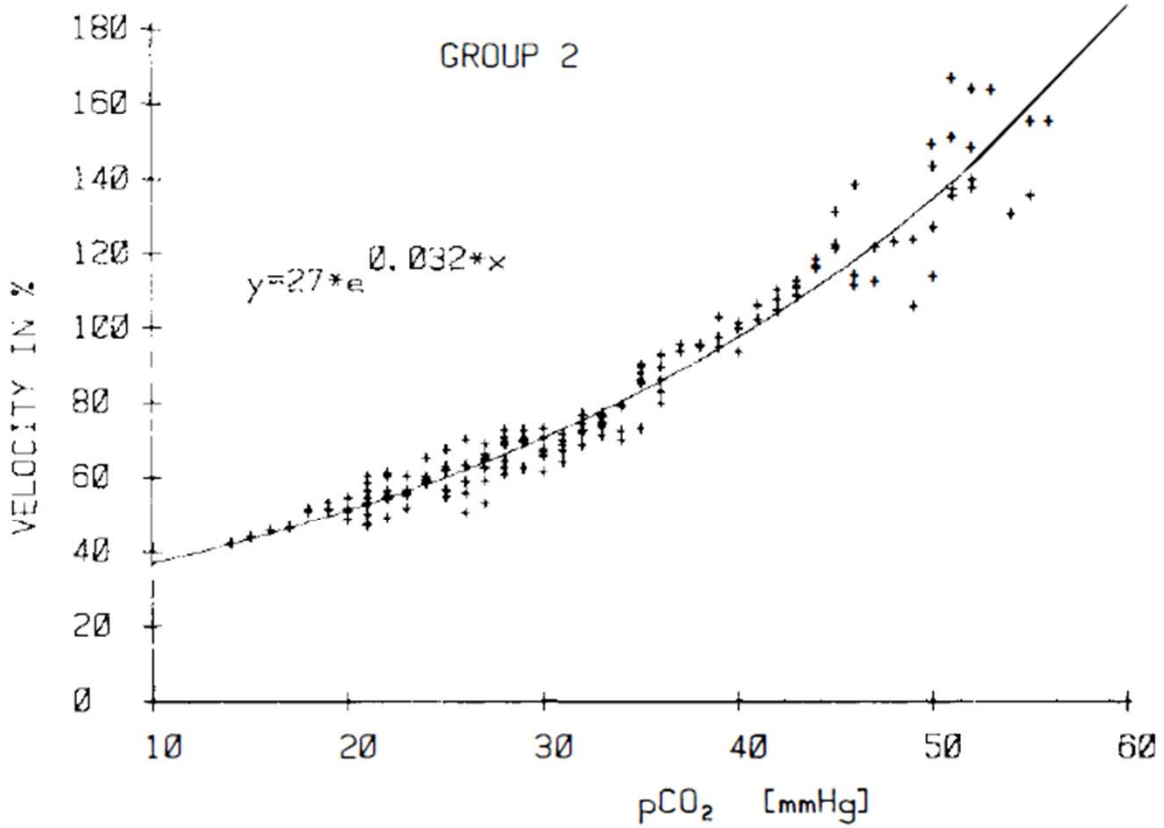

FIG. 3. Blood flow velocity (*V*) of the middle cerebral artery as percentage of the *V* value at an end-tidal P_{CO_2} of 40 mm Hg (Group 2: 10 subjects between 16 and 40 years of age; r = 0.97).

Markwalder, T. M., Grolimund, P., Seiler, R. W., Roth, F., and Aaslid, R., 1984, "Dependency of blood flow velocity in the middle cerebral artery on end-tidal carbon dioxide partial pressure--a transcranial ultrasound Doppler study," Journal of cerebral blood flow and metabolism : official journal of the International Society of Cerebral Blood Flow and Metabolism, 4(3), pp. 368-372.

$$y = 77.6 + (-29.1)(x - 0.918)$$

Human data

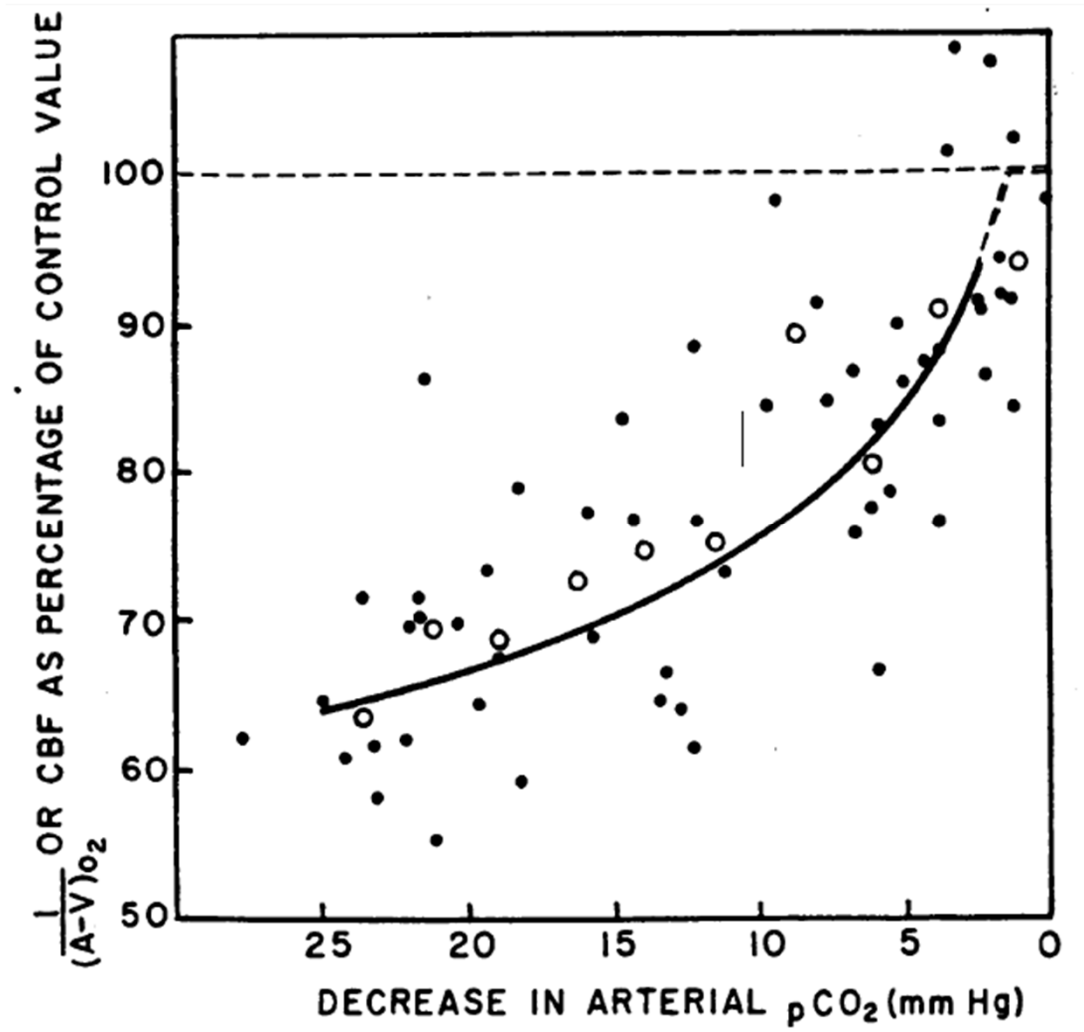

Wasserman, A. J., and Patterson, J. L., Jr., 1961, "The cerebral vascular response to reduction in arterial carbon dioxide tension," J Clin Invest, 40, pp. 1297-1303.

- Dog data

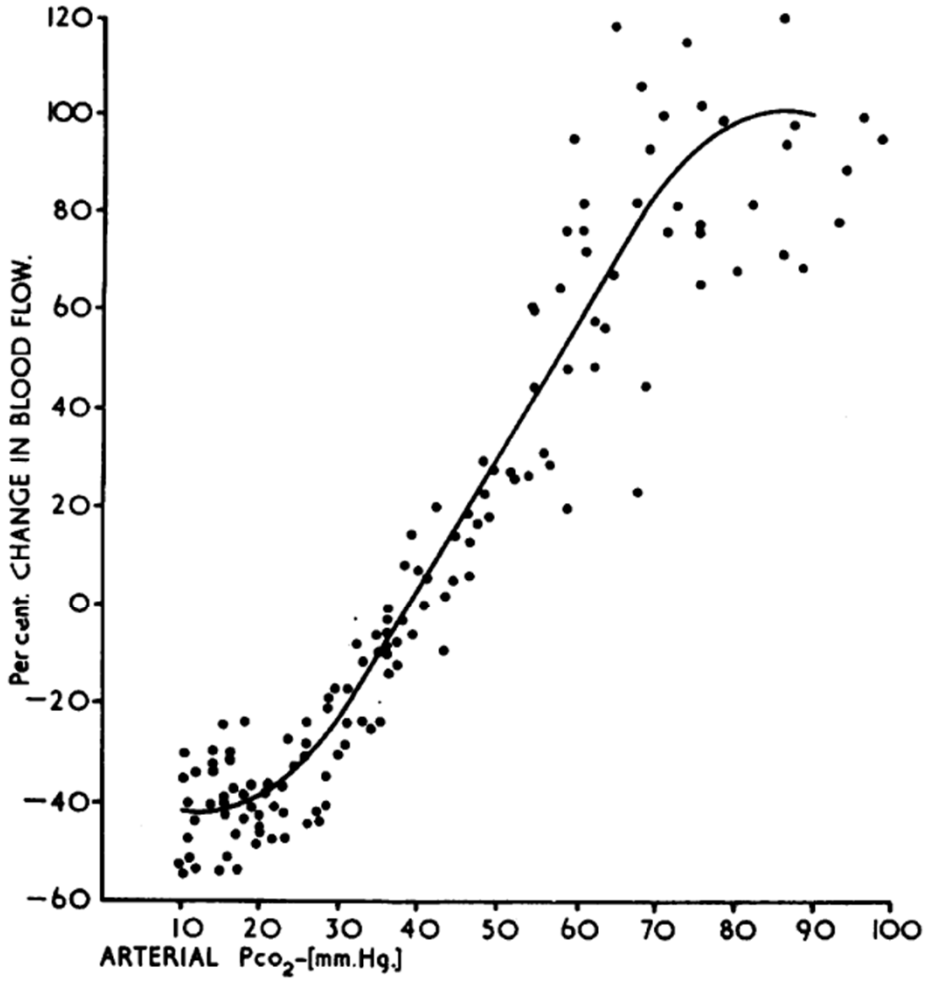

FIG. 1. *The effect of alterations in* Pa_{CO_2} *in normotensive animals on the cortical blood flow. Zero reference line for blood flow is at* Pa_{CO_2} *of 40 mm.Hg. (Tables giving the data from which this and subsequent figures were constructed will be sent by the authors on request.)*

Harper, A. M., and Glass, H. I., 1965, "Effect of alterations in the arterial carbon dioxide tension on the blood flow through the cerebral cortex at normal and low arterial blood pressures," Journal of neurology, neurosurgery, and psychiatry, 28(5), pp. 449-452.

CBF in cats

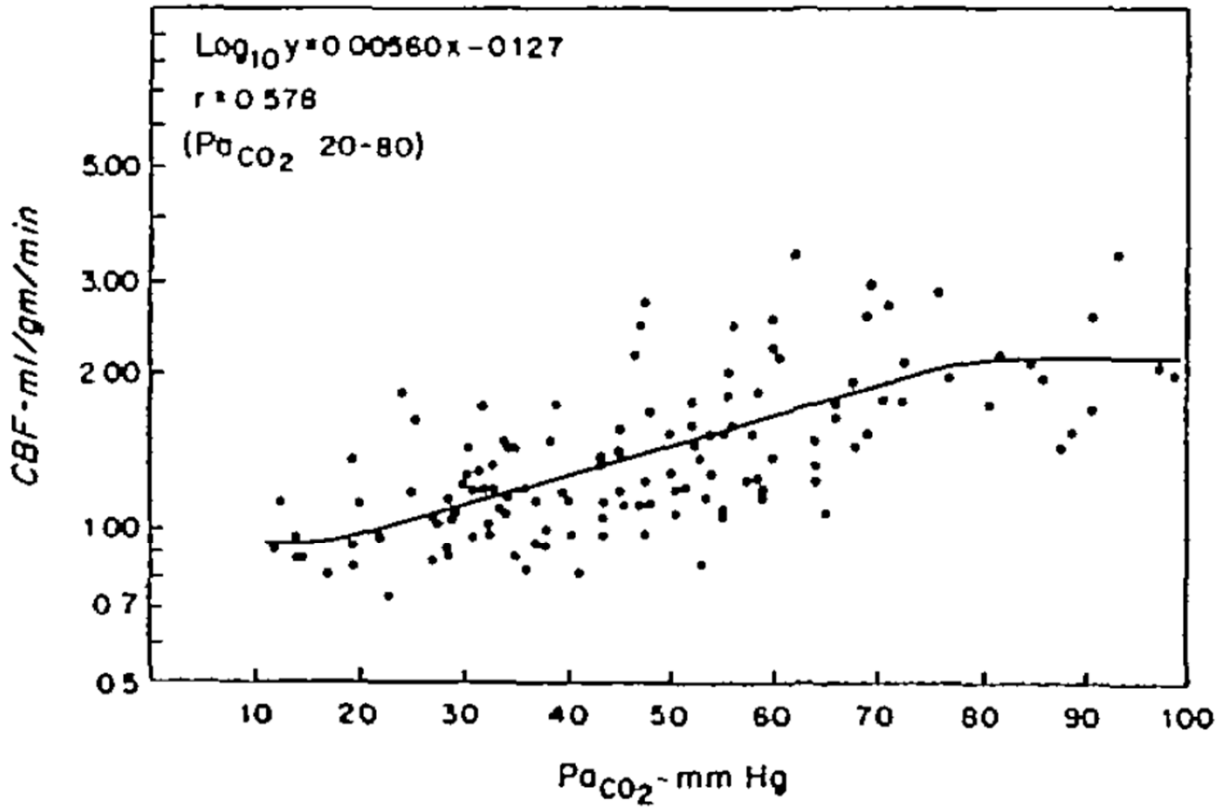

FIGURE 2

Relationship between log_{10} CBF and Pa_{CO_2} in non-ischemic cerebral cortex. Correlation coefficient, r, is statistically significant ($P < 0.005$).

Waltz, A. G., 1970, "Effect of Pa CO2 on blood flow and microvasculature of ischemic and nonischemic cerebral cortex," Stroke; a journal of cerebral circulation, 1(1), pp. 27-37.

CBF and PCO2

- Rehsus monkeys

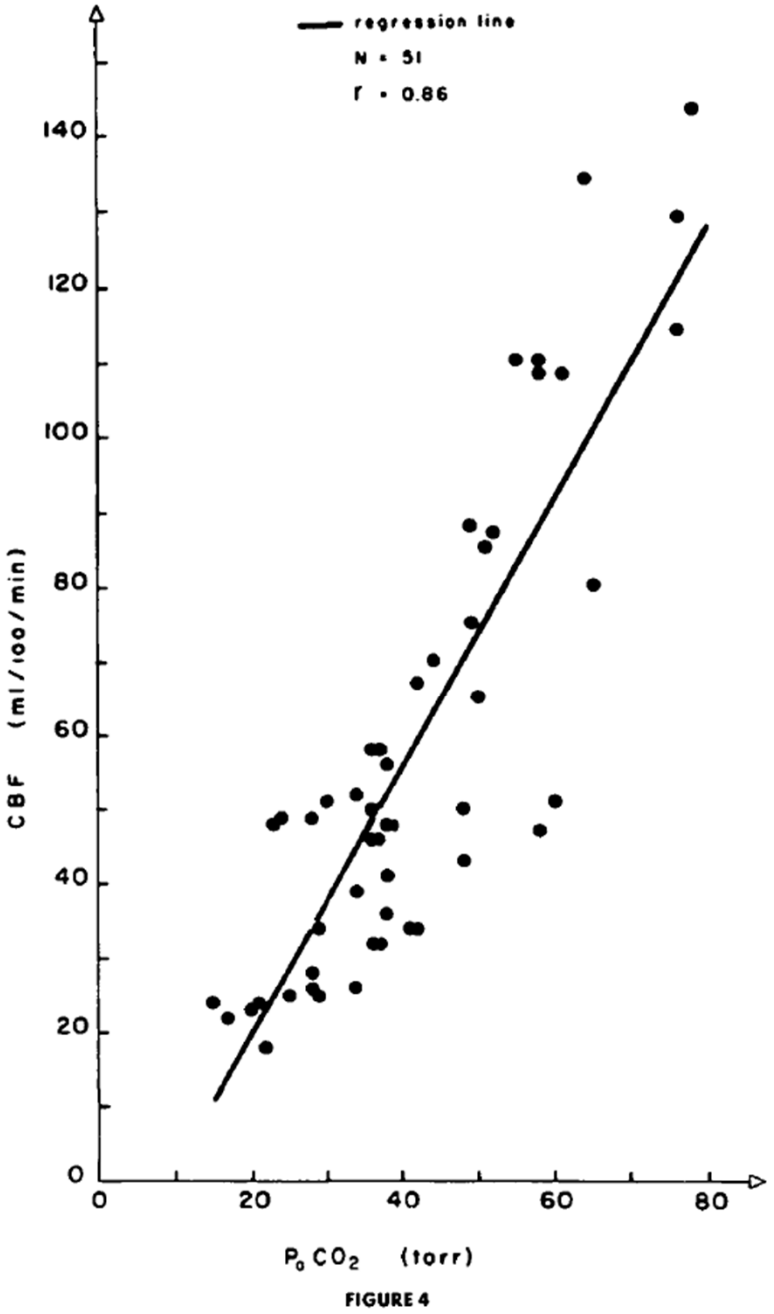

FIGURE 4

CBF versus $Paco_2$ in rhesus monkeys. The equation of the regression line is: $CBF = 1.8\ Paco_2 - 16.75$ ($P < 0.001$).

Grubb, R. L., Jr., Raichle, M. E., Eichling, J. O., and Ter-Pogossian, M. M., 1974, "The effects of changes in PaCO2 on cerebral blood volume, blood flow, and vascular mean transit time," Stroke; a journal of cerebral circulation, 5(5), pp. 630-639.

- Rat data

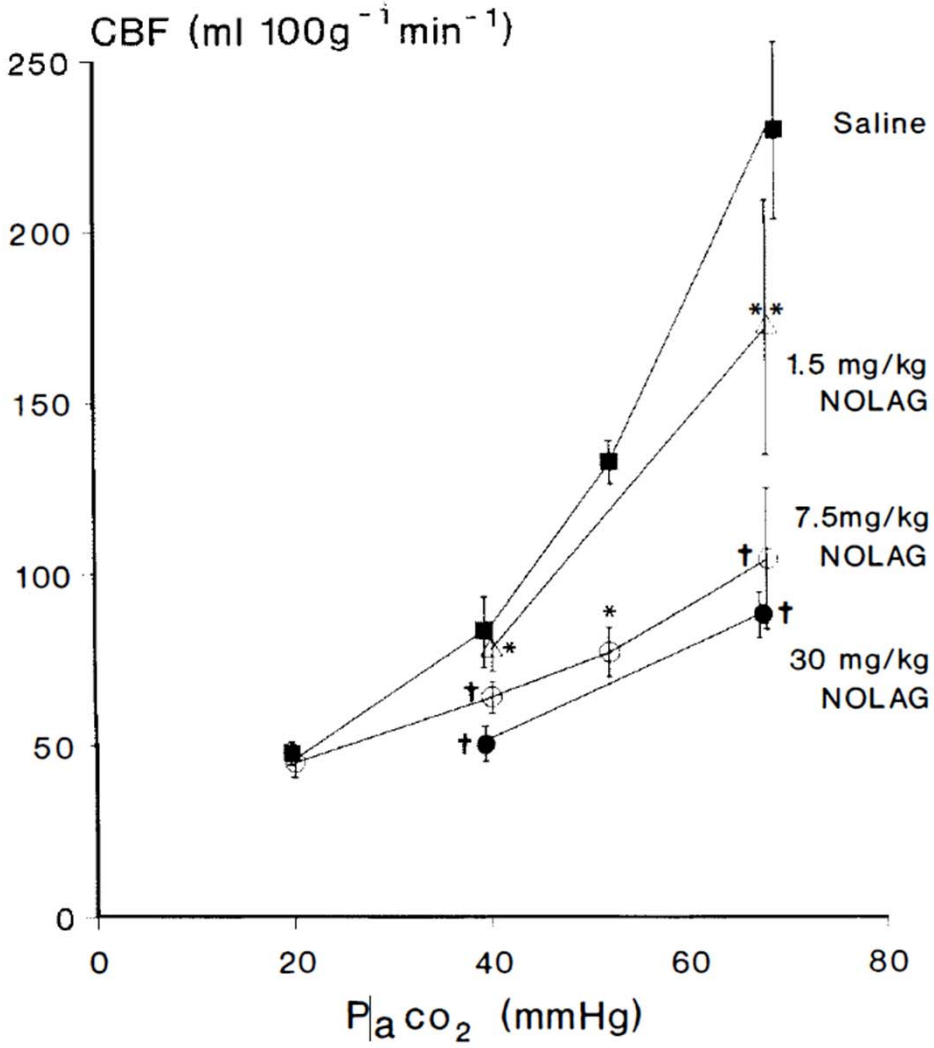

FIG. 2. Effect of N^G-nitro-L-arginine (NOLAG) on CBF-P_aCO_2 response. *$p < 0.05$, **$p < 0.01$, †$p < 0.001$ versus saline-treated animals.

Wang, Q., Paulson, O. B., and Lassen, N. A., 1992, "Effect of nitric oxide blockade by NG-nitro-L-arginine on cerebral blood flow response to changes in carbon dioxide tension," Journal of cerebral blood flow and metabolism : official journal of the International Society of Cerebral Blood Flow and Metabolism, 12(6), pp. 947-953.

- infants

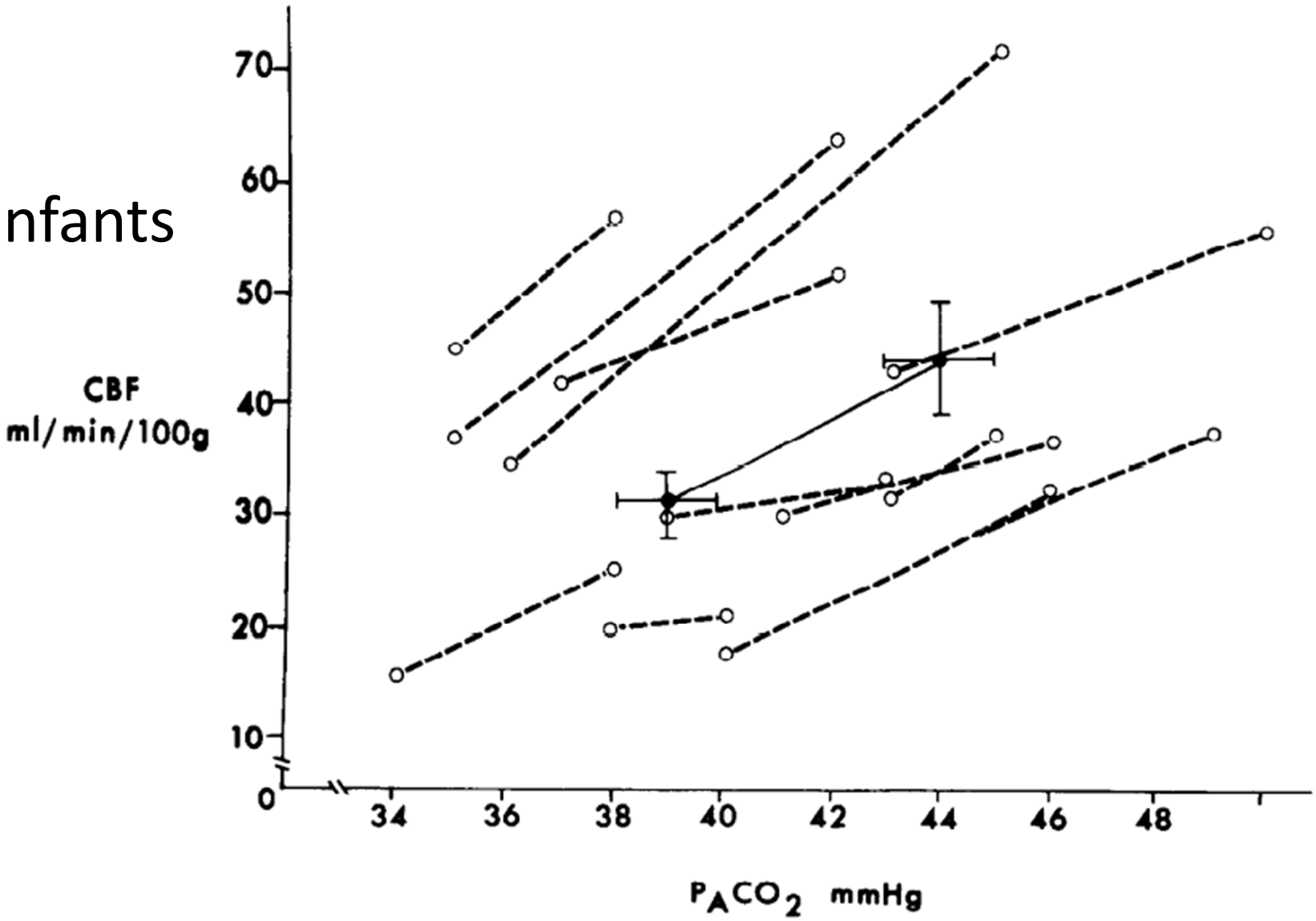

Leahy, F. A., Cates, D., MacCallum, M., and Rigatto, H., 1980, "Effect of CO2 and 100% O2 on cerebral blood flow in preterm infants," Journal of applied physiology: respiratory, environmental and exercise physiology, 48(3), pp. 468-472.

- human

Vmca (% of awake Vmca-40)

TABLE 4. The Absolute and Relative Slopes of CO_2 Reactivity during the Awake State and during Anesthesia with Propofol and Propofol–N_2O

Conditions	Absolute Slope ($cm \cdot s^{-1} \cdot mmHg^{-1}$)	Relative Slope ($\% \cdot mmHg^{-1}$)
Awake	2.1 ± 0.1	3.2 ± 0.1 (2.9–3.5)
Propofol	1.5 ± 0.2*	2.1 ± 0.1* (1.8–2.5)
Propofol–N_2O	1.6 ± 0.2*	2.5 ± 0.2* (2.0–2.9)

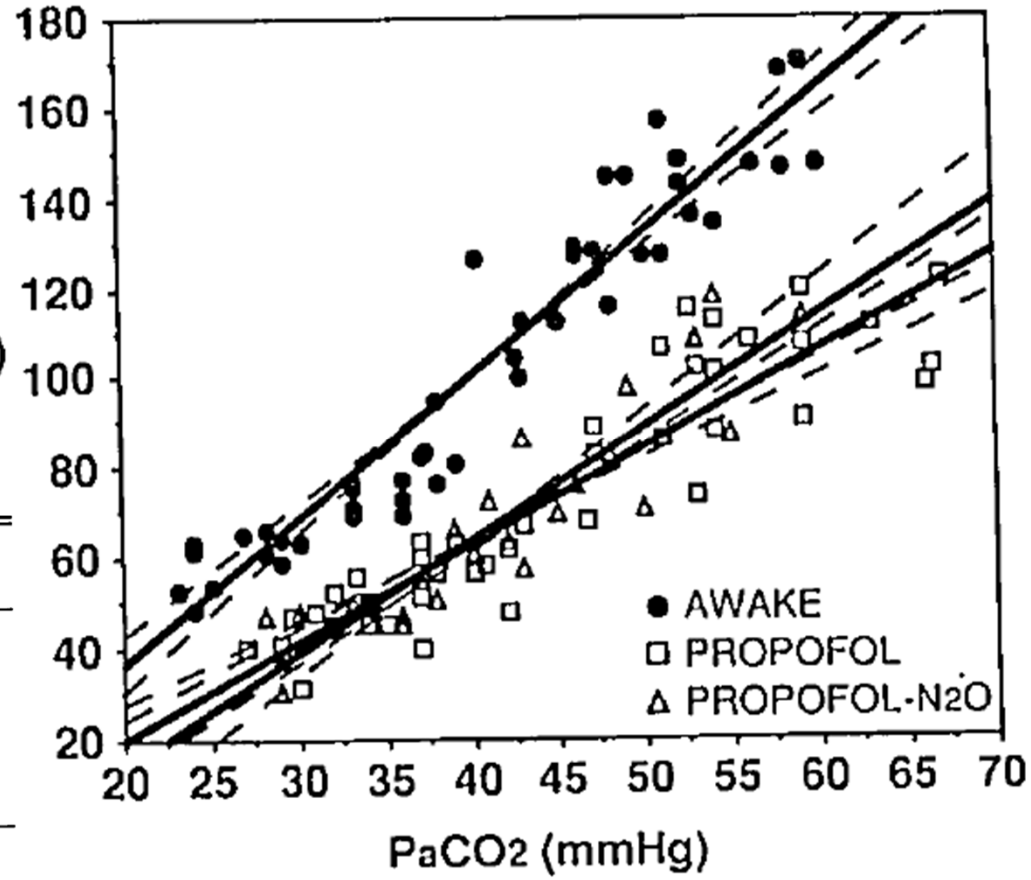

Eng, C., Lam, A. M., Mayberg, T. S., Lee, C., and Mathisen, T., 1992, "The influence of propofol with and without nitrous oxide on cerebral blood flow velocity and CO2 reactivity in humans," Anesthesiology, 77(5), pp. 872-879.

Patients undergoing nonneurologic suergery

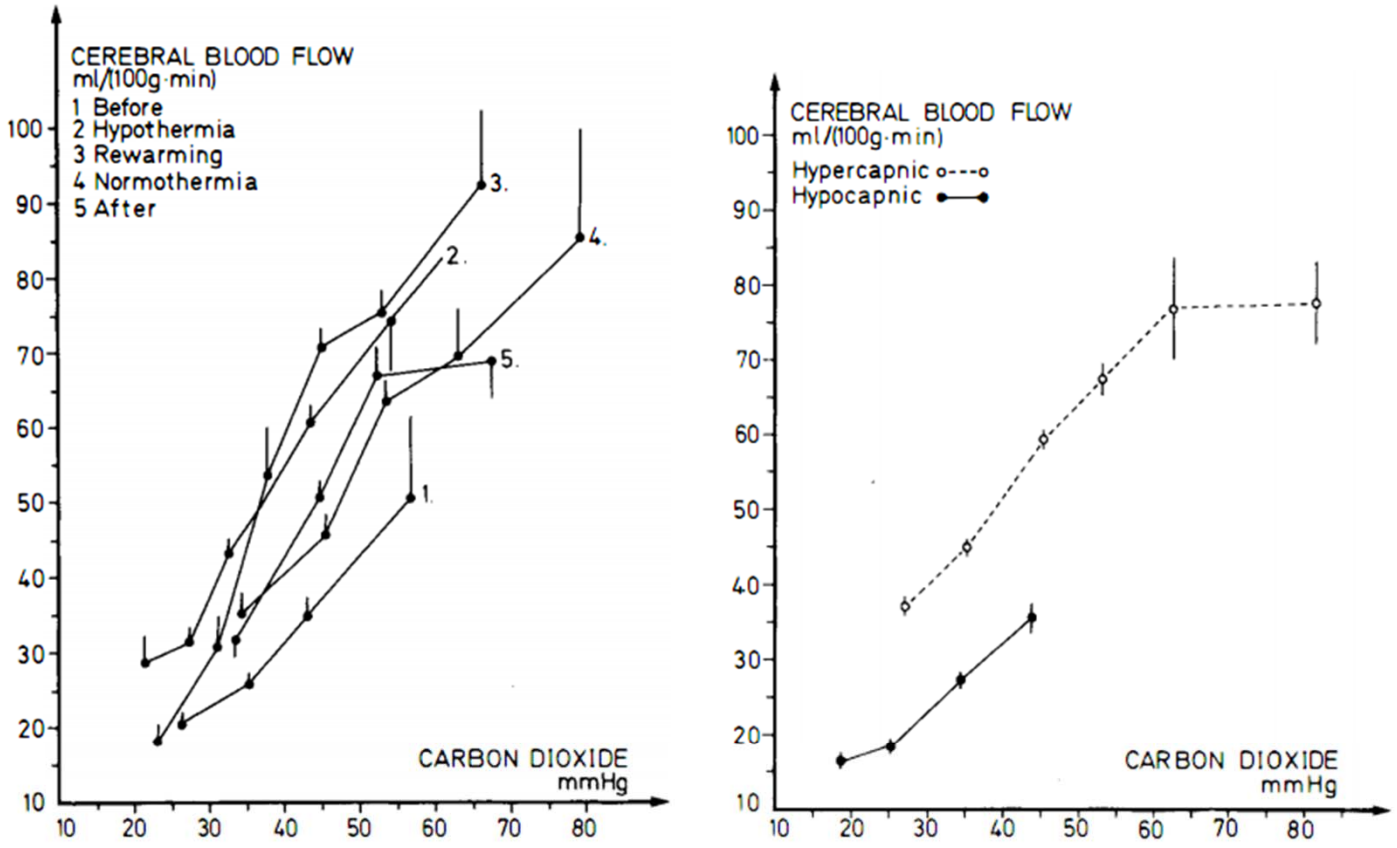

FIG. 2. Normal relationship between CBF and P_aCO_2 was found during all five periods of the surgery. CO_2 reactivity (% change in CBF/mm Hg change in P_aCO_2) was ~4%, there being no difference in sensitivity between the various periods. **Left:** All measurements from the 68 patients (n = 879) with blood pressure of ≥40 mm Hg during the five periods are presented. **Right:** Measurements before bypass are excluded (owing to a higher hematocrit) and the other measurements are pooled together to give the general CBF–P_aCO_2 relationship. The 9 patients with no CO_2 added to the oxygenator (hypocapnia, n = 100) showed the same CO_2 reactivity in the CO_2 range studied as the group of 59 hypercapnic patients (n = 723). Resetting of CBF to higher values in the hypercapnic patients illustrates that the hyperperfusion must be caused by other means than CO_2 per se. Values are means ± 1 SEM.

Henriksen, L., 1986, "Brain luxury perfusion during cardiopulmonary bypass in humans. A study of the cerebral blood flow response to changes in CO2, O2, and blood pressure," Journal of cerebral blood flow and metabolism : official journal of the International Society of Cerebral Blood Flow and Metabolism, 6(3), pp. 366-378.

Spinal cord arteries

- There is a lot of anatomical variation in SC blood supply

1. Intercostal artery
2. Posterior inter. art. branch
3. Anterior inter. art. branch
4. Radiculomedullary art.
5. Muscular branch
6. Artery of Adamkiewicz
7. Anterior spinal artery (ASA)

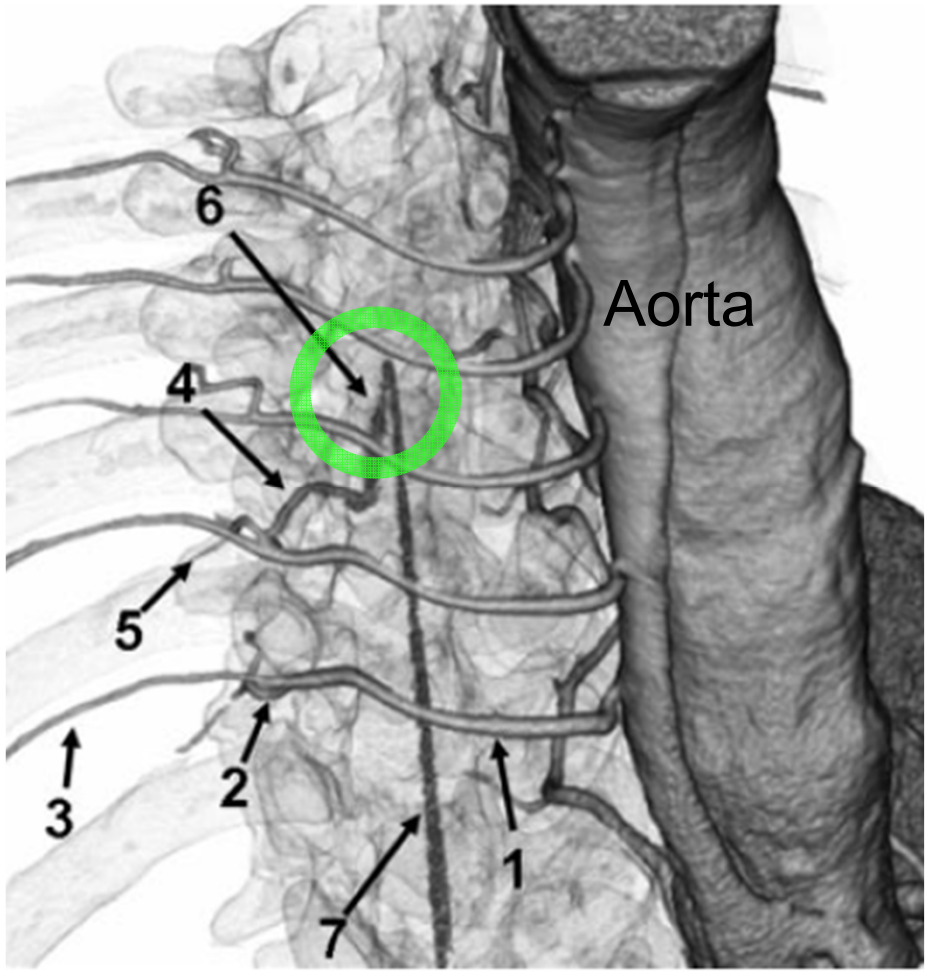

Uotani, K., N. Yamada, et al. (2008). "Preoperative visualization of the artery of Adamkiewicz by intra-arterial CT angiography." AJNR Am J Neuroradiol **29**(2): 314-8.

More on spinal cord blood supply

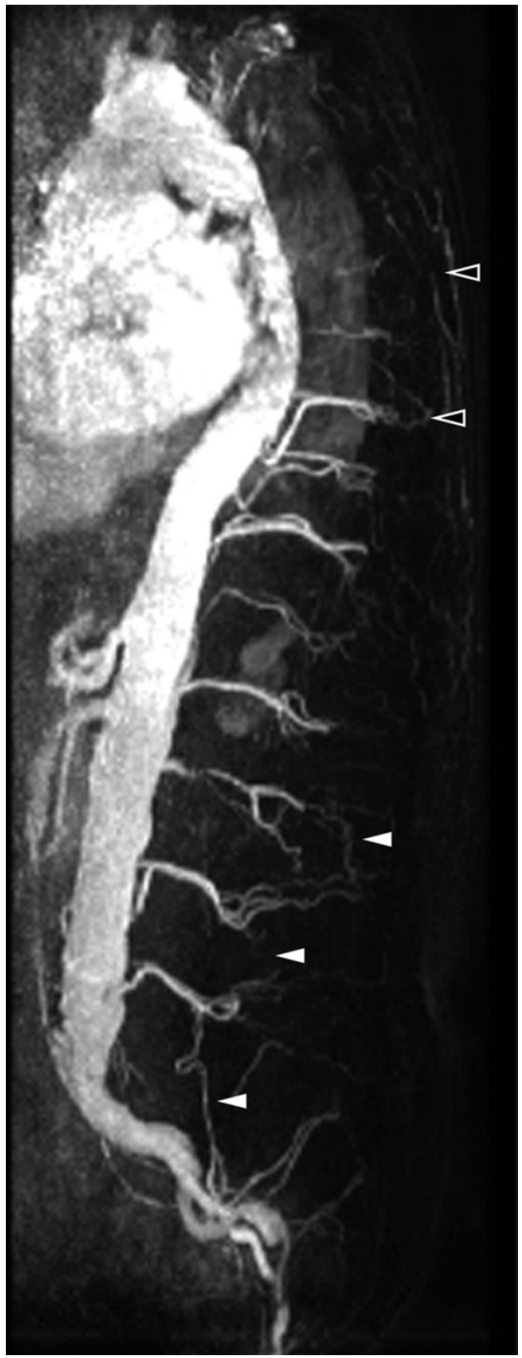

Backes WH, Nijenhuis RJ, Mess WH, Wilmink FA, Schurink GW, and Jacobs MJ. Magnetic resonance angiography of collateral blood supply to spinal cord in thoracic and thoracoabdominal aortic aneurysm patients. *Journal of vascular surgery : official publication, the Society for Vascular Surgery [and] International Society for Cardiovascular Surgery, North American Chapter* 48: 261-271, 2008.

Spinal cord gross anatomy

Section of lumbar spinal cord. The dura-arachnoid has been removed to expose pial and root sheath surfaces. Dorsal **(DR)** and ventral **(VR)** nerve roots have been cut proximal to their exit through the duraarachnoid. **A** denticulate ligament **(DL)** extends along the lateral side of the cord. Arteries **(A)** and veins **(V)** lie on the pial surface. x ***28.***

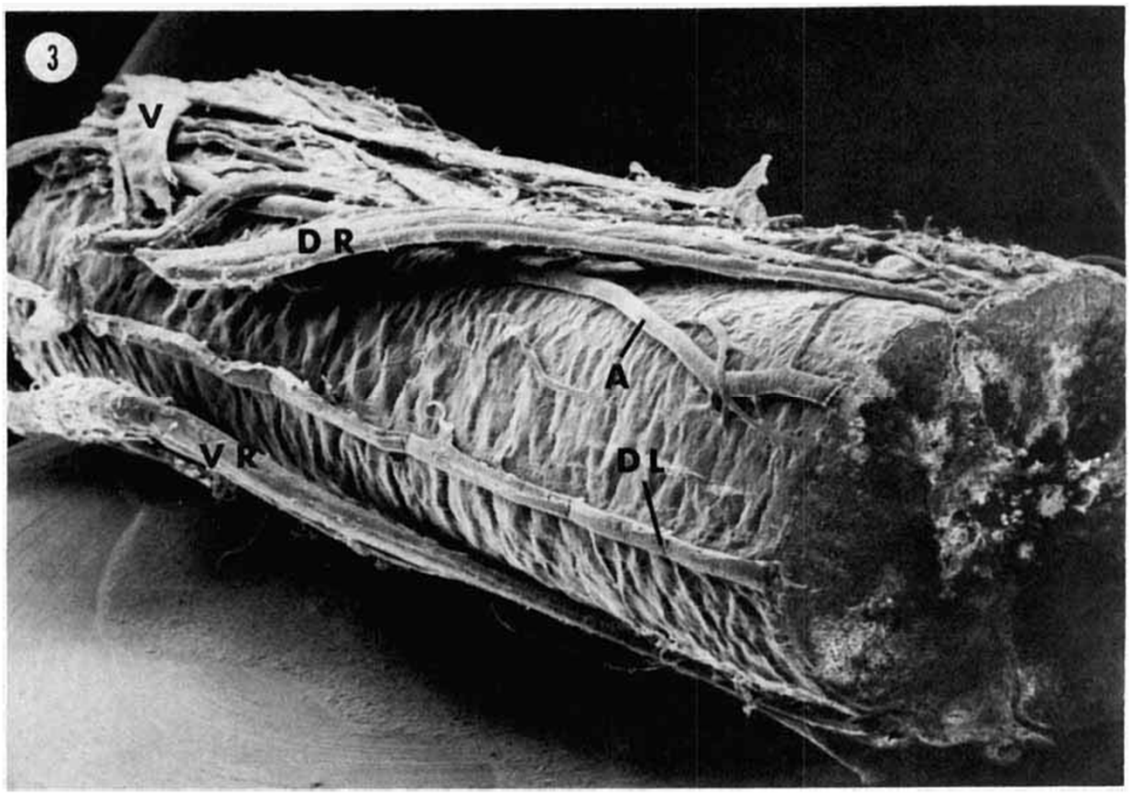

(3) Cloyd, M. W. and F. N. Low (1974). "Scanning electron microscopy of the subarachnoid space in the dog. I. Spinal cord levels." The Journal of comparative neurology **153**(4): 325-368.

Spinal cord microstructure at conus

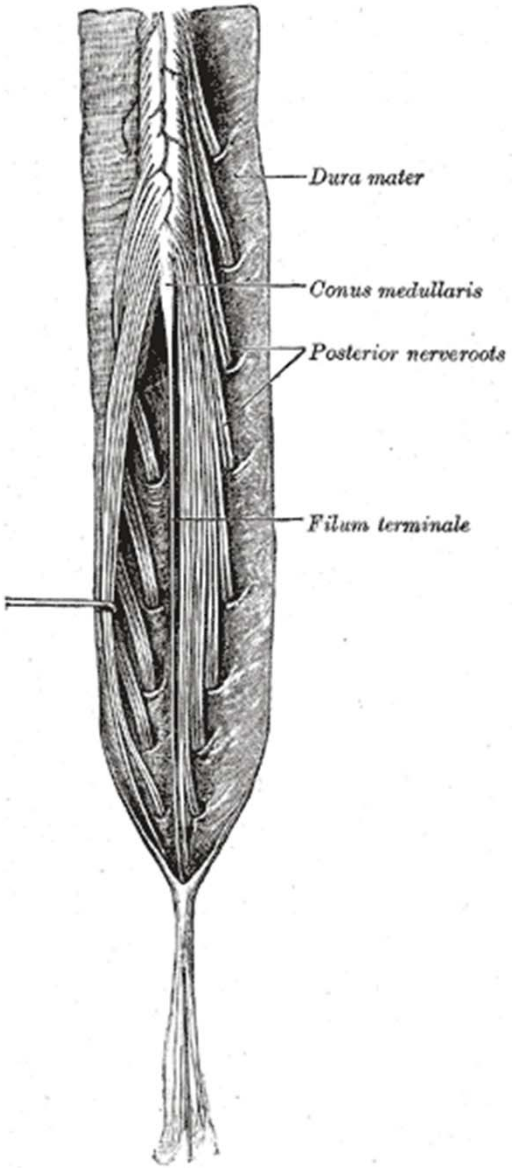

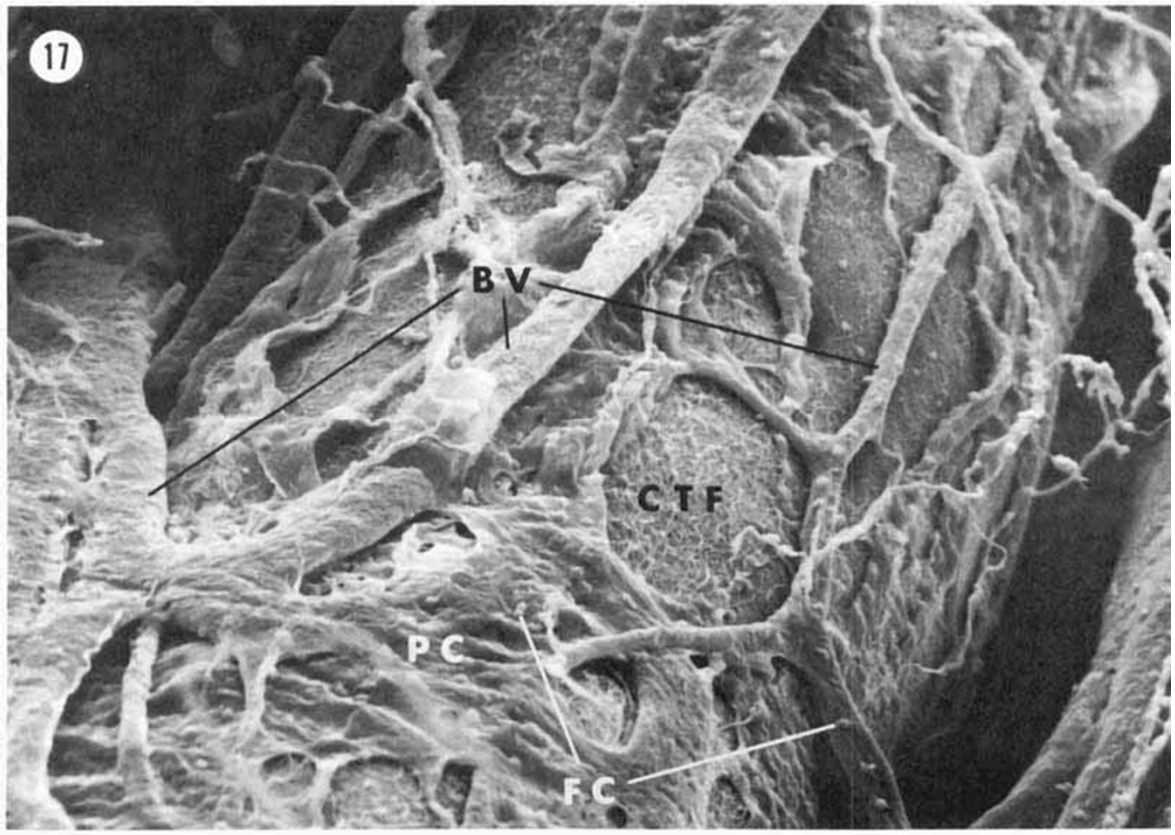

Spinal pia at the conus medullaris region. Here the cellular layer of the pia (PC) is highly fenestrated. Large areas lack **a** surface cellular layer, with the result **that** connective tissue fibers (CTF) are exposed to the subarachnoid space. A network of blood vessels (BV) is intimately associated with the pia mater. Free cells (FC) can be observed. x 140.

(3) Cloyd, M. W. and F. N. Low (1974). "Scanning electron microscopy of the subarachnoid space in the dog. I. Spinal cord levels." The Journal of comparative neurology **153**(4): 325-368.

Perivascular spaces

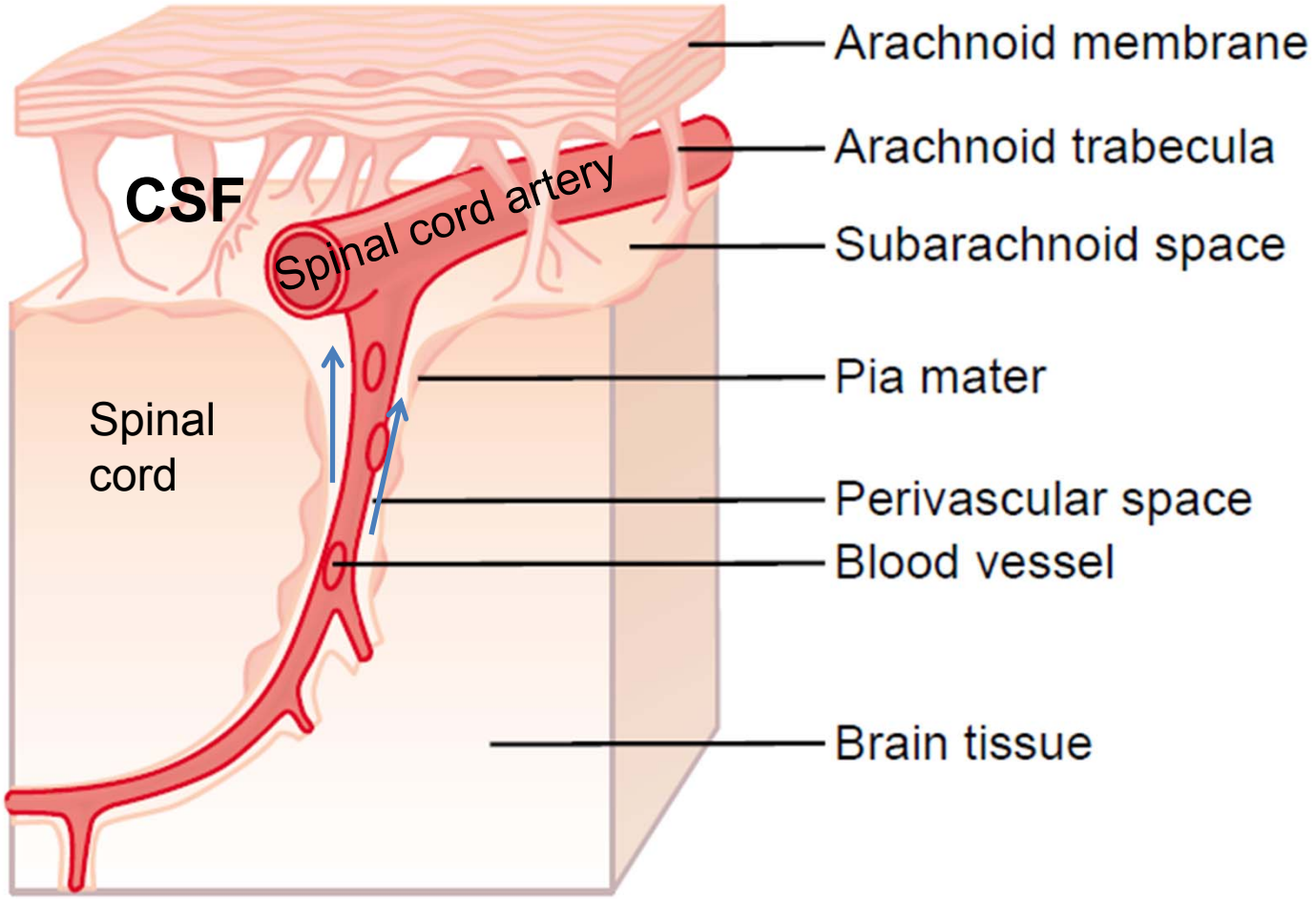

- Spinal cord perivascular spaces are a “specialized lymphatic system” (Guyton et al.)

Guyton, A. C. and J. E. Hall (2006). Textbook of medical physiology. Philadelphia, Elsevier Saunders.

Arterioles entering spinal cord

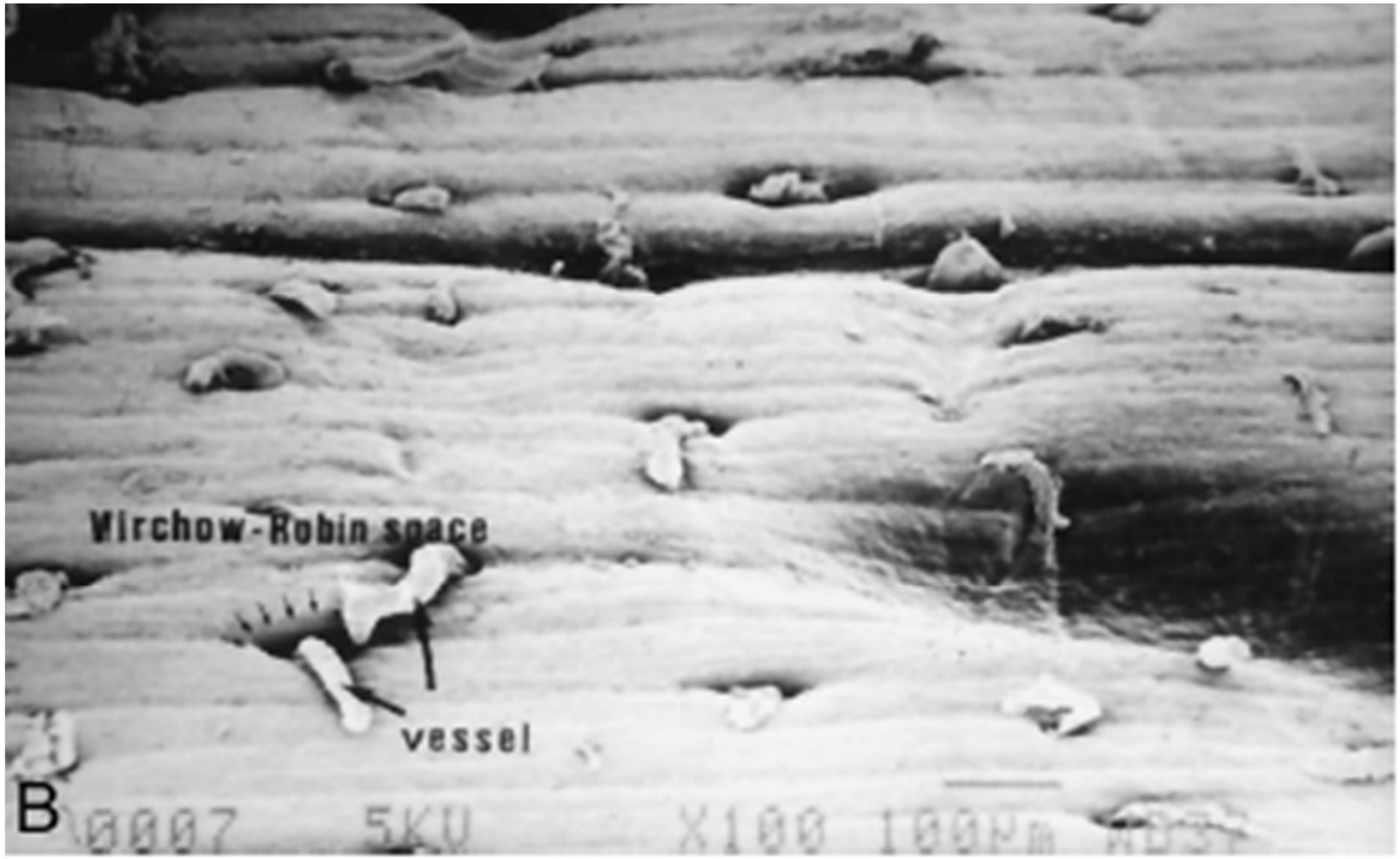

Yoshizawa, H. (2002). "Presidential address: pathomechanism of myelopathy and radiculopathy from the viewpoint of blood flow and cerebrospinal fluid flow including a short historical review." Spine (Phila Pa 1976) **27**(12): 1255-63.

Arterioles entering brain surface

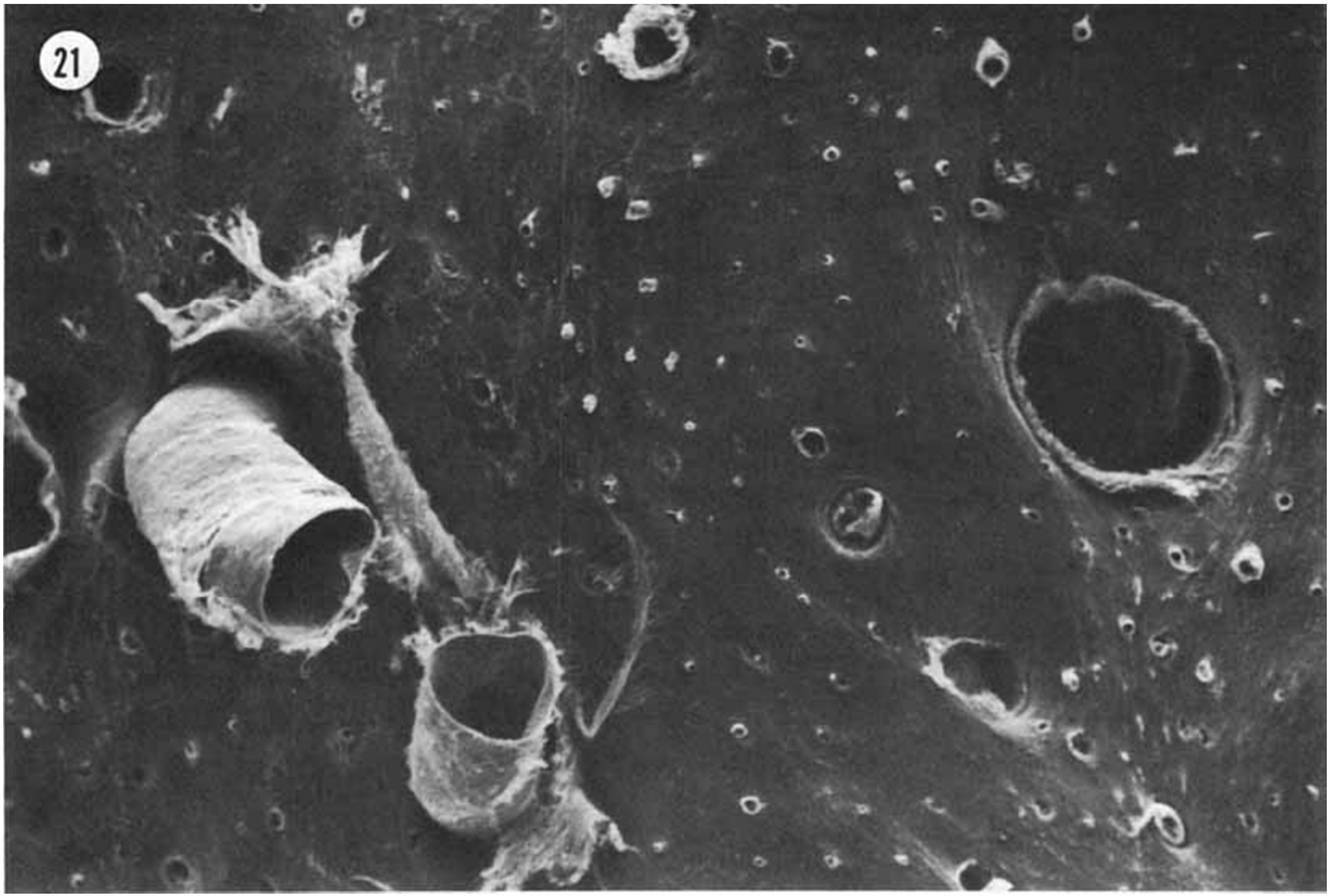

Allen, D. J. and F. N. Low (1975). "Scanning electron microscopy of the subarachnoid space in the dog. III. Cranial levels." The Journal of comparative neurology **161**(4): 515-539.

Spinal cord perivascular space (detailed)

"…the subpial space and the perivascular space communicate with the subarachnoid space via the fenestrae of the superficial layer of the pia mater. When horseradish peroxidase is injected into the subarachnoid space, it infiltrates gradually from the surface into the spinal cord over time from a few minutes to 1 hour, but reaches the interior of the spinal cord rapidly through the perivascular spaces." (Yoshizawa 2002)

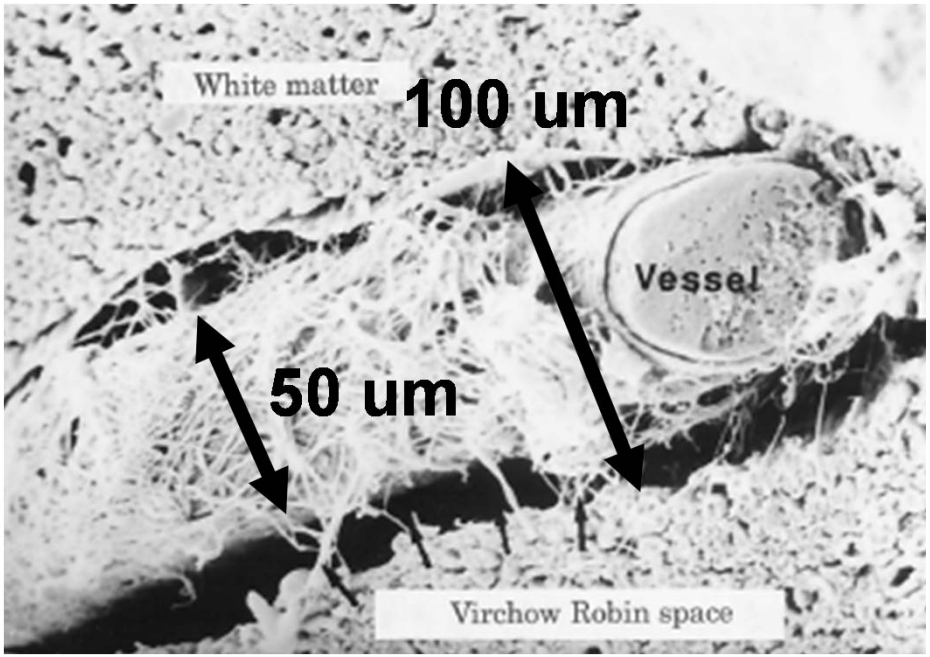

Yoshizawa, H. (2002). "Presidential address: pathomechanism of myelopathy and radiculopathy from the viewpoint of blood flow and cerebrospinal fluid flow including a short historical review." Spine (Phila Pa 1976) **27**(12): 1255-63.

Pia matter fenestration

Fenestration in spinal pia mater. Fenestrations of various sizes are common in the pial surface. This moderate sized fenestration results from a lack of surface pial cells. Pial connective tissue fibrils are revealed through the fenestration. The fibers are of various diameters and most appear to be arranged in the same direction. The smallest fibers are more random in arrangement. The edge of the fenestration **is** thickened (large arrow). The edges **of** flat pial cells (small arrows), and numerous microvilli can be observed. x 1,400. (Cloyd)

Interstitial brain fluid and CSF are nearly homogenous in composition due to the permeability of the pia mater (Guyton)

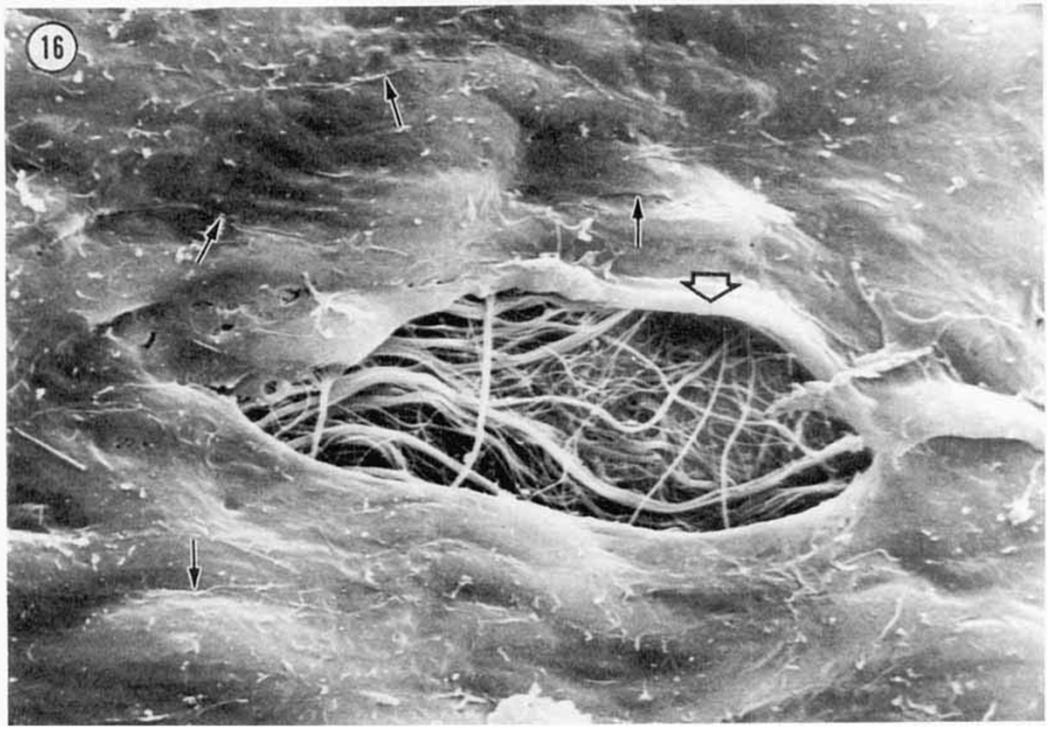

(3) Cloyd, M. W. and F. N. Low (1974). "Scanning electron microscopy of the subarachnoid space in the dog. I. Spinal cord levels." The Journal of comparative neurology **153**(4): 325-368.

Pia mater microstructure

View of transected spinal pia mater. The cut end of spinal cord (SPC) and its pia mater (PM) illustrates the arrangement of pial connective tissue fibers. There appear to be two layer of fibers. The first is a surface lamella (large arrows) which is covered by a smooth cellular lining facing the subarachnoid space. This delicate cellular lining is easily lacerated during preparation (small arrow). The connective tissue fibers in the surface lamella appear closely packed and are arranged longitudinal to the axis of the spinal cord. The second layer of connective tissue fibers lies deeper in the pial connective tissue space and is considerably thicker. The fibers of this layer for the most part either run longitudinal or circumferential to the cord. Some fibers are grouped into large bundles. x 320.

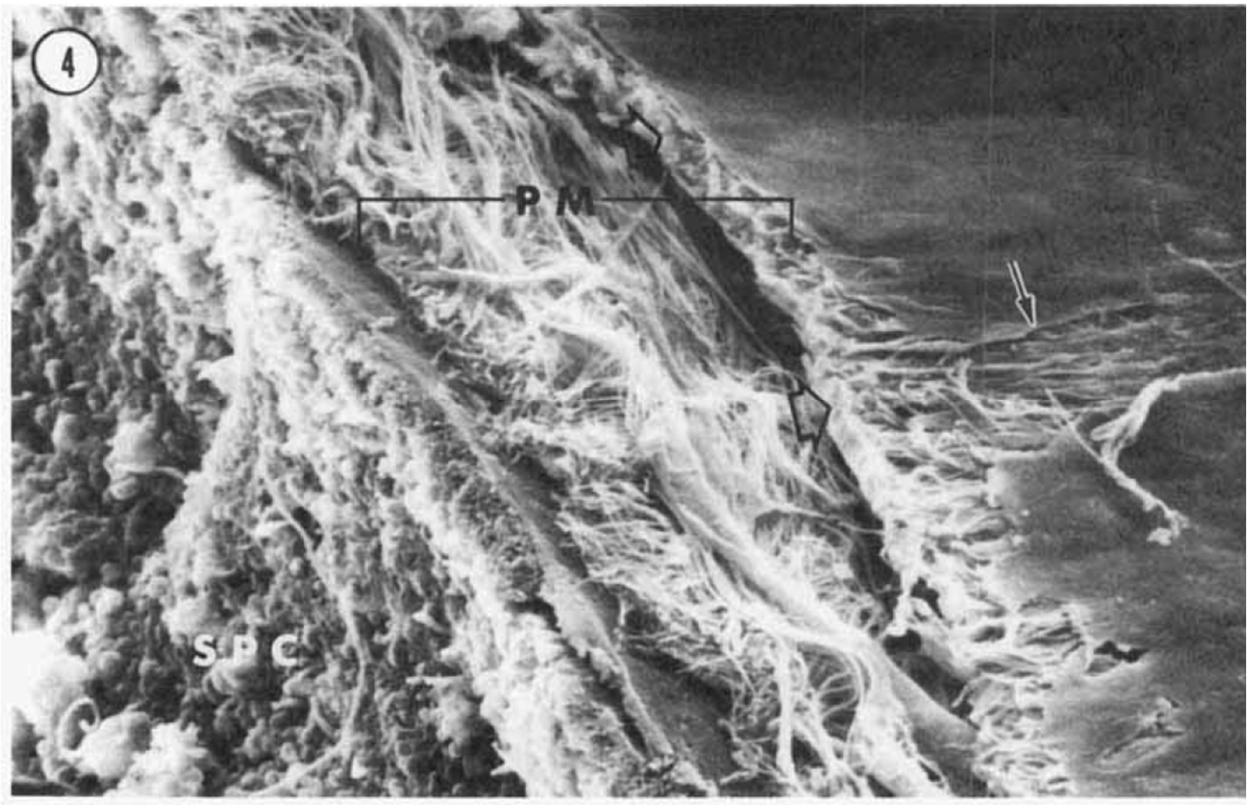

(3) Cloyd, M. W. and F. N. Low (1974). "Scanning electron microscopy of the subarachnoid space in the dog. I. Spinal cord levels." The Journal of comparative neurology **153**(4): 325-368.

Human Subarachnoid Space (SAS)

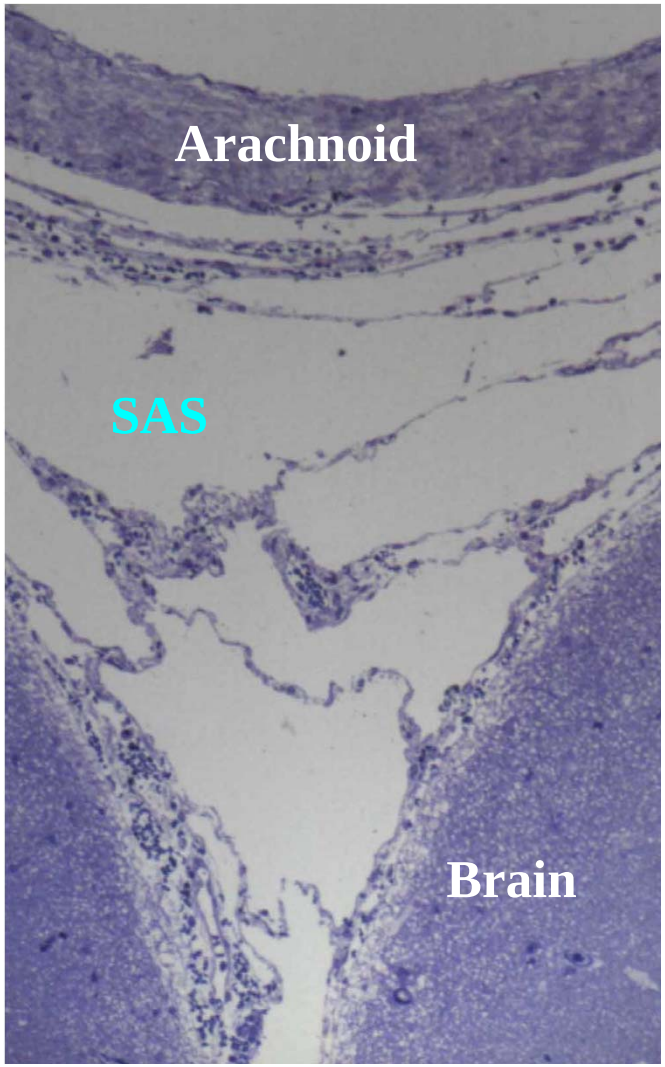

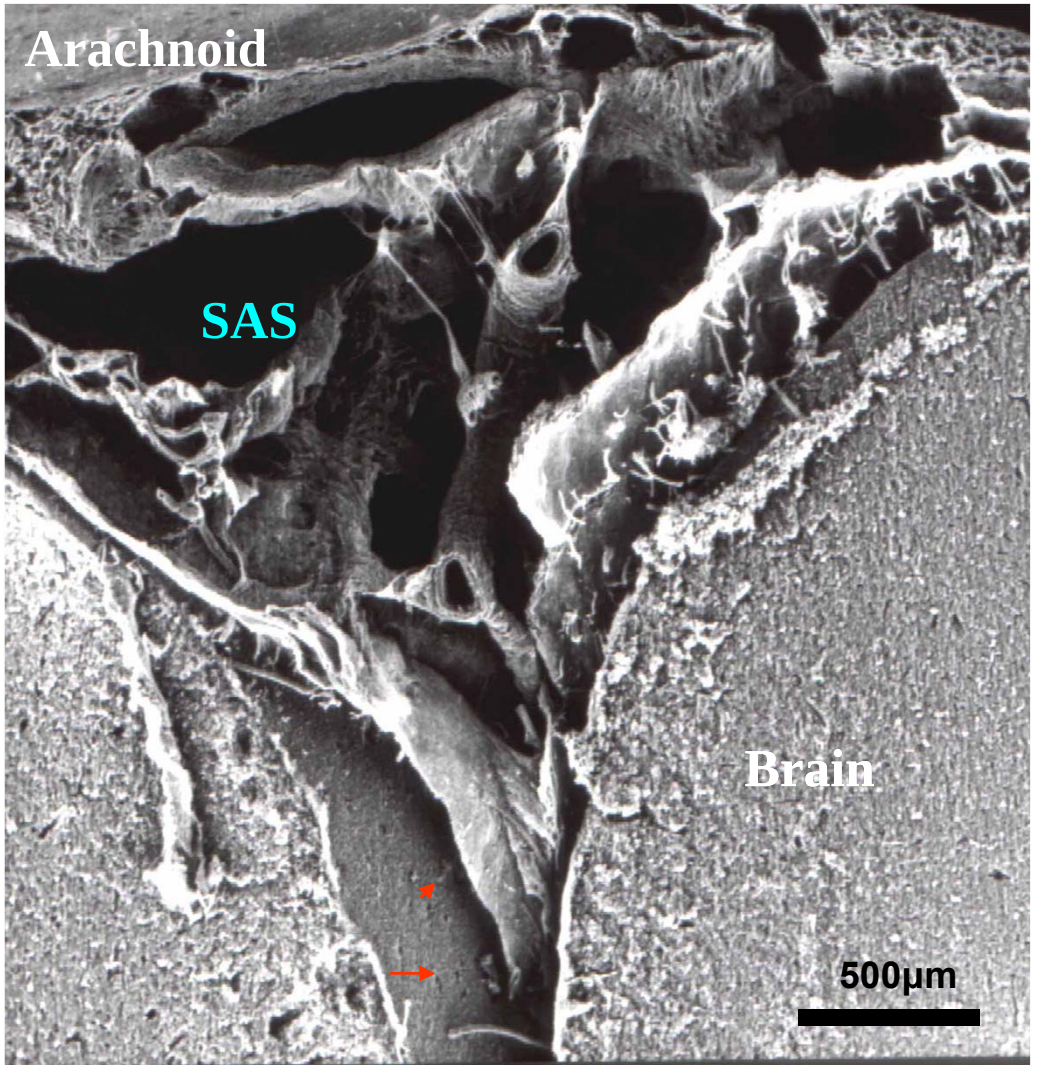

Figure from: Margaret Hutchings

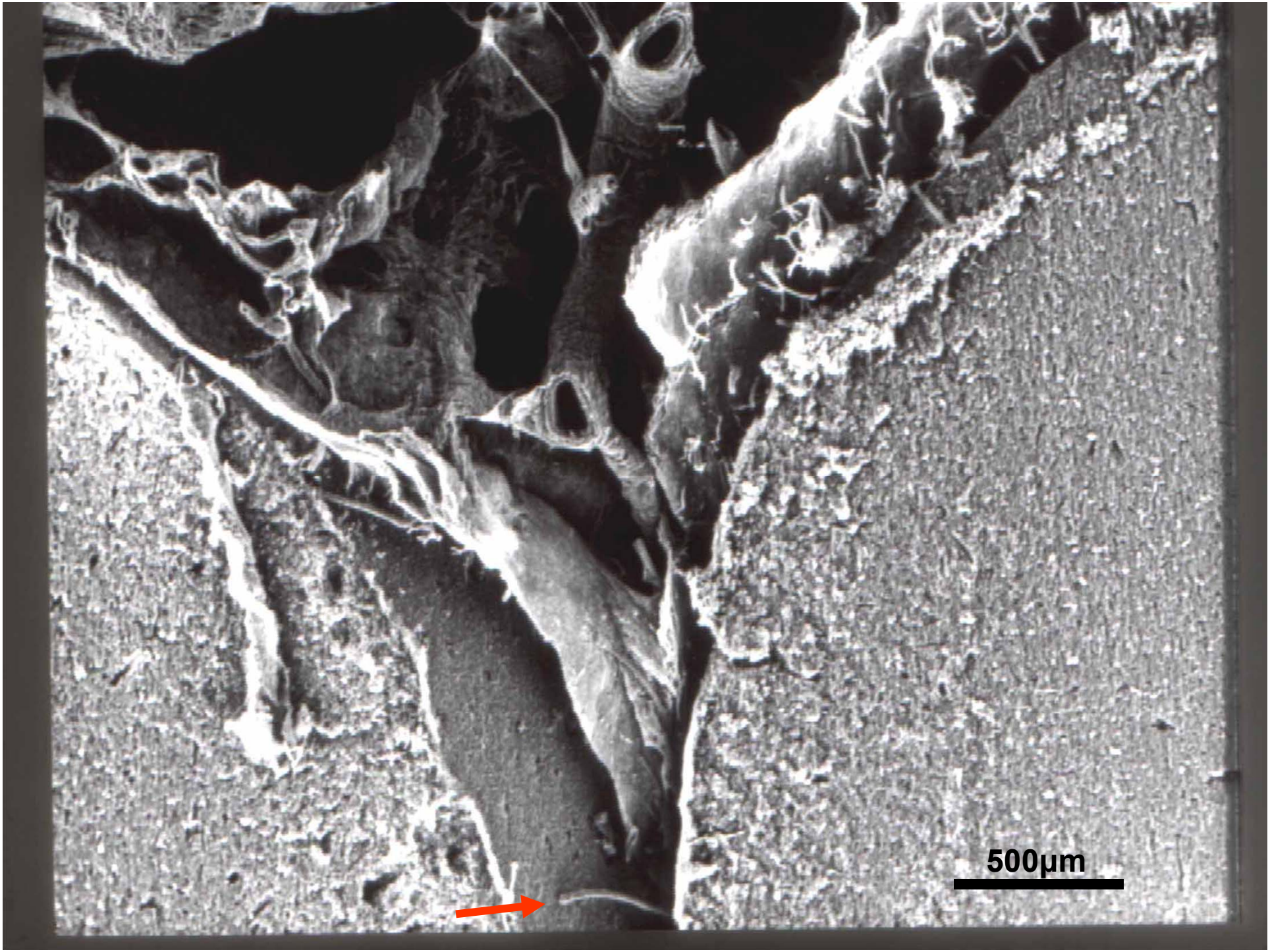
500µm

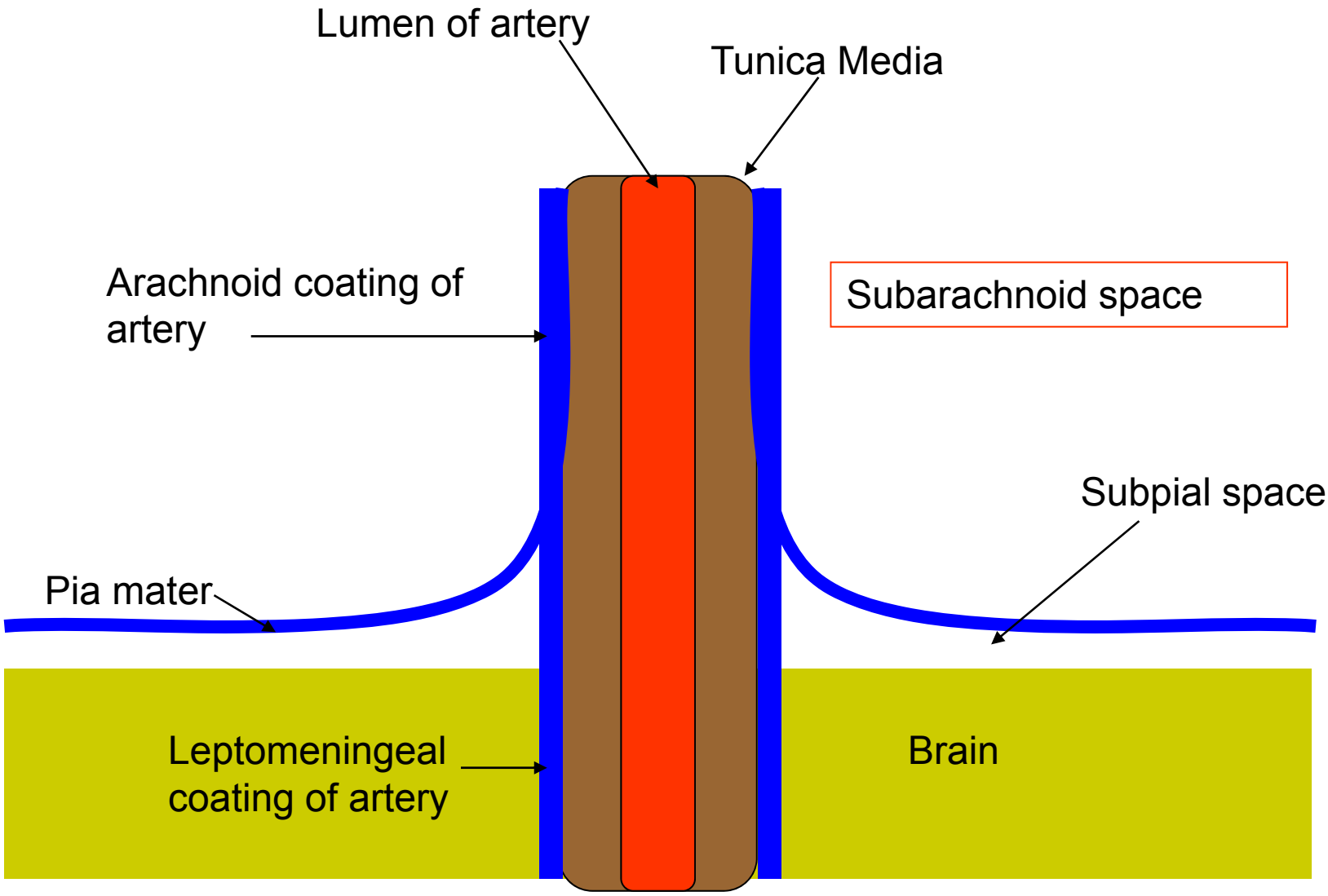

Arrangements of the Leptomeninges at the surface of the cerebral cortex (Hutchings and Weller 1986)(Zhang and Weller 1990)

Hutchings M, and Weller RO. Anatomical relationships of the pia mater to cerebral blood vessels in man. *Journal of Neurosurgery* 65: 316-325, 1986.

Zhang ET, Inman CB, and Weller RO. Interrelationships of the pia mater and the perivascular (Virchow-Robin) spaces in the human cerebrum. *J Anat* 170: 111-123, 1990.

Meninges (layers) of the CNS

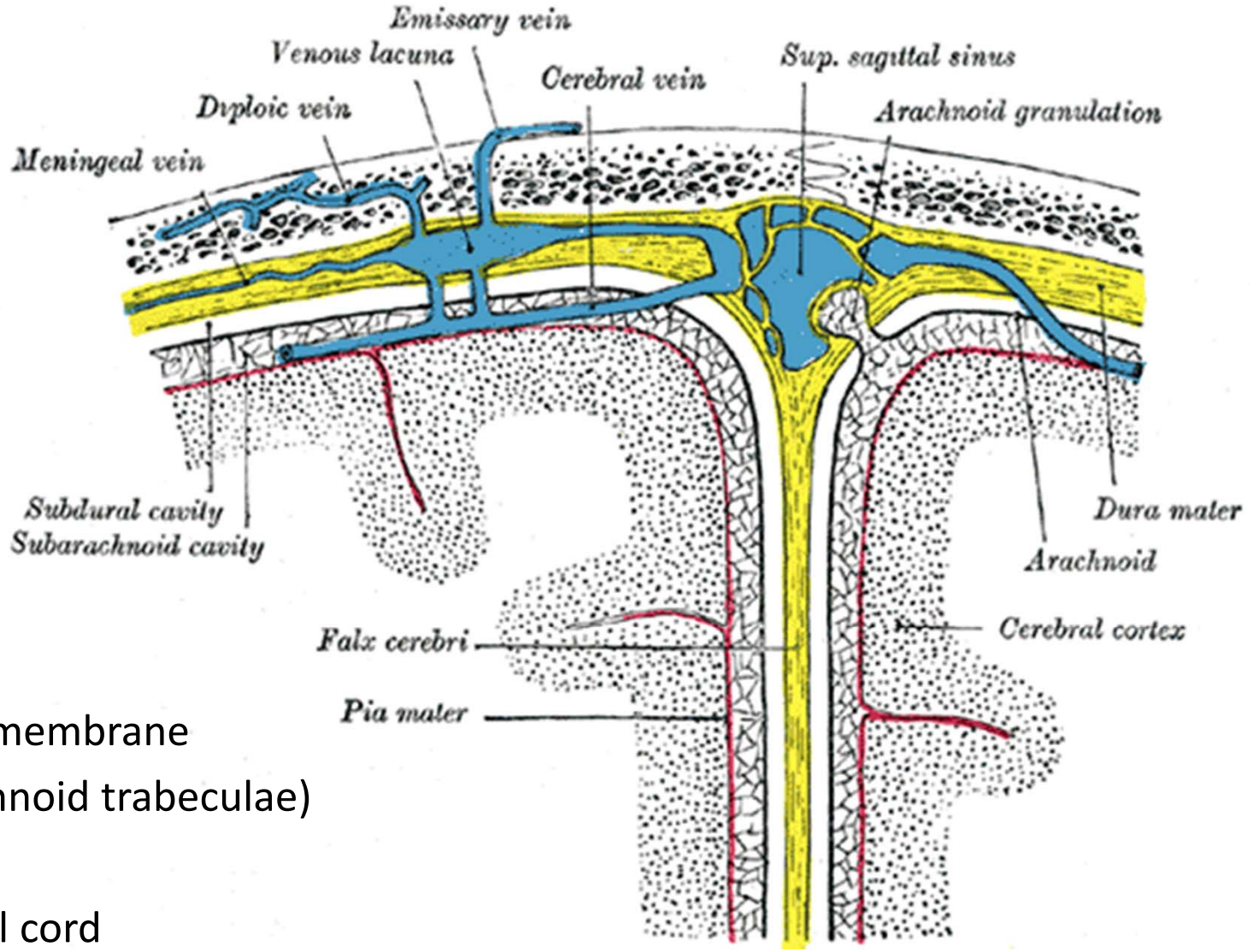

Outer to inner:

1. Skull
2. Dura mater
3. Arachnoid membrane
4. (CSF / arachnoid trabeculae)
5. Pia mater
6. Brain/spinal cord

Cranial meninges and subarachnoid space

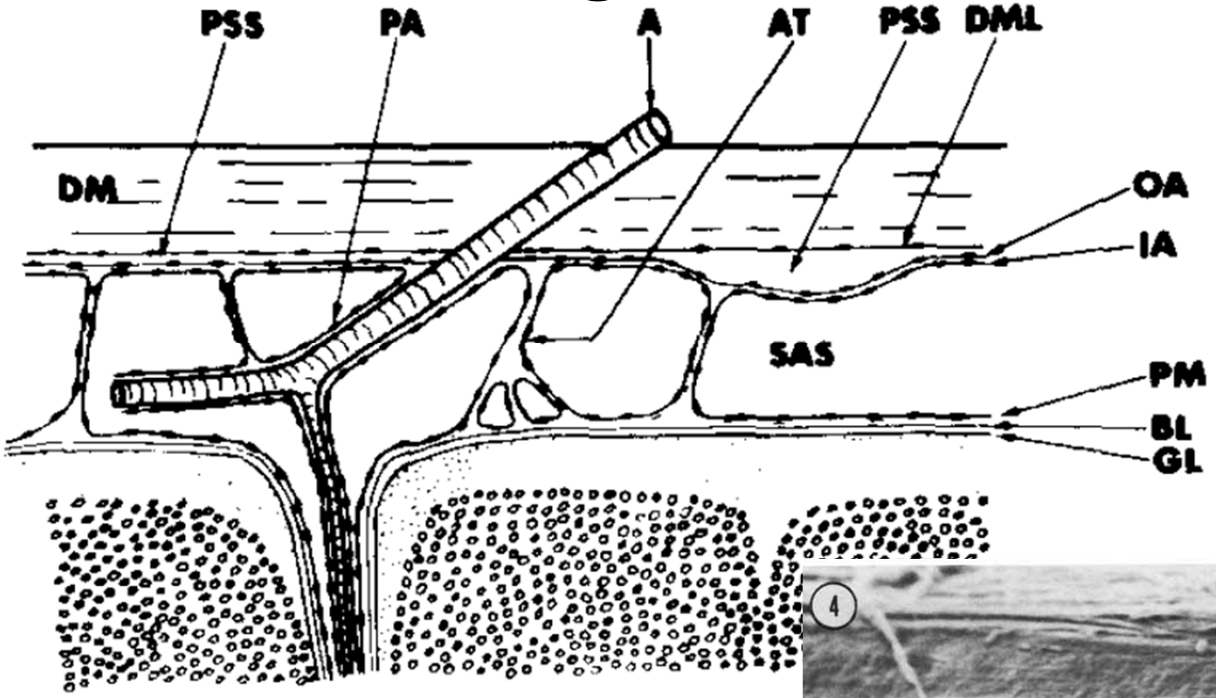

PSS, potential subdural space
DM, dura mater
PA, pia-arachnoid / leptomeninges
A, blood vessels
AT, arachnoid trabeculae
DML, inner suface of dura mater
OA, outer arachnoid (facing dura mater
IA, inner arachnoid (facing subarachnoid space
PM, pia mater
BL, basal lamina
GL, glia limitans

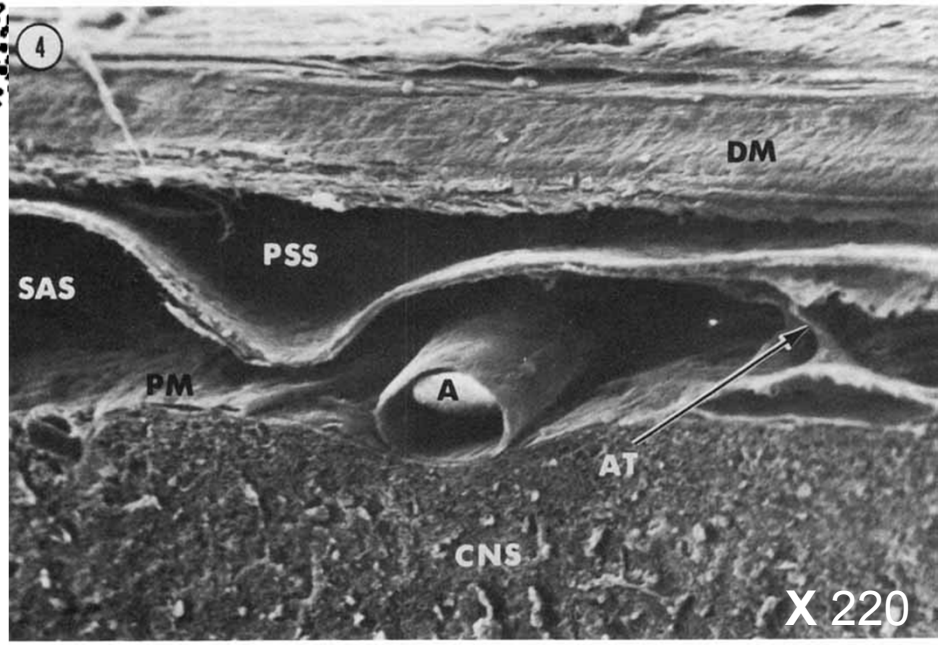

Allen, D. J. and F. N. Low (1975). "Scanning electron microscopy of the subarachnoid space in the dog. III. Cranial levels." The Journal of comparative neurology **161**(4): 515-539.

Brain and spinal cord anatomy

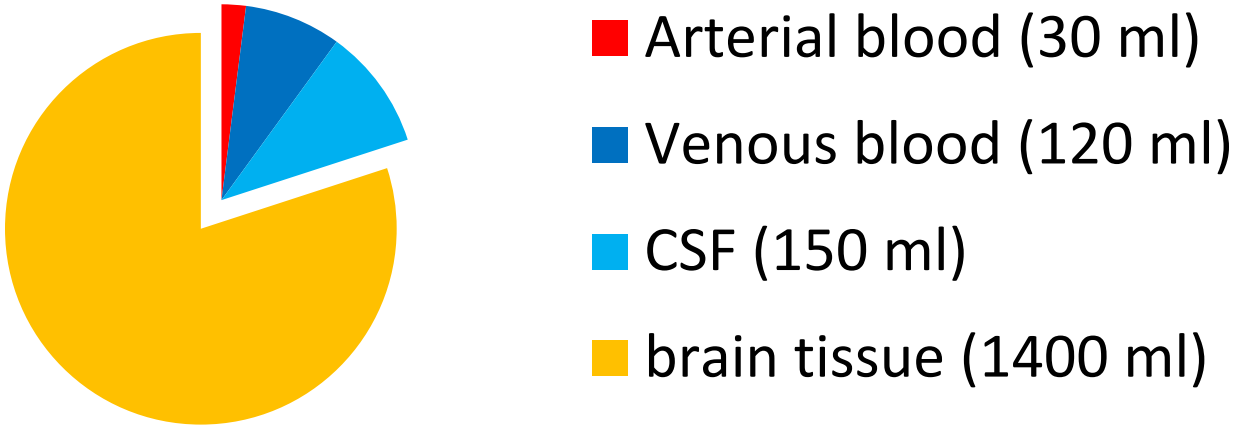

The brain has highly complex mechanical properties

- Anisotropic white matter
- Isotropic grey matter
- Viscoelastic throughout
- Shear modulus *10-10,000* Pa (lower in white)
- Porous (Nicholson)
  - 10x smaller in direction of fibers

Nicholson, C. and E. Syková (1998). "Extracellular space structure revealed by diffusion analysis." Trends in Neurosciences **21**(5): 207-215.
Pierpaoli, C. and P. J. Basser (1996). "Toward a quantitative assessment of diffusion anisotropy." Magnetic Resonance in Medicine **36**(6): 893-906.

Fiber tract geometry

- ~ 15% fiber undulation results in a complex non-linear elasticity

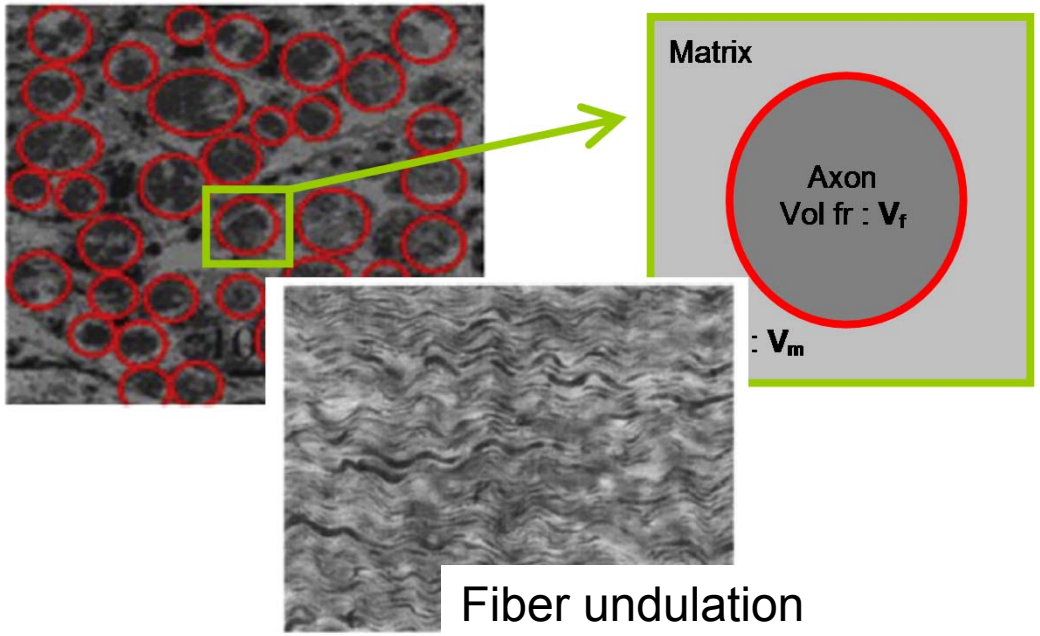

Bain, A. C., D. I. Shreiber, et al. (2003). "Modeling of Microstructural Kinematics During Simple Elongation of Central Nervous System Tissue." Journal of Biomechanical Engineering **125**(6): 798-804.
Karami, G., N. Grundman, et al. (2009). "A micromechanical hyperelastic modeling of brain white matter under large deformation." Journal of the Mechanical Behavior of Biomedical Materials **2**(3): 243-254.

Effect of fiber undulation could be to make two separate elasticity regimes

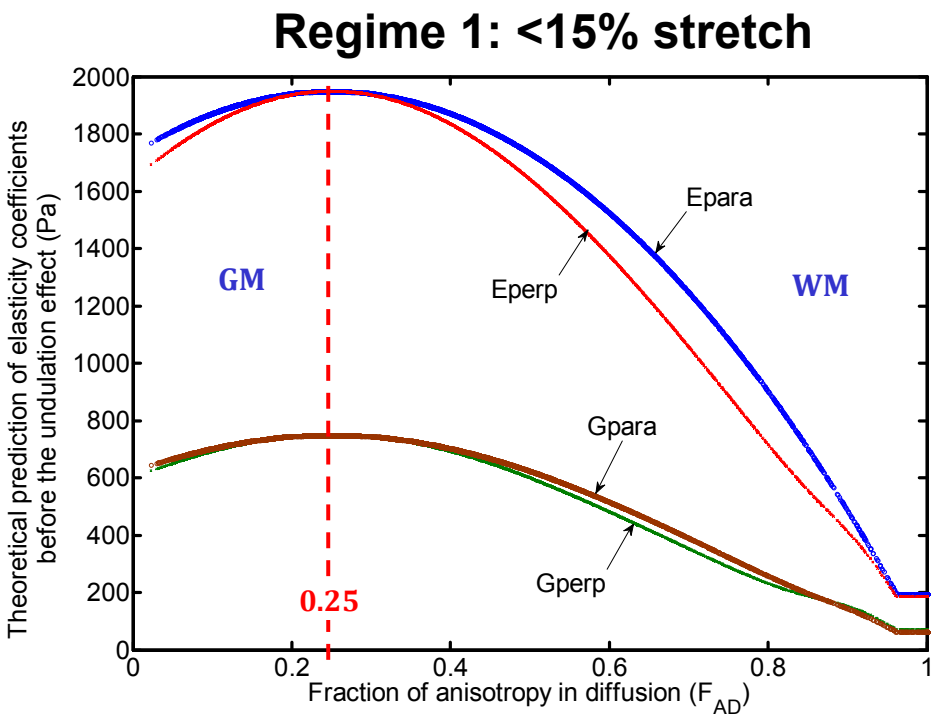

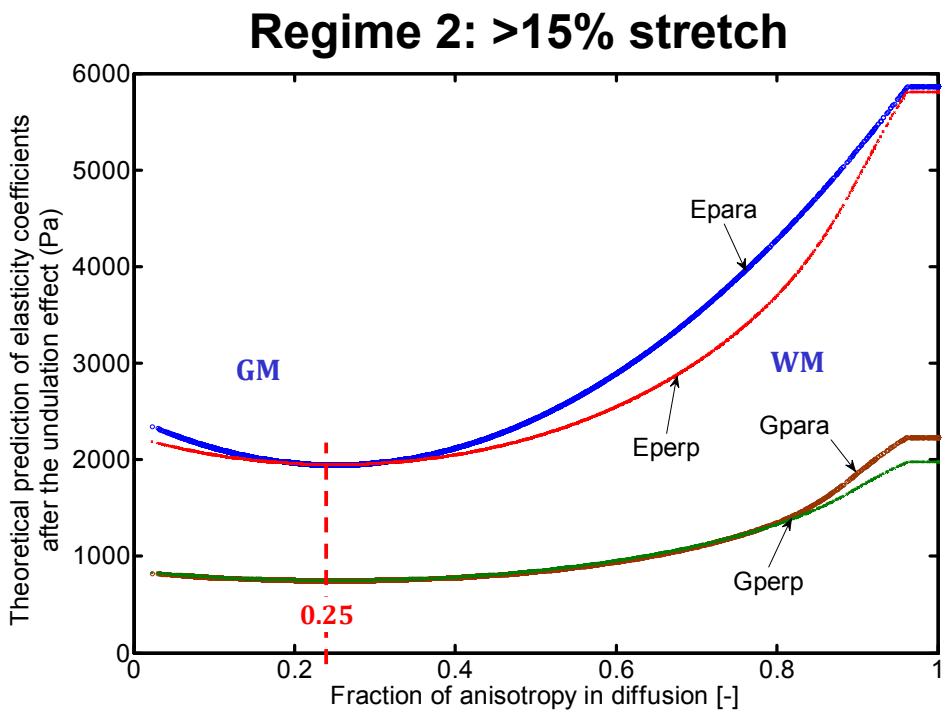

Unpublished, K. Shahim, Bryn A. Martin, J.-M. Drezet, R. Sinkus, J.-F. Molinari, S. Momjian, "Evolution of brain parenchyma elastic properties in the development of normal pressure hydrocephalus," (submitted, January 2011).

Spinal cord nerve roots

- Various types in different regions of the SC

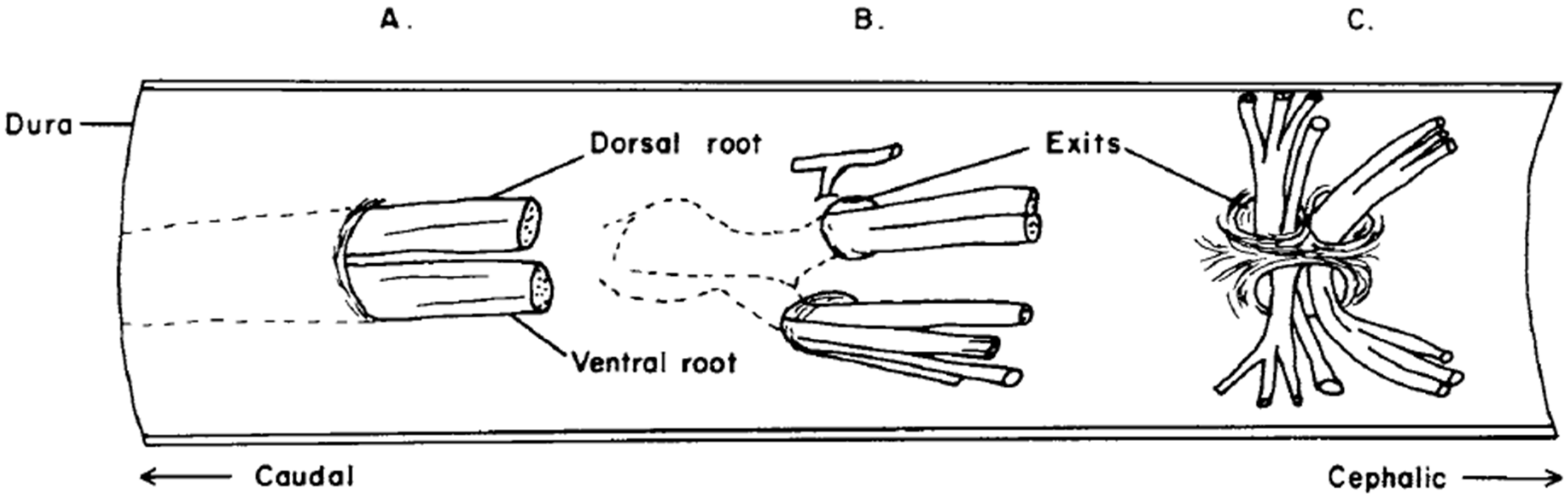

Fig. 1 *Nerve root exits.* A is a single exit of the type found in lower lumbar and sacral levels. B is a typical double exit from the thoracic region and C a more complicated type from the lower cervical region. Drawn from laboratory observations.

Malloy, J. J. and F. N. Low (1974). "Scanning electron microscopy of the subarachnoid space in the dog. II. Spinal nerve exits." The Journal of comparative neurology **157**(1): 87-107.

Spinal cord nerve roots

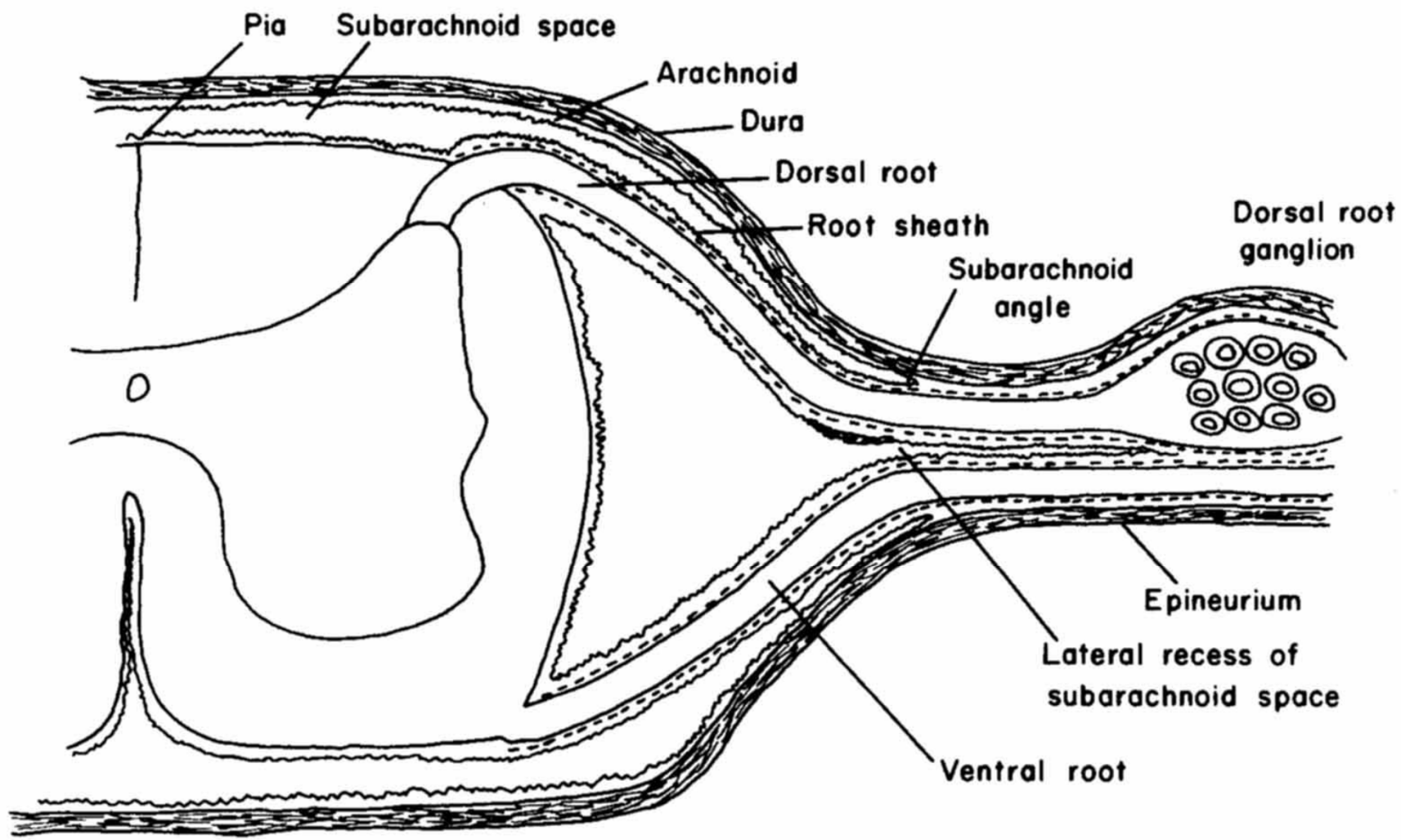

Figure redrawn and modified from McCabe and Low ('69) and Himango and Low ('71) by: Malloy, J. J. and F. N. Low (1974). "Scanning electron microscopy of the subarachnoid space in the dog. II. Spinal nerve exits." The Journal of comparative neurology **157**(1): 87-107.

Nerve root anatomy

The dorsal root **(DR)** and ventral root **(VR)** converge on one another and pass through the dura-arachnoid **(DA)** by means of a single exit. The cerebrospinal artery **(A)** enters the subarachnoid space cephalic to the ventral root. An attachment **of** the denticulate ligament **(DL)** is located caudally and is slightly dorsal to the nerve exit. Numerous arachnoid trabeculae (arrows) can be seen in this **35** mm light micrograph. x **15.**

Cervical nerve root

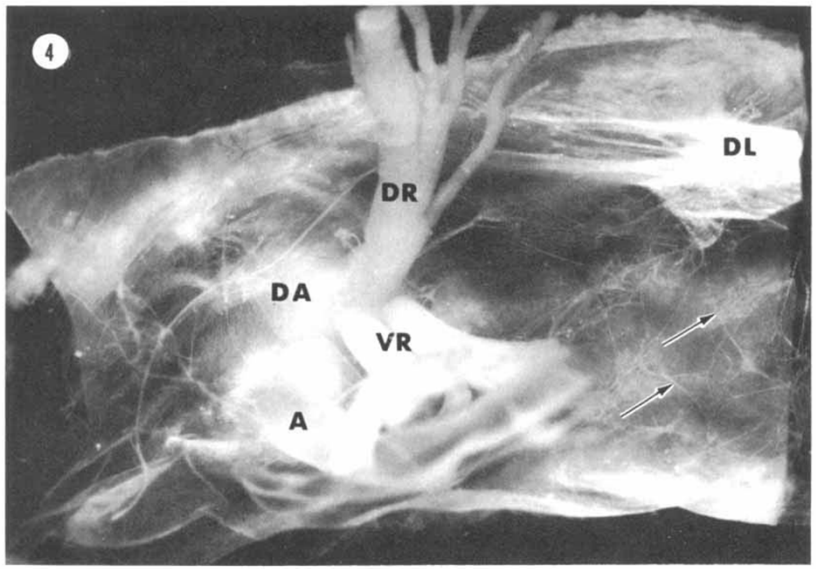

Lumbar nerve root

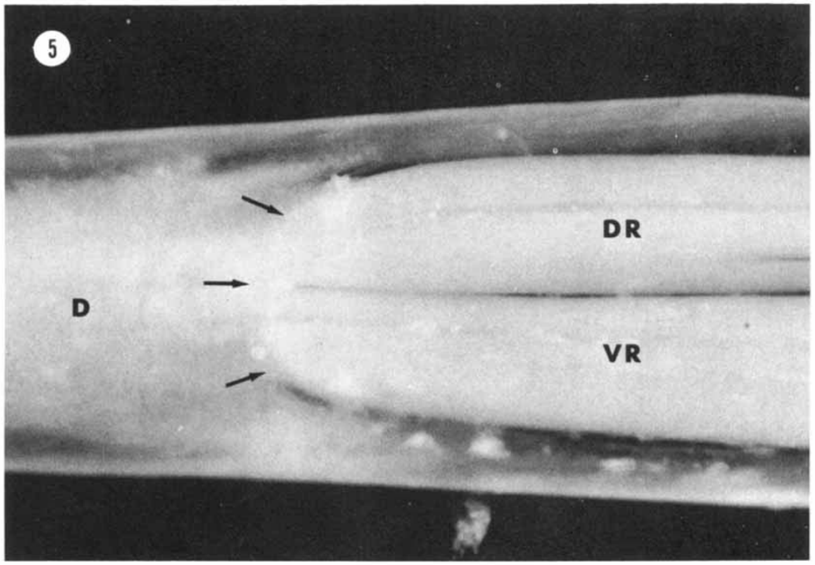

Malloy, J. J. and F. N. Low (1974). "Scanning electron microscopy of the subarachnoid space in the dog. II. Spinal nerve exits." The Journal of comparative neurology **157**(1): 87-107.

More on nerve roots

Cervical multiple exit nerve root

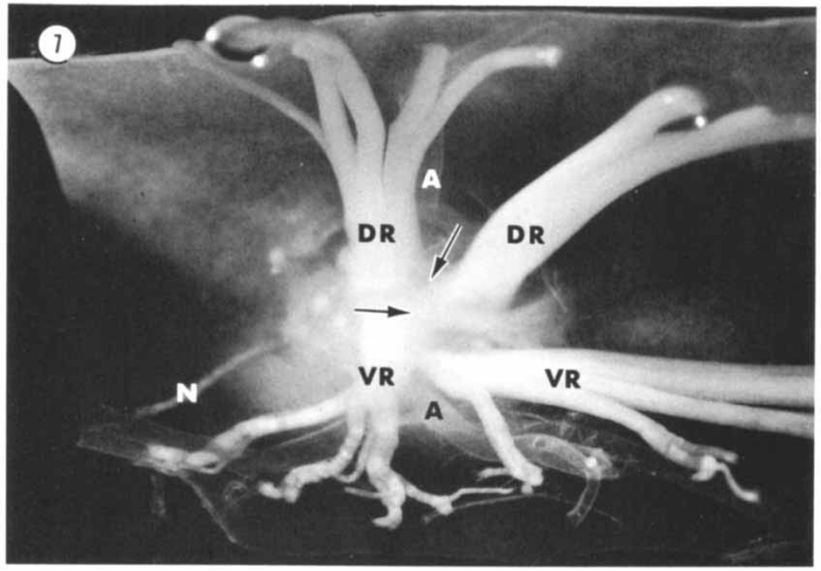

Lumbar double nerve root

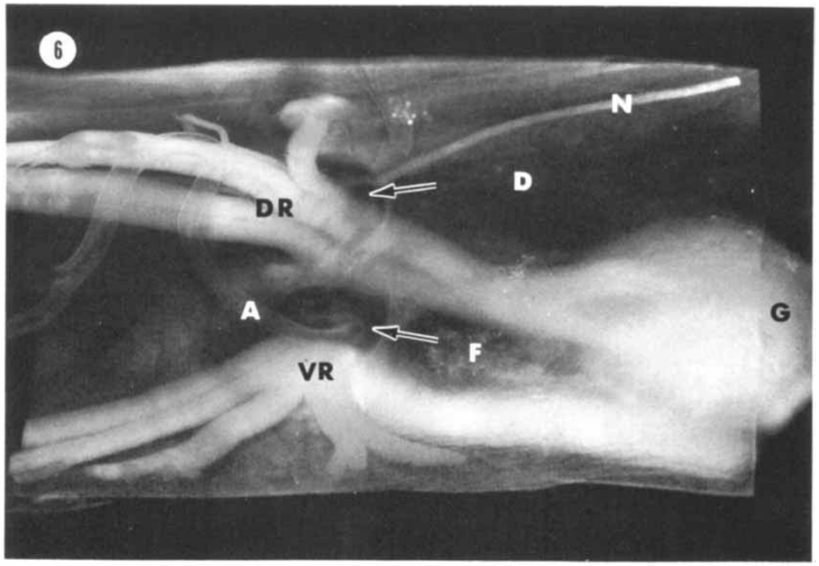

Malloy, J. J. and F. N. Low (1974). "Scanning electron microscopy of the subarachnoid space in the dog. II. Spinal nerve exits." The Journal of comparative neurology **157**(1): 87-107.

Current areas of research in neurohydrodynamics

Craniospinal disorders: Chiari malformation

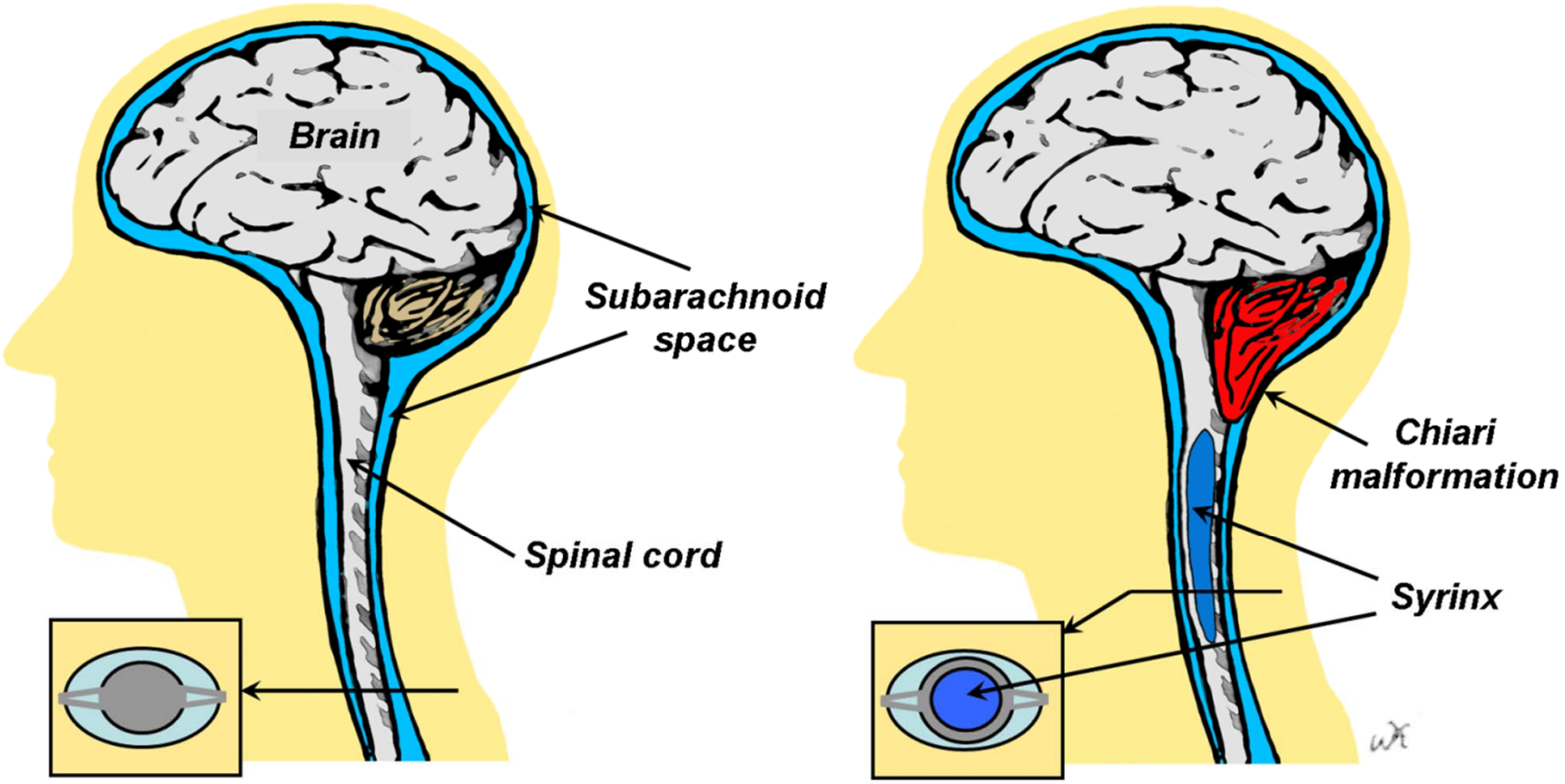

Shaffer, N., Martin, B., and Loth, F., 2011, "Cerebrospinal fluid hydrodynamics in type I Chiari malformation," Neurological research, 33(3), pp. 247-260.

Type I Chiari Malformation (CMI)

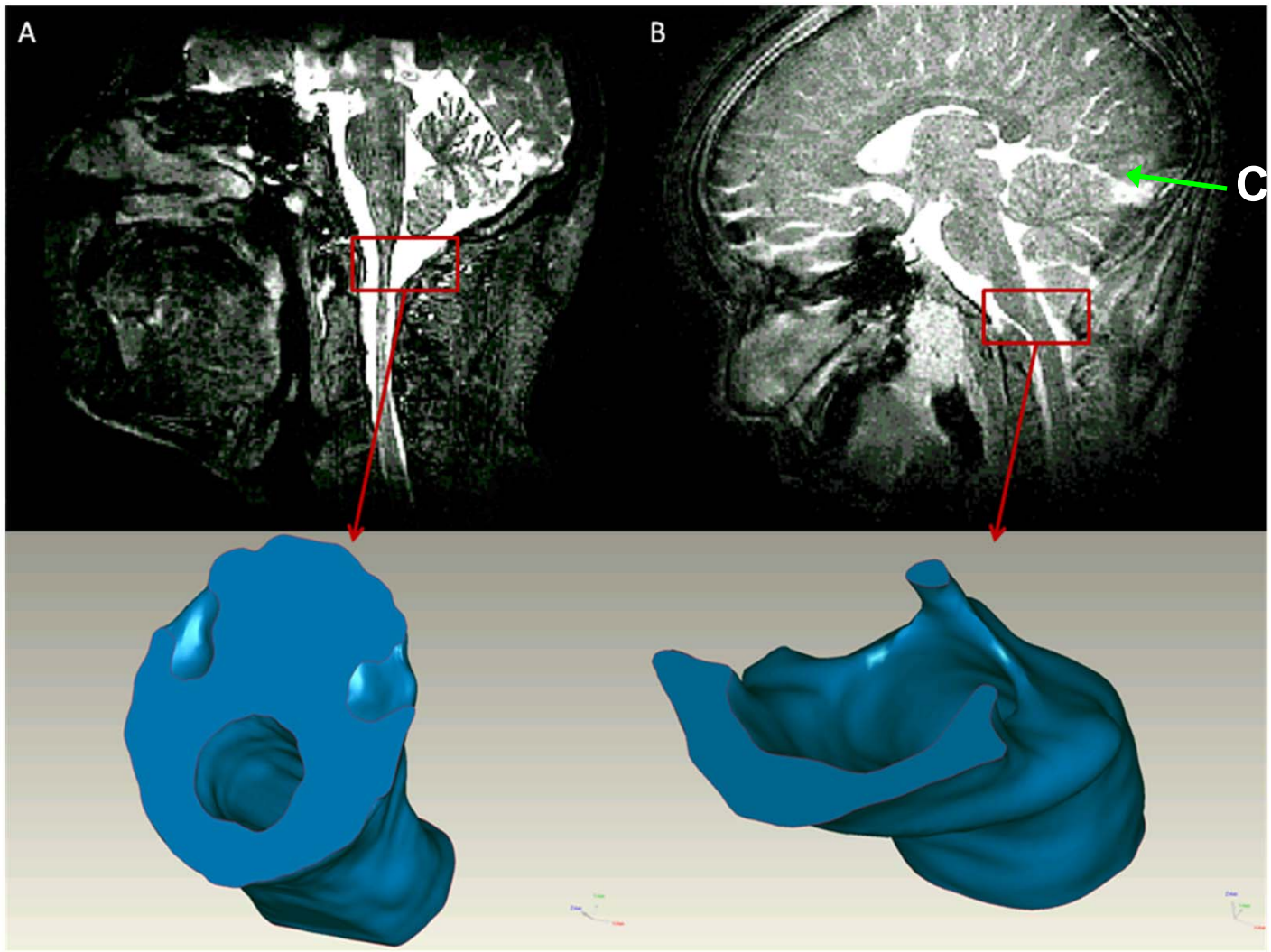

A: Healthy Subject **B: Subject with Symptomatic CMI**

Figure courtesy of Francis Loth and Nicolas Schaffer, University of Akron, OH

Could flow resistance through the craniospinal junction be an indicator of **Chiari "0"**

- Higher CSF flow resistance in Chiari patients?

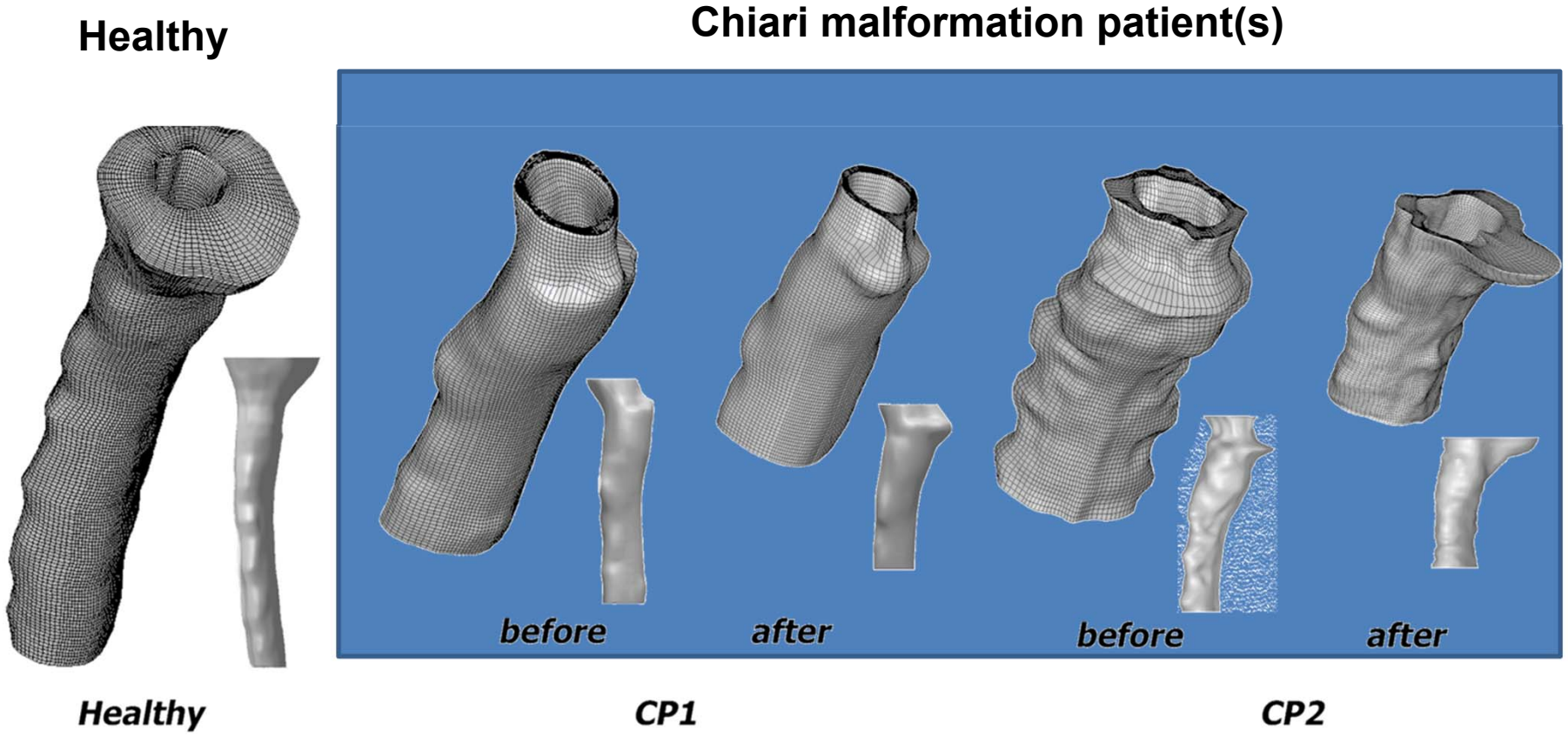

Image courtesy of Dr. Francis Loth, University of Akron, Biofluids Laboratory

Successful decompression surgery decreases flow resistance?

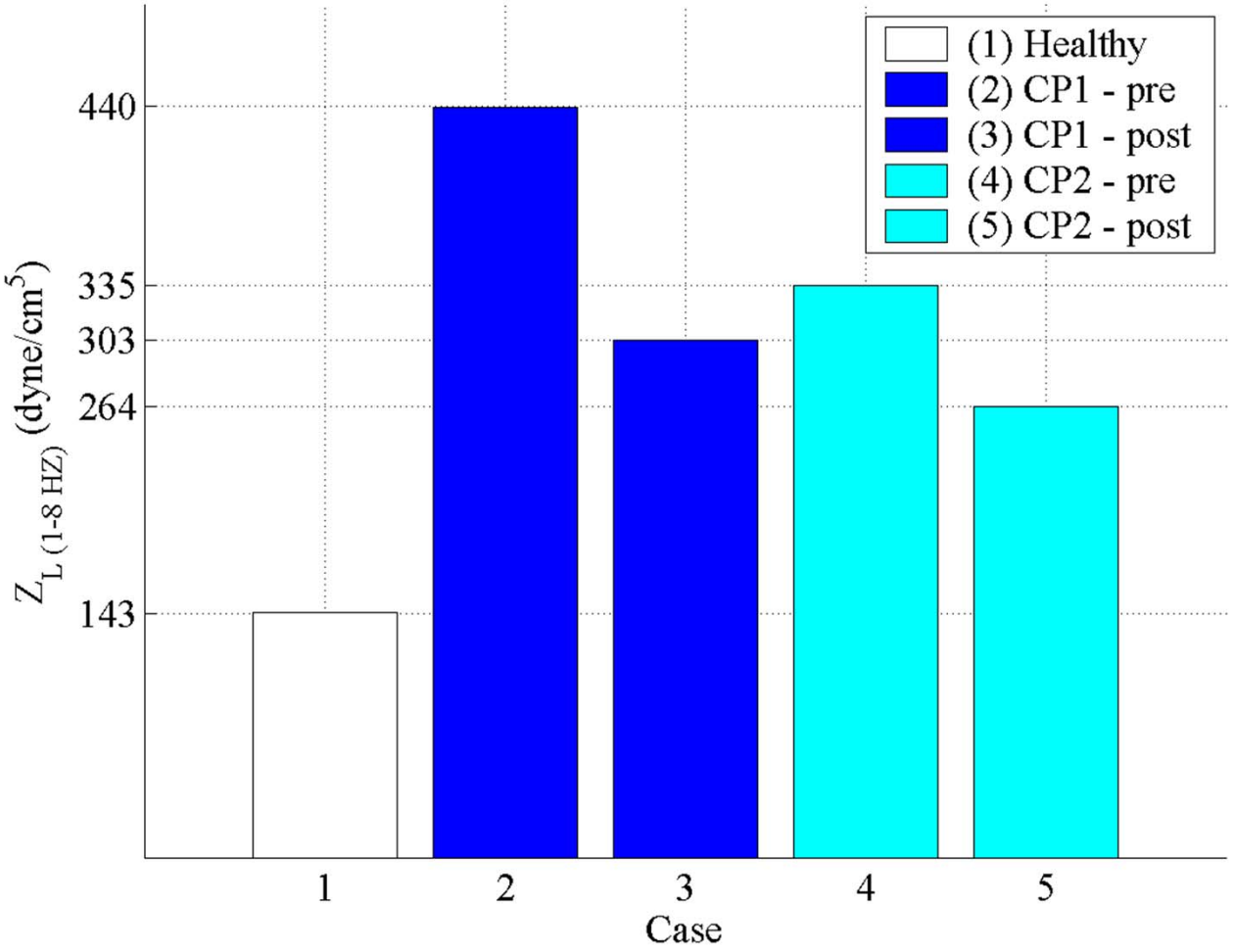

Image courtesy of Dr. Francis Loth, University of Akron, Biofluids Laboratory

Impedance to Cerebrospinal Fluid Flow in the Cervical Spinal Canal is Dominated by Geometric Complexity

Nicholas Shaffer, MS, Francis Loth, PhD

Department of Mechanical Engineering, University of Akron

Brandon Rocque, MD, Bermans Iskandar, MD

Department of Neurological Surgery, University of Wisconsin

Oliver Wieben, PhD

Departments of Medical Physics and Radiology, University of Wisconsin

John Oshinski, PhD

Department of Radiology, Emory University

Funding Provided by the Chiari and Syringomyelia Patient Education Foundation

Integrated Longitudinal Impedance (ILI)

$$Z_{L_n} = \frac{FFT(\Delta P)}{FFT(Q)} = \frac{\Delta P_n}{Q_n} \Rightarrow M_n = \left| Z_{L_n} \right| \Rightarrow ILI = \int_{n=1}^{8} M_n dn$$

Can ILI be used as a measure of the altered state of the conduit geometry in the cervical spinal SAS affected by CMI?

- Function of conduit geometry [Curi et al, J Surg Res, 2002].
- Has predictive value for patency in vein grafts; measure of favorable conduit size and material properties [Schwartz et al, J Vasc Surg, 1997].
- Compare ILI, mean hydraulic radius, and cervical SAS volume between symptomatic, asymptomatic and volunteer groups using one-way analysis of variance by ranks (Kruskal-Wallis Test) for a = 0.05, df = 3.

Statistical Analysis

- Generic Statistical Hypothesis:
  - H0: Distribution of values is the same for all groups
  - HA: Median value is not the same for all groups

Slide information courtesy of Francis Loth and Nicolas Schaffer, University of Akron, OH

Methods: geometry and meshing

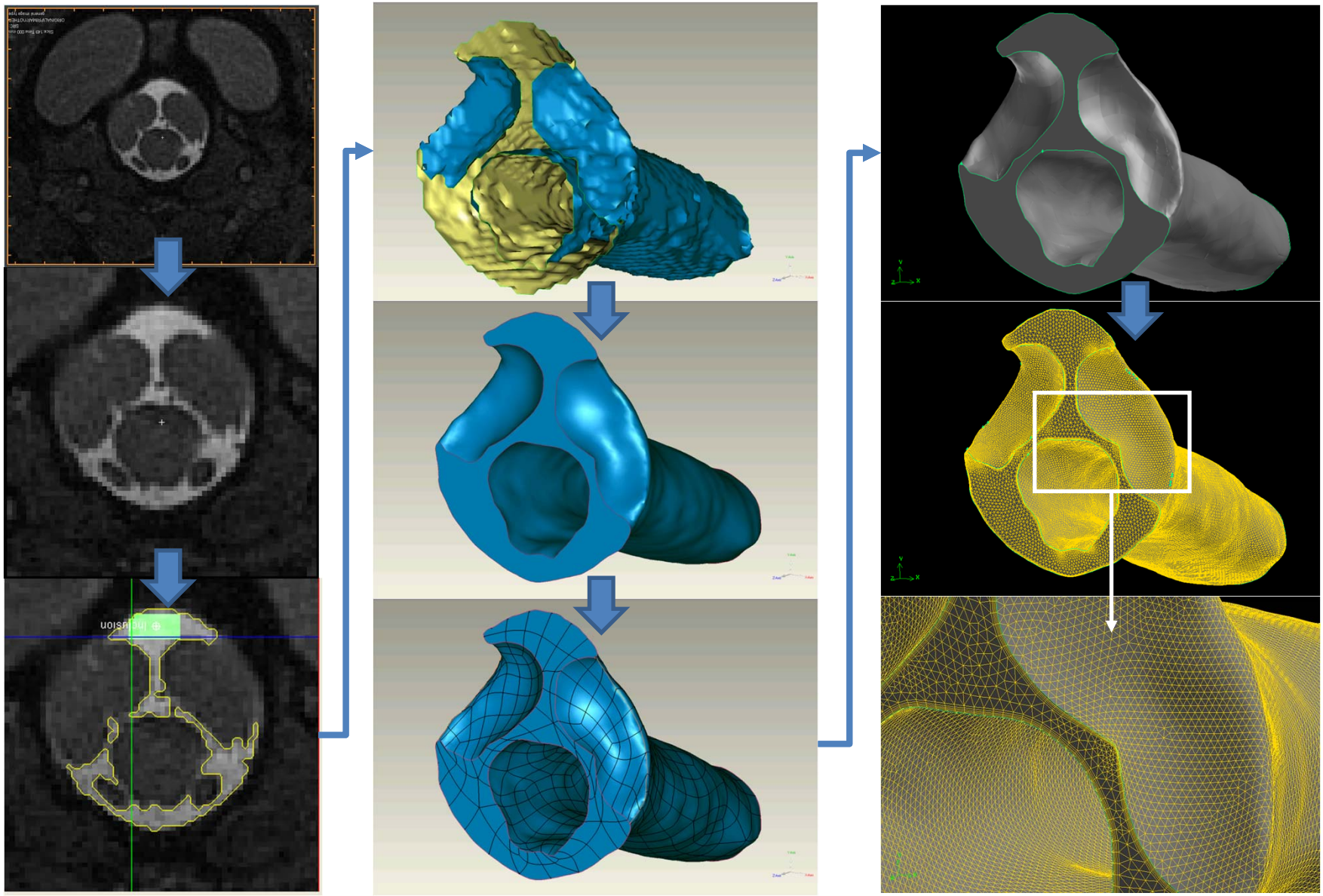

Figure courtesy of Francis Loth and Nicolas Schaffer, University of Akron, OH

Inlet Flow Boundary Condition Study

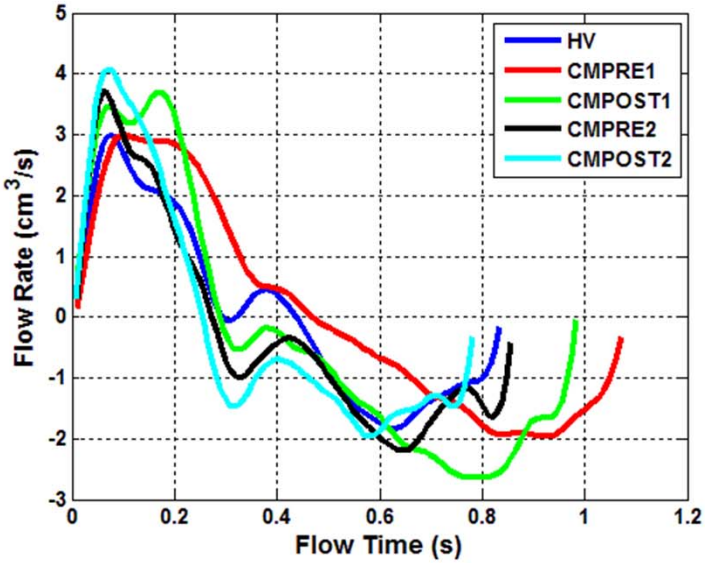

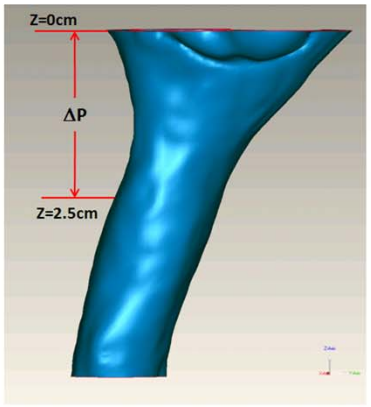

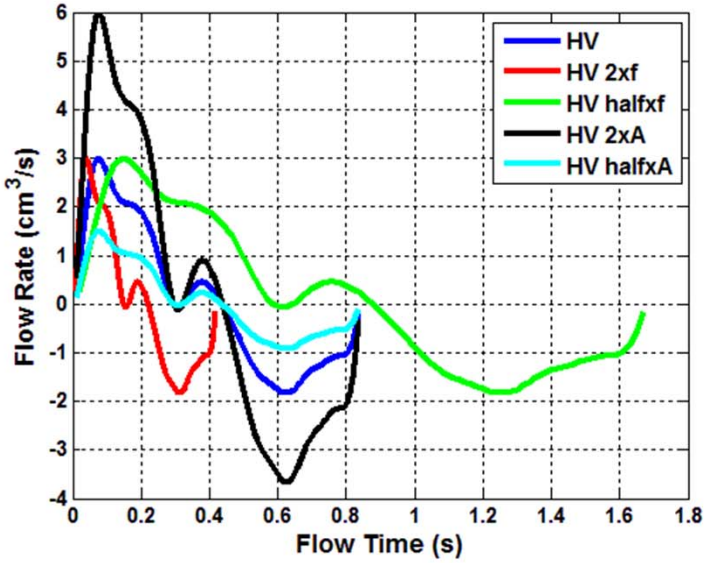

Maximum and minimum integrated LI vary from mean by 1.3% and 0.7%, respectively.

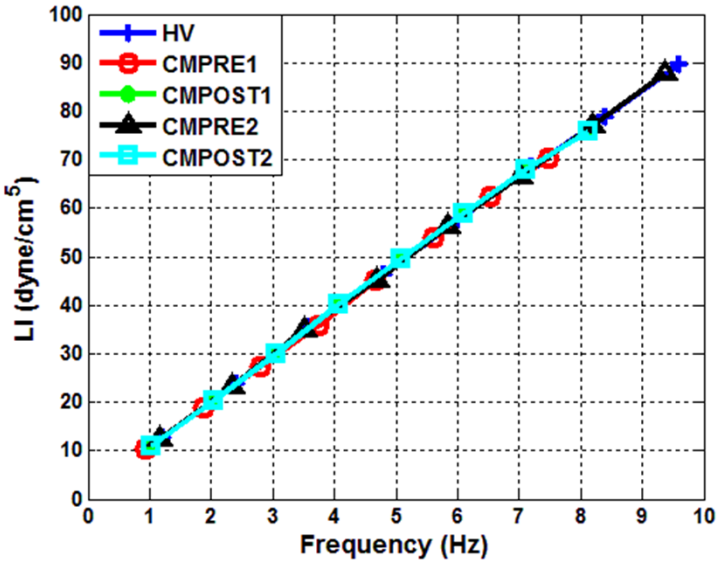

Figure courtesy of Francis Loth and Nicolas Schaffer, University of Akron, OH

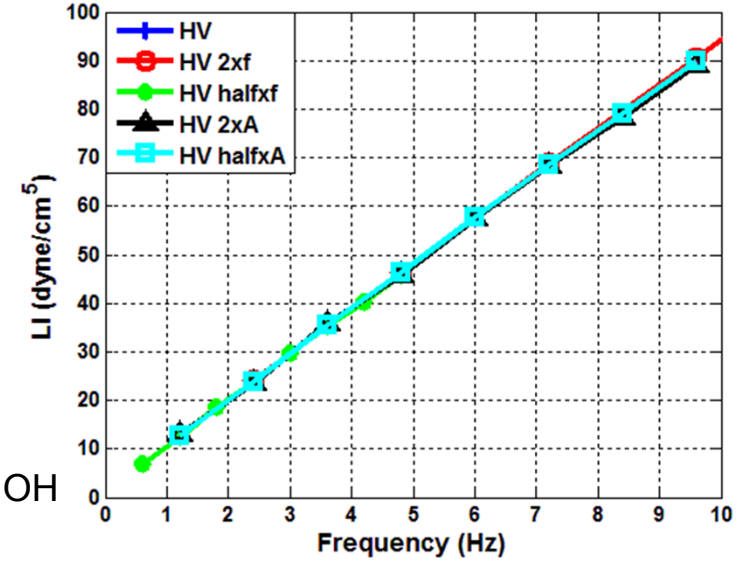

Longitudinal impedance in a straight tube

$$\left|\frac{\Delta P}{Q}\right| = \left|\frac{i\mu\alpha^2 L}{\pi R_H^4}\left[1 - \frac{2J_1\left(i^{3/2}\alpha\right)}{i^{3/2}\alpha J_0\left(i^{3/2}\alpha\right)}\right]^{-1}\right| = f\left(HR, \mu, \frac{1}{R_H^2}\right)$$

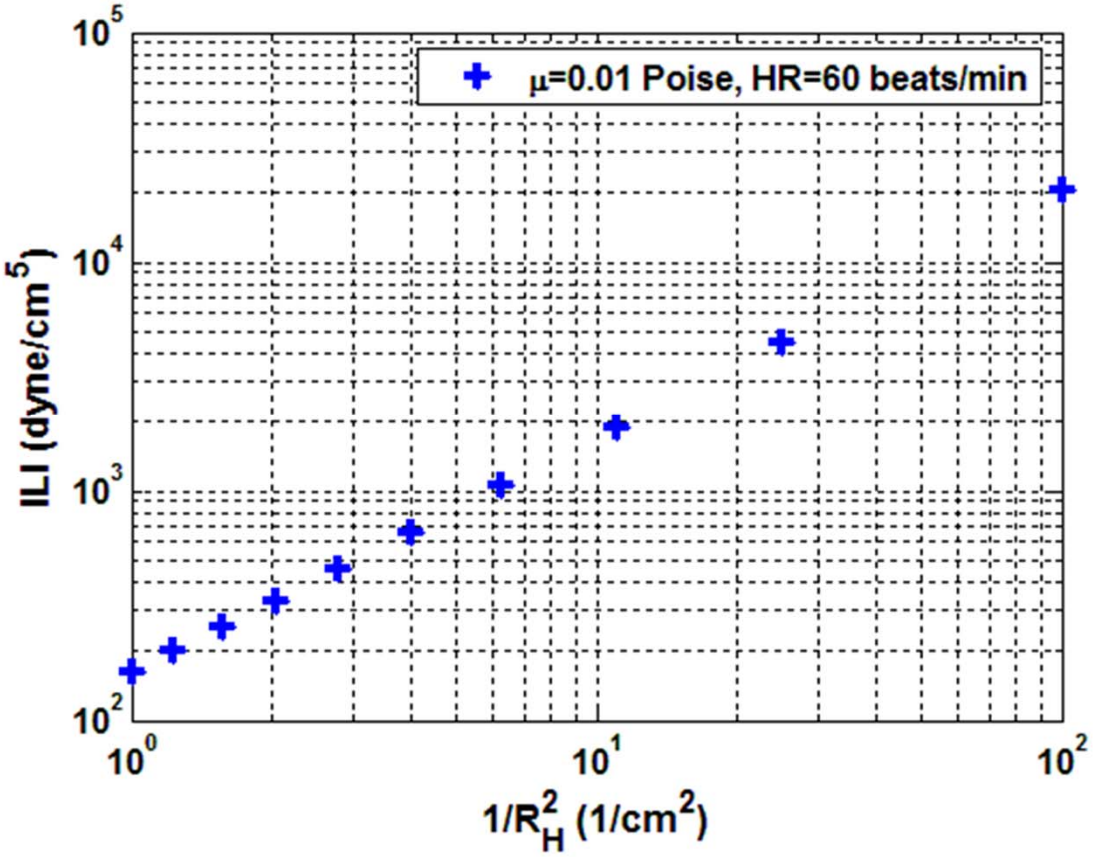

Figure courtesy of Francis Loth and Nicolas Schaffer, University of Akron, OH

ILI results: 21 subjects

Black = Volunteers; Blue = Asymptomatic;
Green = Symptomatic; Red = Equivocal/Indeterminate

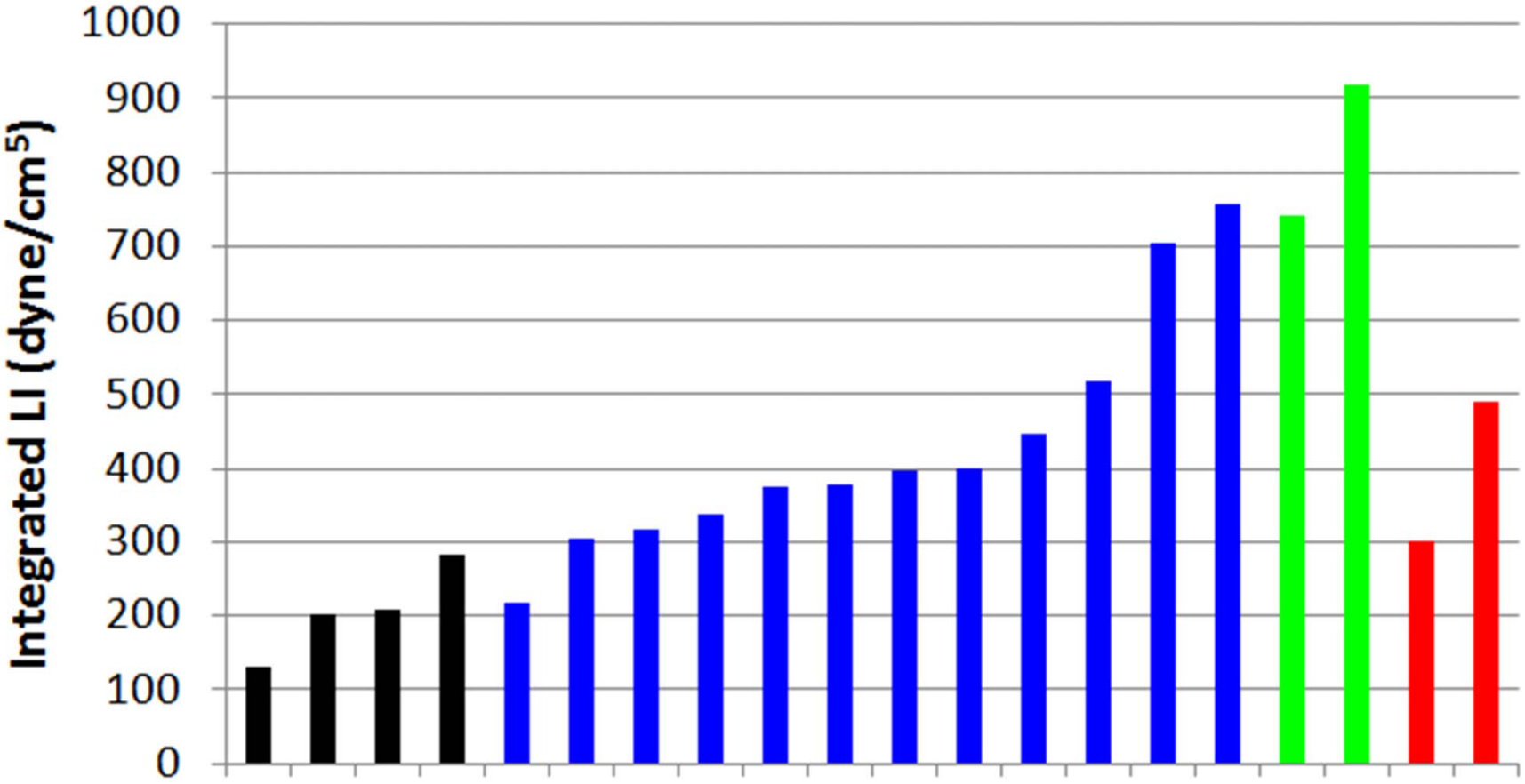

Figure courtesy of Francis Loth and Nicolas Schaffer, University of Akron, OH

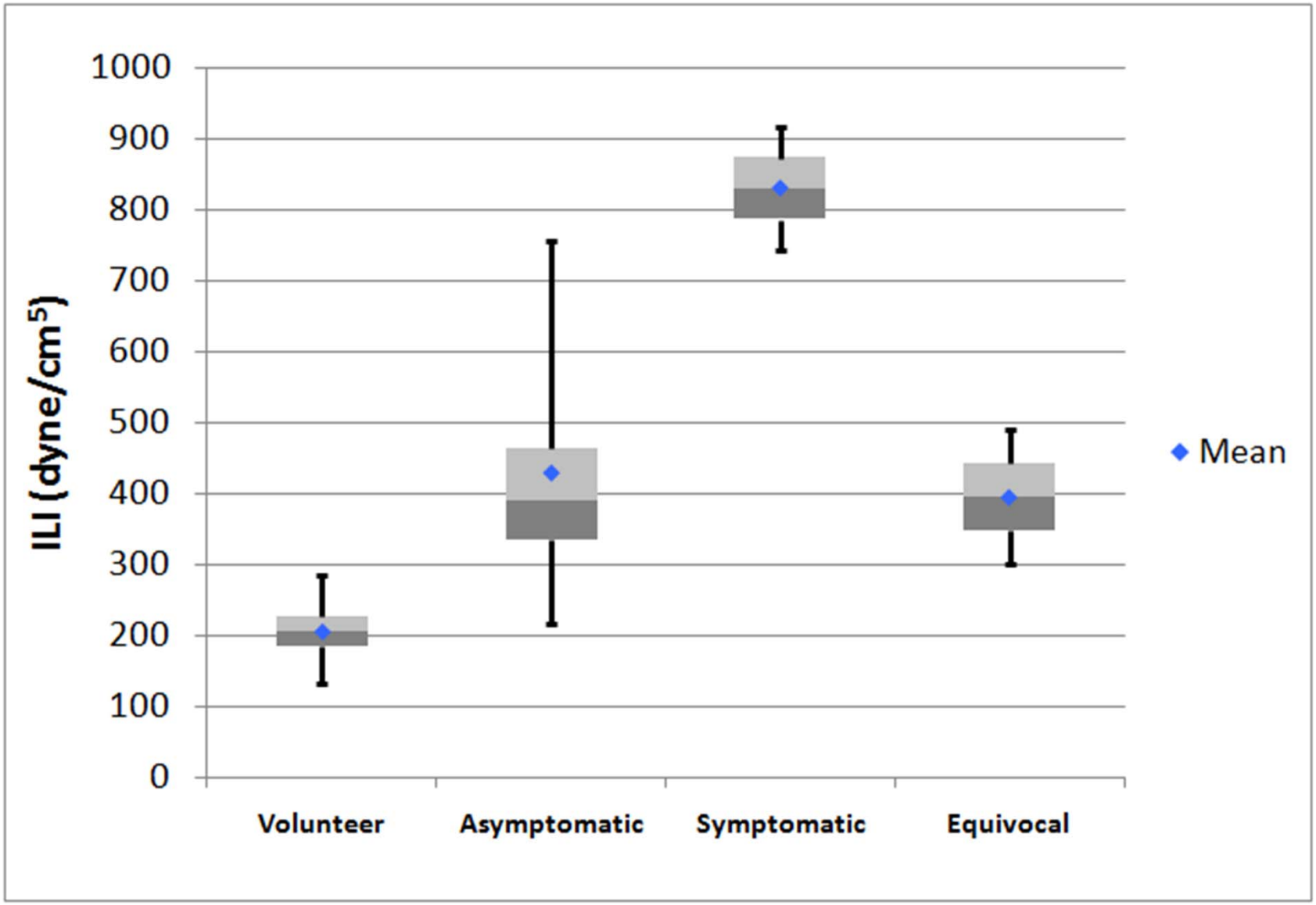

***Median integrated LI in each group is NOT the same (p<0.01)**

Figure courtesy of Francis Loth and Nicolas Schaffer, University of Akron, OH

ILI conclusions

Integrated Longitudinal Impedance

- Independent of the shape of the C2 volume flow waveform
- Controlled by cervical SAS geometry
- On average, increases with symptom severity.
- More subjects required to confirm this as a trend.
- Correlates nearly linearly with average hydraulic radius and cervical SAS volume.

However…

- Standard geometric parameters such as hydraulic radius and SAS volume are not always predictive of the impedance to flow.
- Do not always reflect geometric complexity of the conduit.

Craniospinal disorders: Syringomyelia

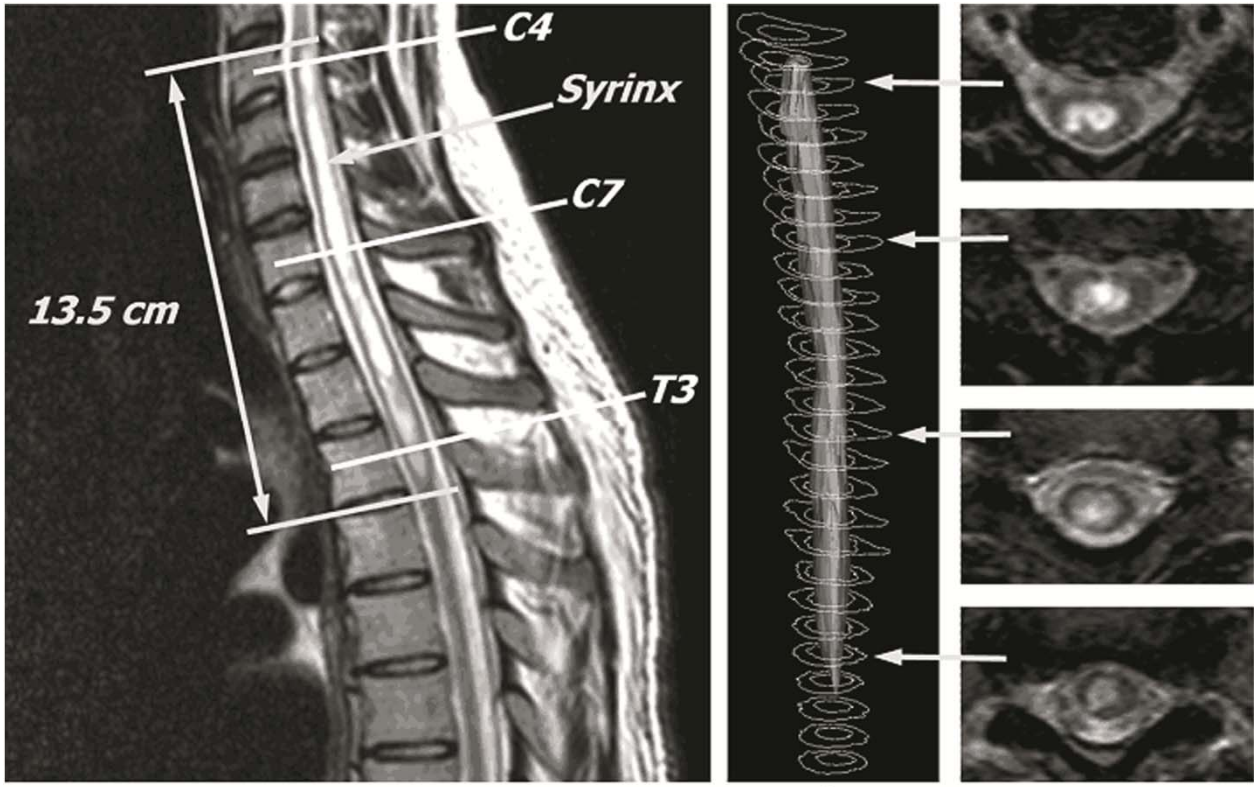

Martin, B. A., W. Kalata, et al. (2005). "Syringomyelia hydrodynamics: an in vitro study based on in vivo measurements." J Biomech Eng **127**(7): 1110-20.

Martin, B.A., et al., *Spinal Canal Pressure Measurements in an In Vitro Spinal Stenosis Model: Implications on Syringomyelia Theories.* J Biomech Eng, 2009. **In Press**(June 2009).

Martin, B.A. and F. Loth, *The influence of coughing on cerebrospinal fluid pressure in an in vitro syringomyelia model with spinal subarachnoid space stenosis.* Cerebrospinal Fluid Res, 2009. **6**(1): p. 17.

Could the relative timing of CSF and blood pulsations help explain **syringomyelia**?

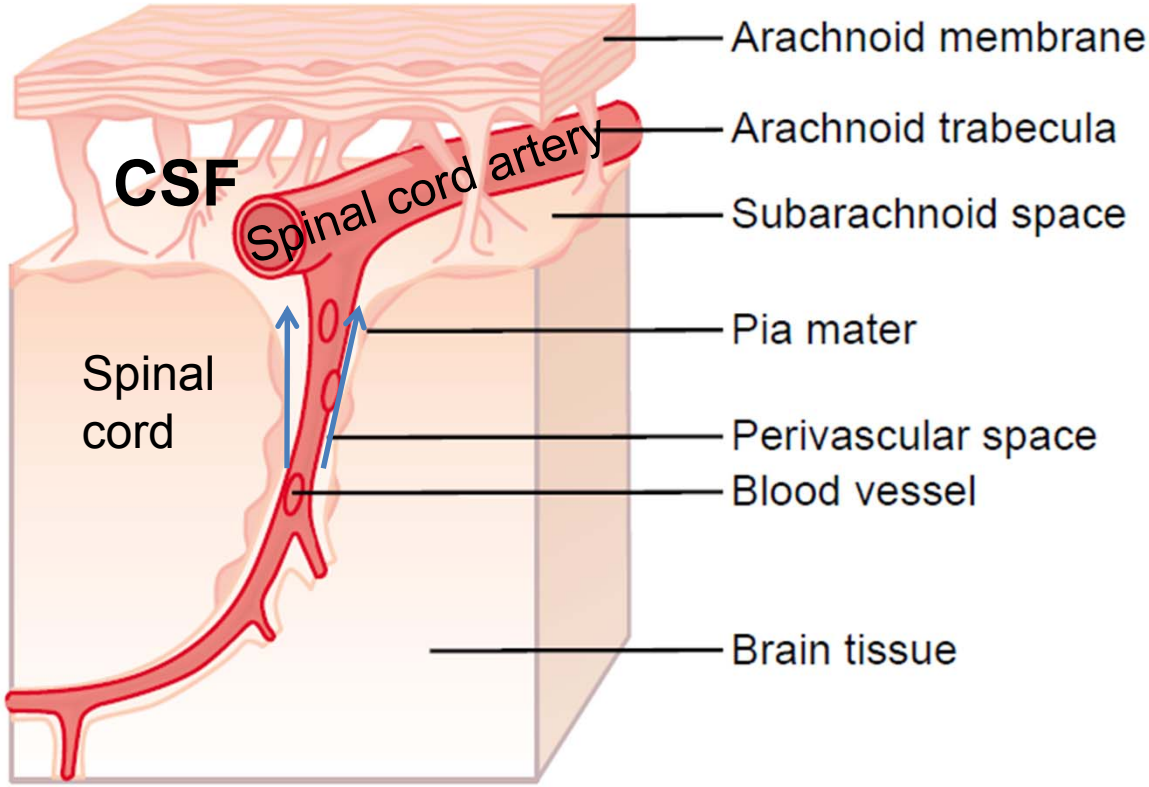

- Spinal cord perivascular spaces are a “specialized lymphatic system” (Guyton et al.)

Guyton, A. C. and J. E. Hall (2006). Textbook of medical physiology. Philadelphia, Elsevier Saunders.

Vessels entering the neural tissue could "milk" fluid in the Virchow-Robin spaces

- CSF/blood phase
- Theory (Madsen , Luciano)
- Simulation (Bilston)
- Experiments (Stoodley)

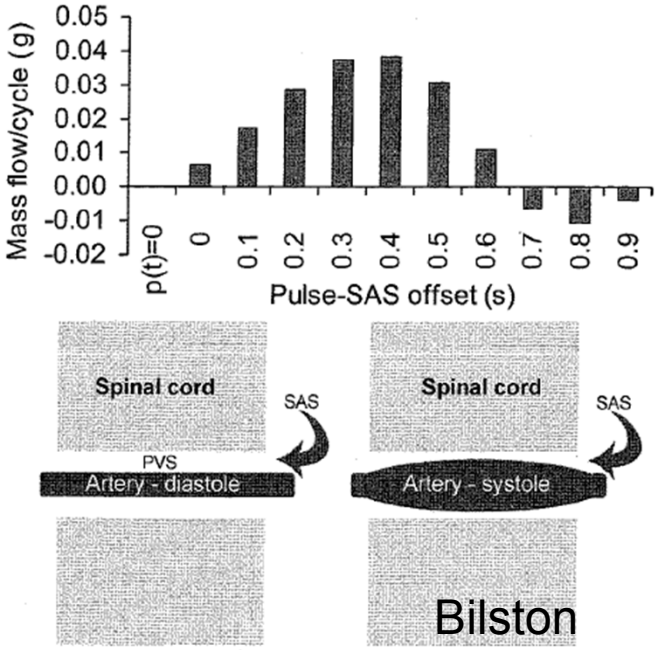

Bilston, L. E., M. A. Stoodley, et al. (2009). "The influence of the relative timing of arterial and subarachnoid space pulse waves on spinal perivascular cerebrospinal fluid flow as a possible factor in syrinx development." J Neurosurg.

Stoodley, M. A., B. Gutschmidt, et al. (1999). "Cerebrospinal fluid flow in an animal model of noncommunicating syringomyelia." Neurosurgery **44**(5): 1065-75; discussion 1075-6.

Luciano, M. and S. Dombrowski (2007). "Hydrocephalus and the heart: interactions of the first and third circulations." Cleve Clin J Med **74 Suppl 1**: S128-31.

Madsen, J. R., M. Egnor, et al. (2006). "Cerebrospinal fluid pulsatility and hydrocephalus: the fourth circulation." Clin Neurosurg **53**: 48-52.

A coupled model of the CSF and cardiovascular system
(and some in vivo and in vitro experiments)

Bryn A. Martin[1], Philippe Reymond[1], Jan Novy[2],
Olivier Balédent[3], Nikolaos Stergiopulos[1]

[1]EPFL, Laboratory of Hemodynamics and Cardiovascular Technology
[2]Department of Neurology, Centre Hospitalier Universitaire Vaudois, Switzerland
[3]Department of Magnetic Resonance Image Processing, University Hospital of Amiens

The crux

- What can we find about perivascular fluid flow to the spinal cord using a coupled model of the cardiovascular and CSF system?

Coupled cardiovascular/CSF system

1. Simulate cardiovascular tree using 1D tube model
2. Obtain blood flow into brain (CBF)
3. Transfer fn. to relate CBF to CSF flow at C2
4. Simulate CSF in spine using 1D tube model

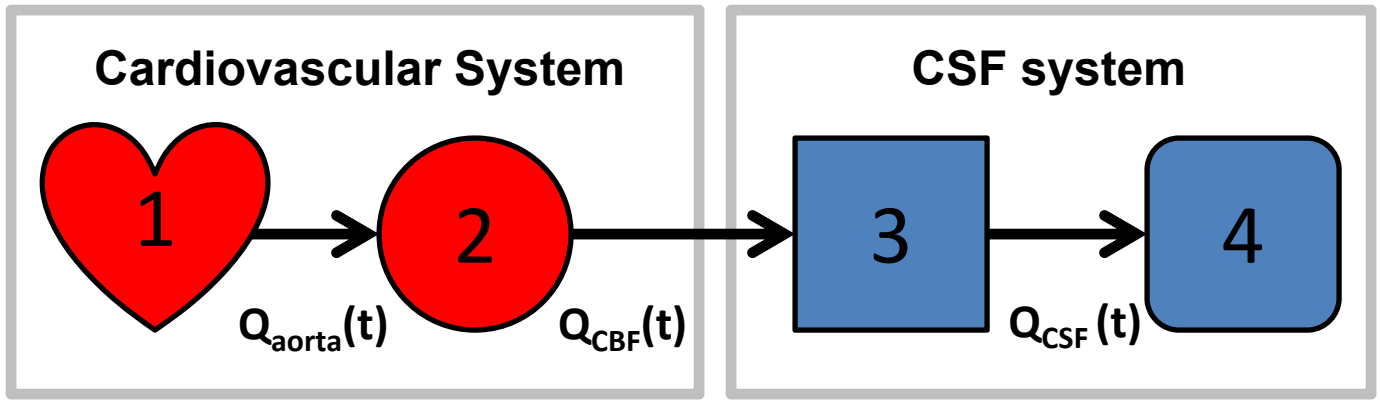

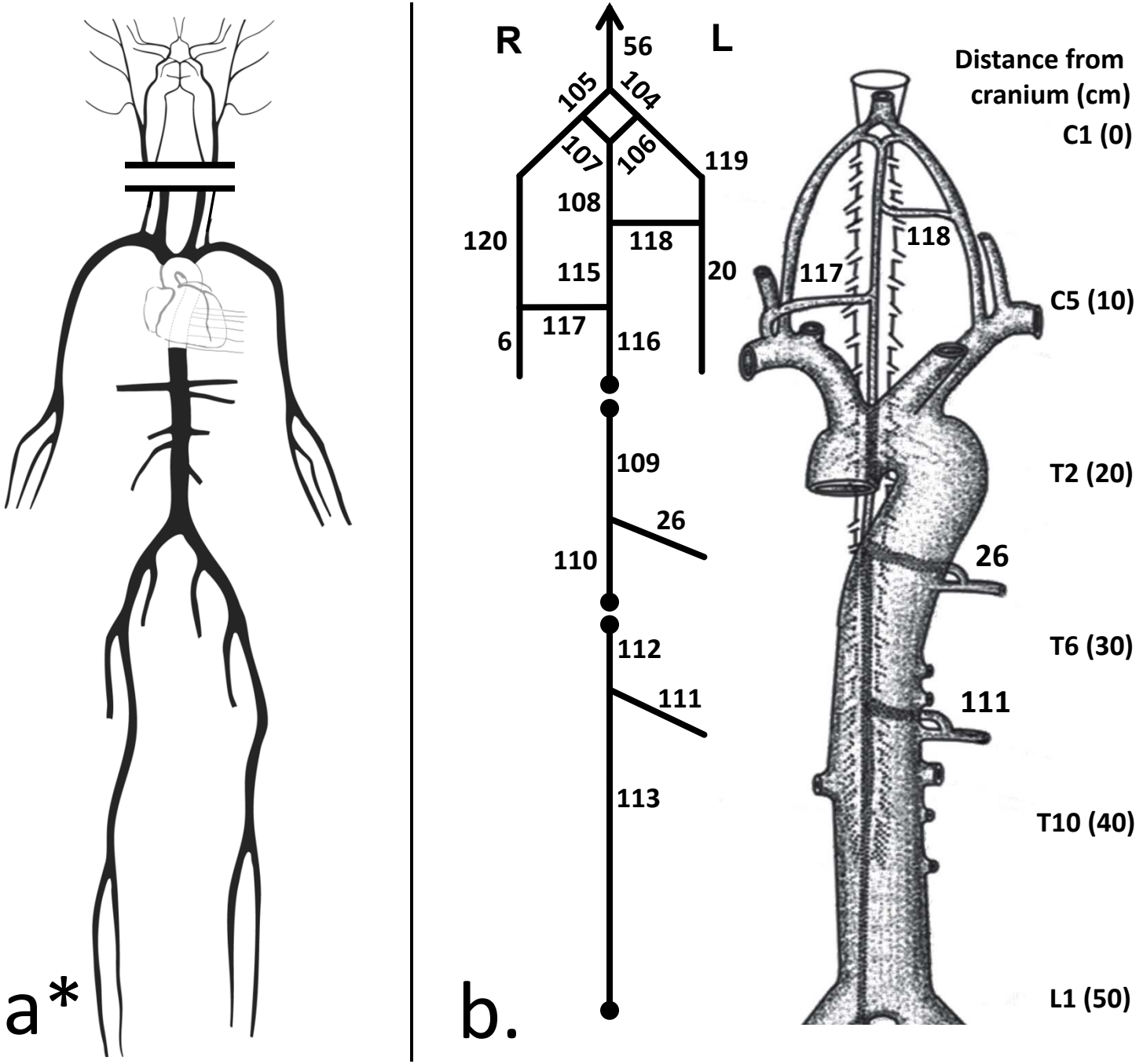

*Reymond, P., F. Merenda, et al. (2009). "Validation of a one-dimensional model." Am J Physiol Heart Circ Physiol **297**(1): H208-22.

Results: SC blood flow

- Similar to in vivo (flow)?
- Signature waveform
- Predictive…

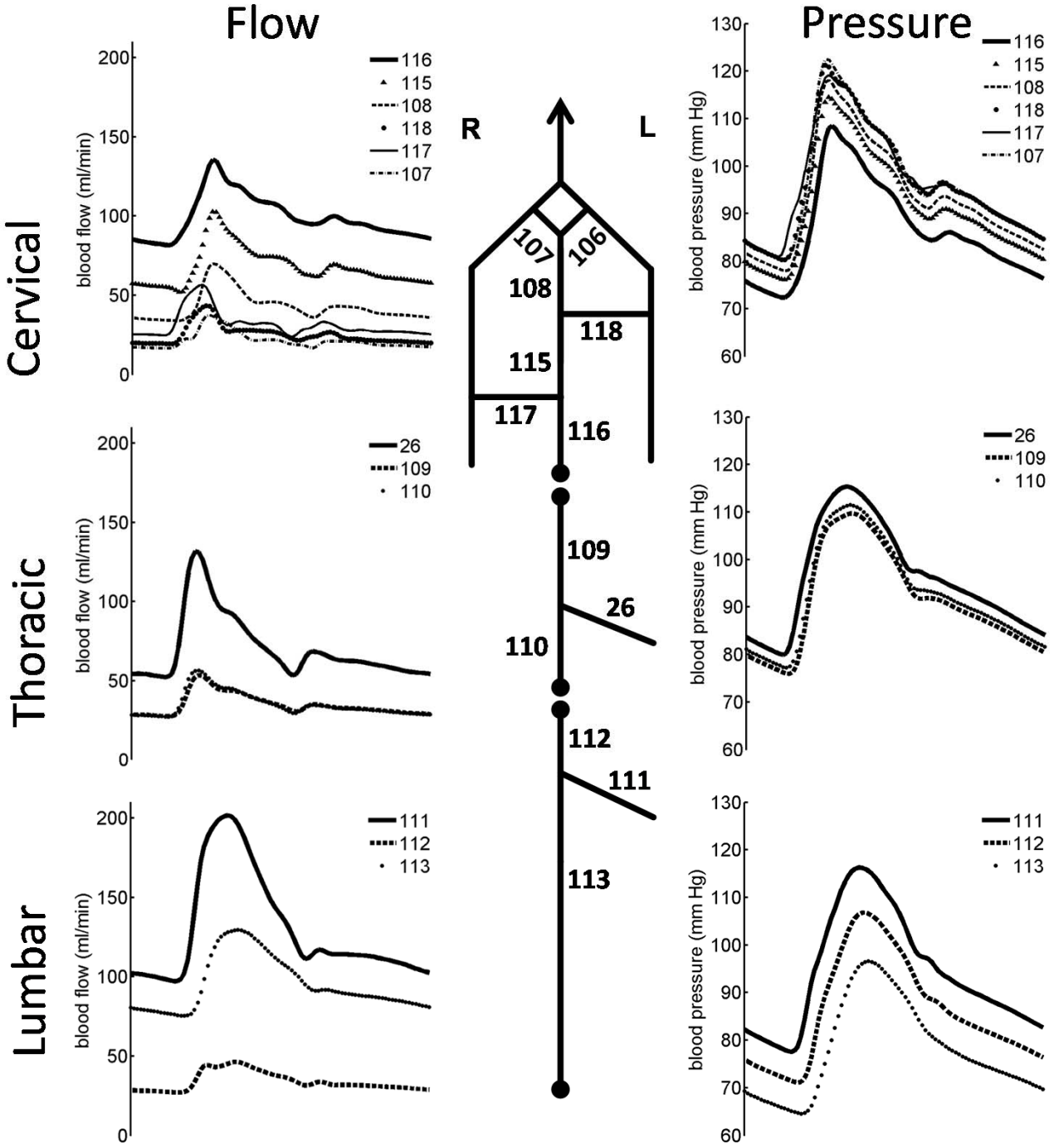

SC blood flow references:

Nystrom B, Stjernschantz J, and Smedegard G. Regional spinal cord blood flow monkey. *Acta Neurol Scand* 70: 307-313, 1984.

Duggal N, and Lach B. lumbosacral spinal cord. *Stroke; a journal of cerebral circulation* 33: 116-121, 2002.

Marcus ML, Heistad DD, Ehrhardt JC, and Abboud FM. spinal cord

Coupled cardiovascular/CSF system

1. Simulate systemic tree using 1D tube model*
2. Obtain blood flow into brain (CBF)
3. Transfer fn. to relate CBF to CSF flow at C2
4. Simulate CSF in spine using 1D tube model

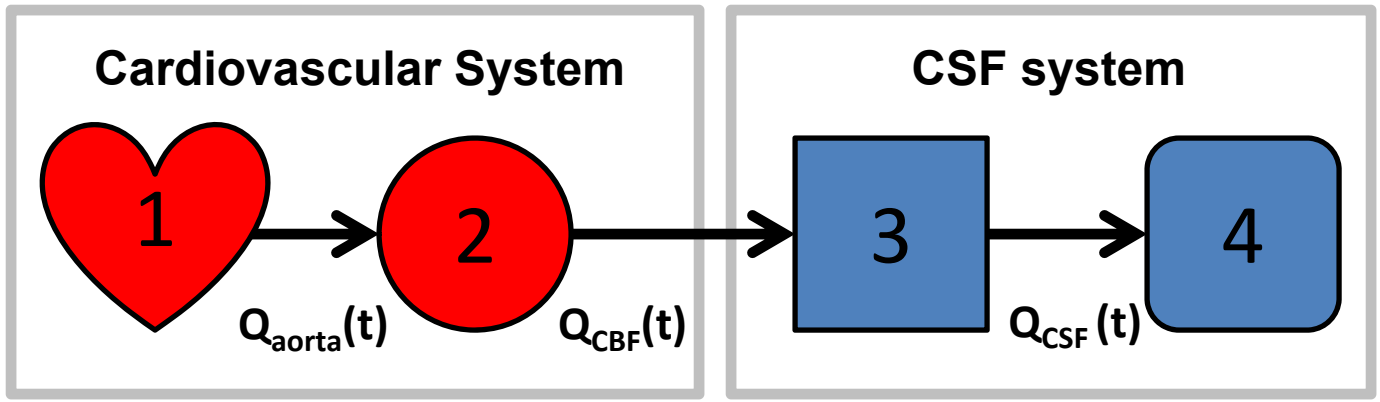

Transfer function

Based on MRI from 17 healthy subjects

Transfer Fn.

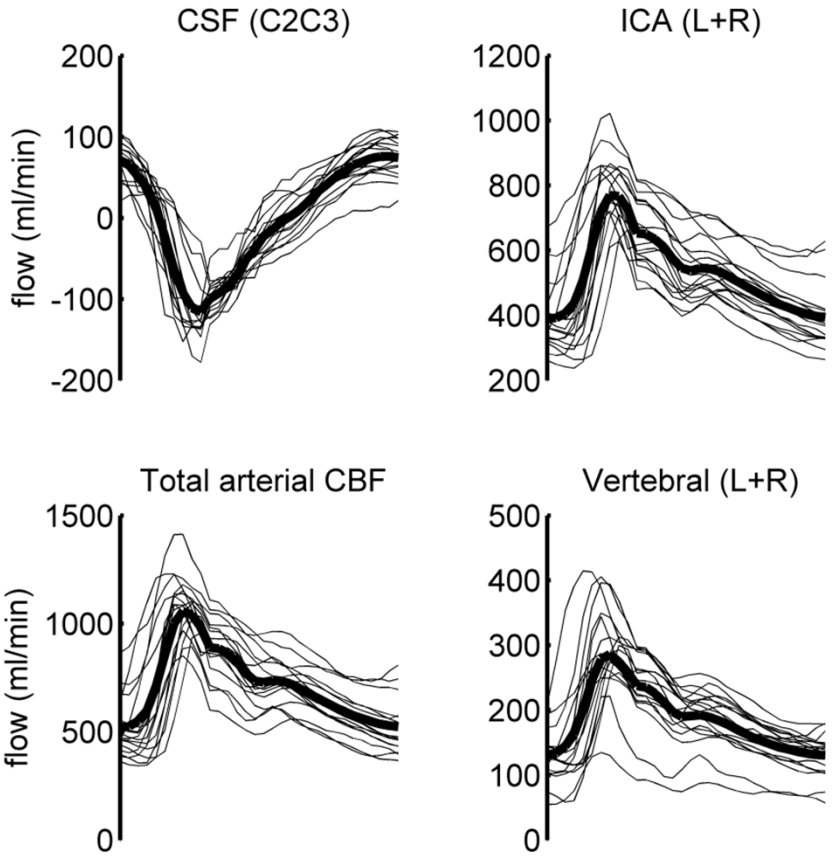

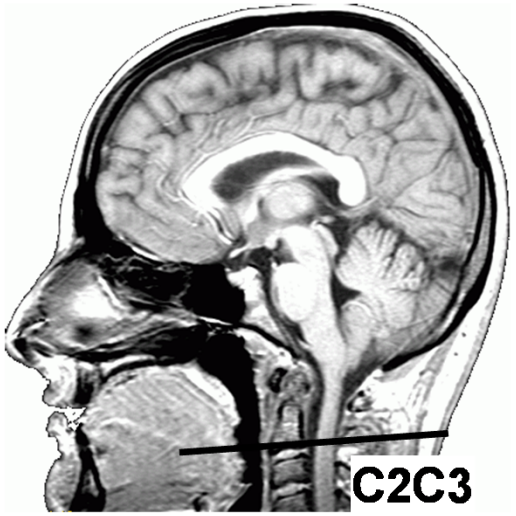

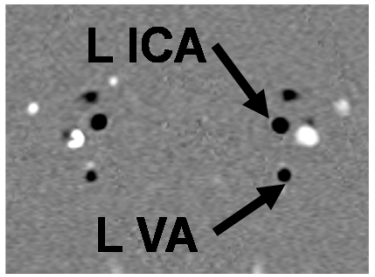

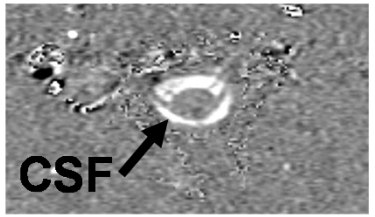

MRI images courtesy of Olivier Baledent, Amien, FR

Transfer fn. results

- Similar flow rate as in vivo
- Stronger systolic accn. in silico (MRI temporal resolution?)

In vivo (MRI)

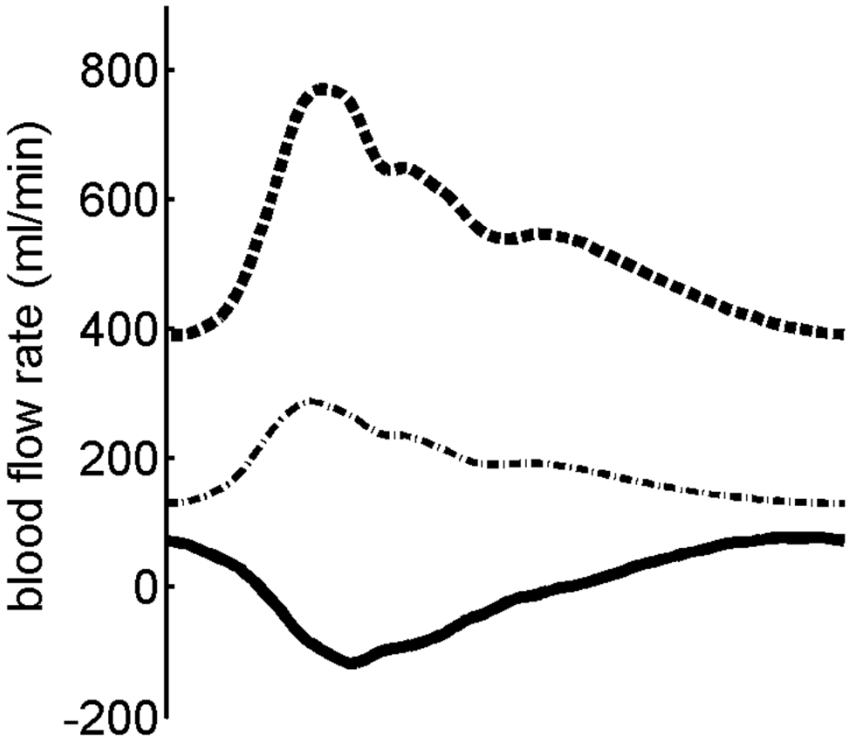

In silico

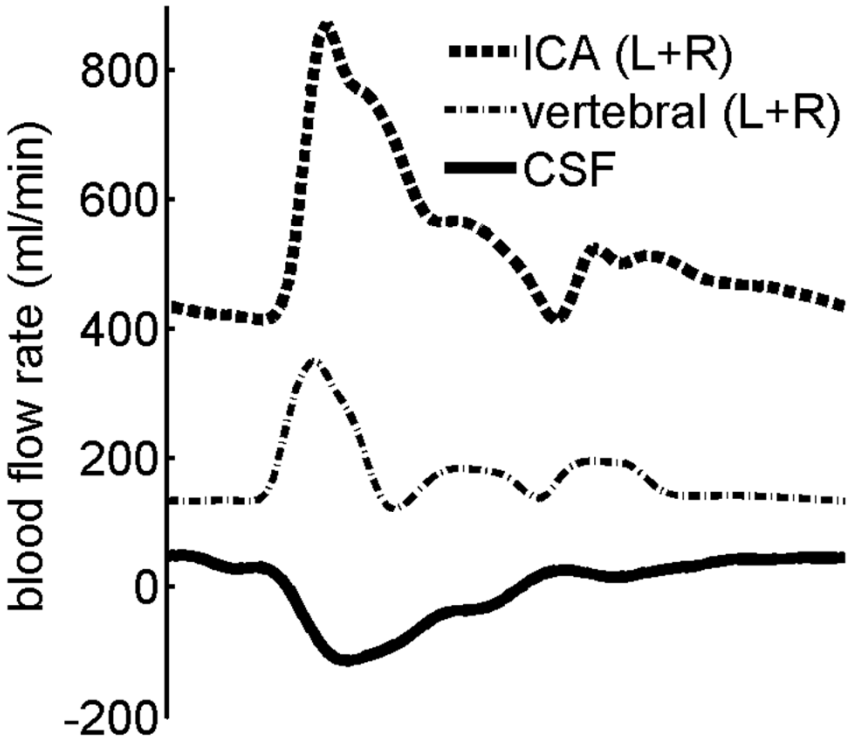

Coupled cardiovascular/CSF system

1. Simulate systemic tree using 1D tube model*
2. Obtain blood flow into brain (CBF)
3. Transfer fn. to relate CBF to CSF flow at C2
4. Simulate CSF in spine using 1D tube model

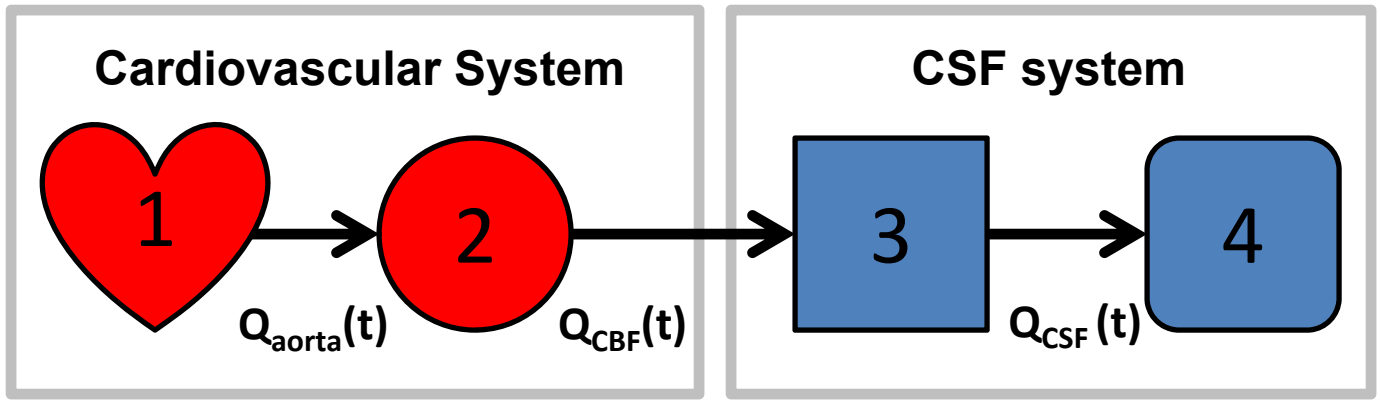

CSF flow and pressure results (healthy)

- Similar to in vivo (waveform / flow / pressure / PWV)
- Strongly modified by changes in spinal compliance

CSF flow (ml/min)

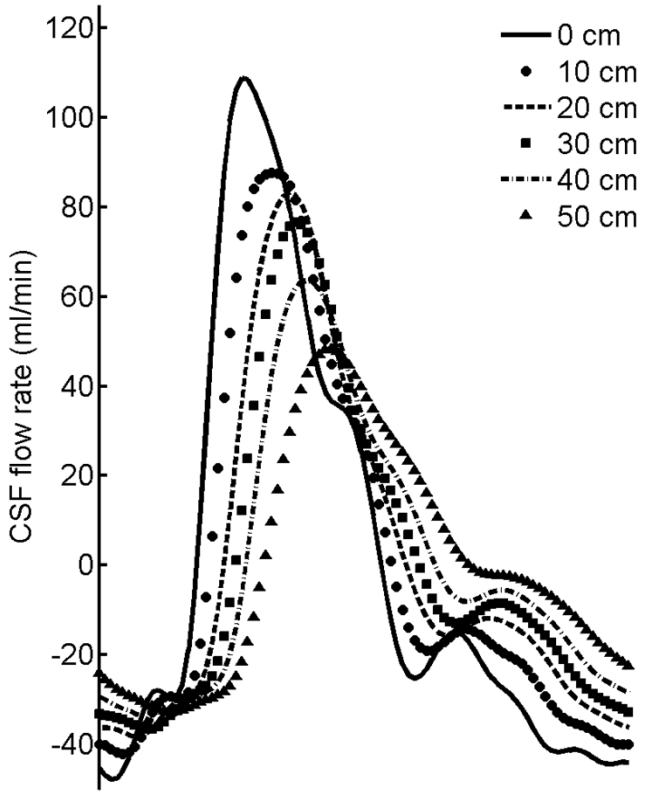

CSF pressure (mmHg)

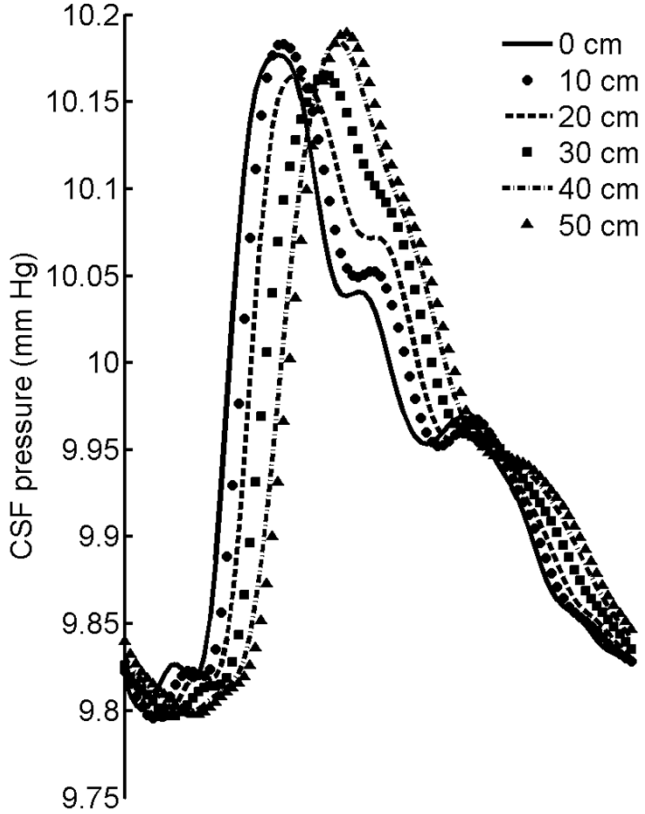

Cardiovascular CSF coupling (in spine)

- Spatial-temporal distribution of flow and P

CSF

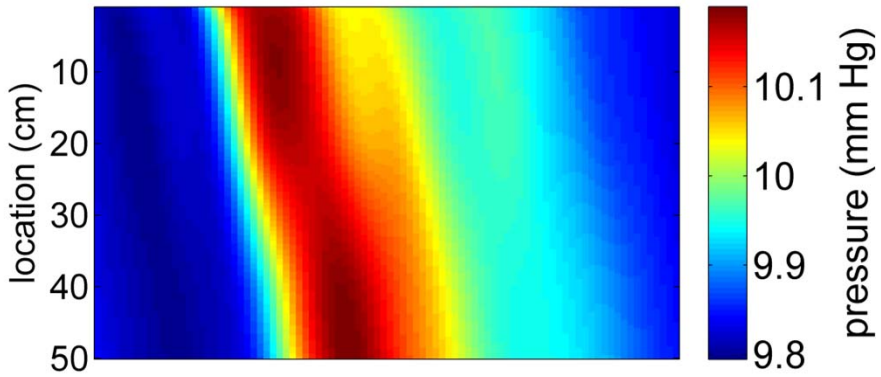

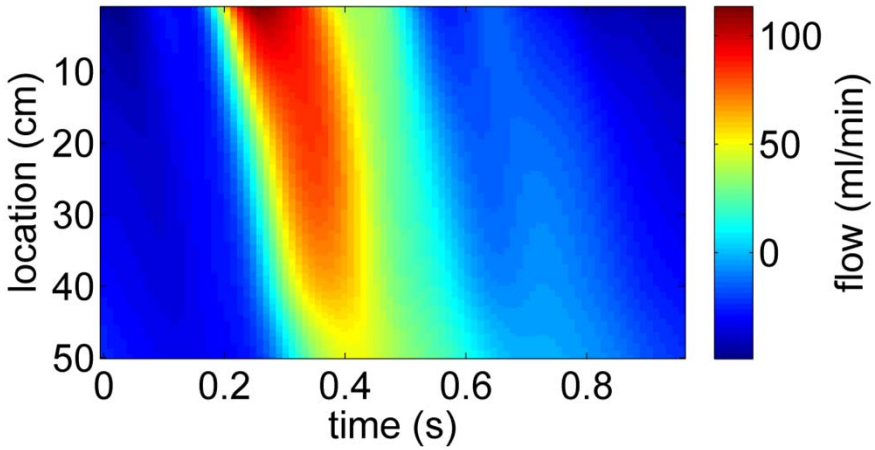

Spinal cord

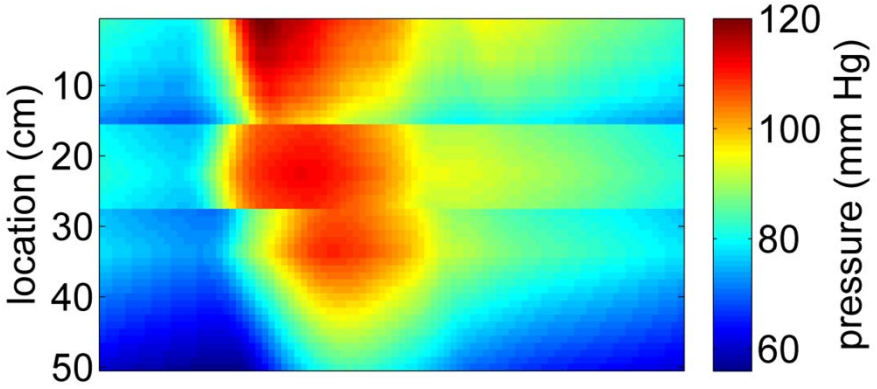

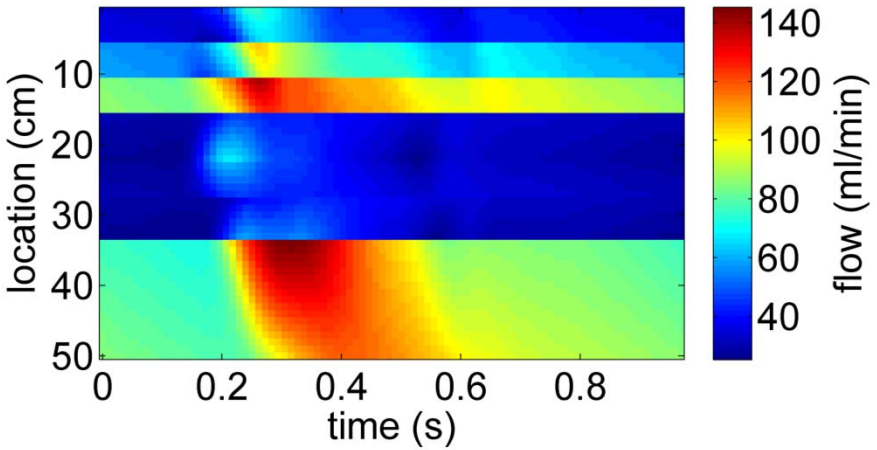

Estimation of SC perivascular flow

Assume:

- 10 arterioles per 1 mm^2
- PVS flow from Bilston
- When arteriole pulse arrives before CSF, PV fluid moves into SC

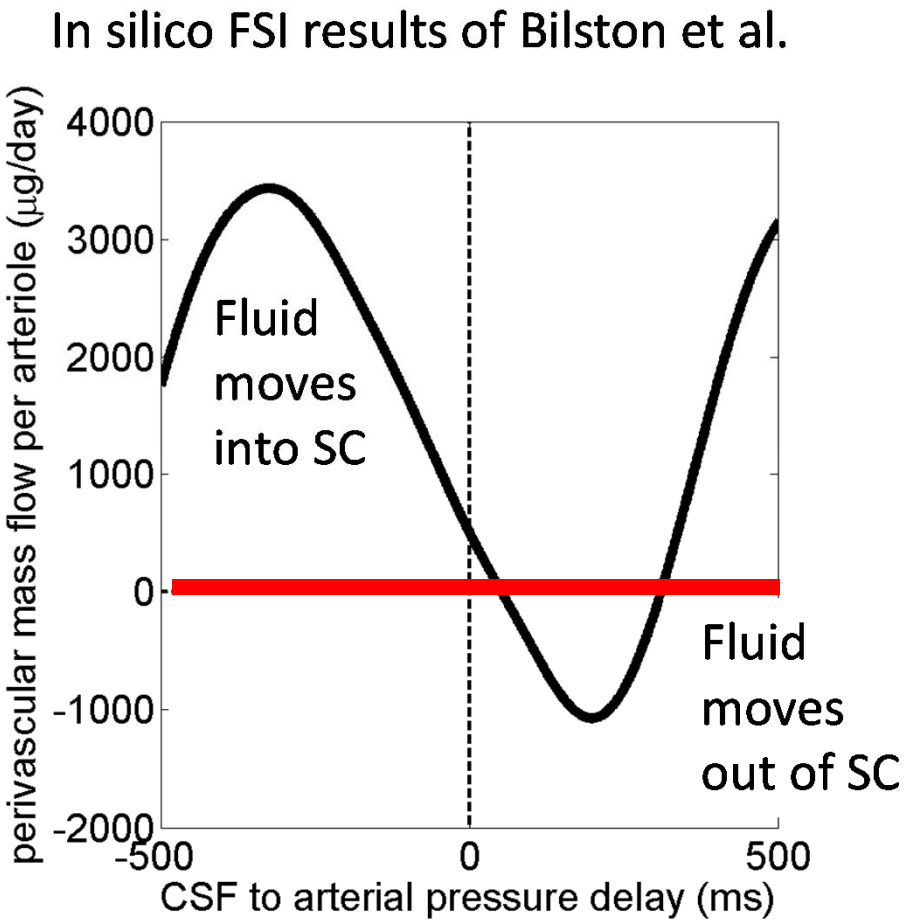

Bilston, L. E., M. A. Stoodley, et al. (2009). "The influence of the relative timing of ." J Neurosurg.

PV flow could be strongly influenced by anatomy and compliance

- Lumbar SC was most active region

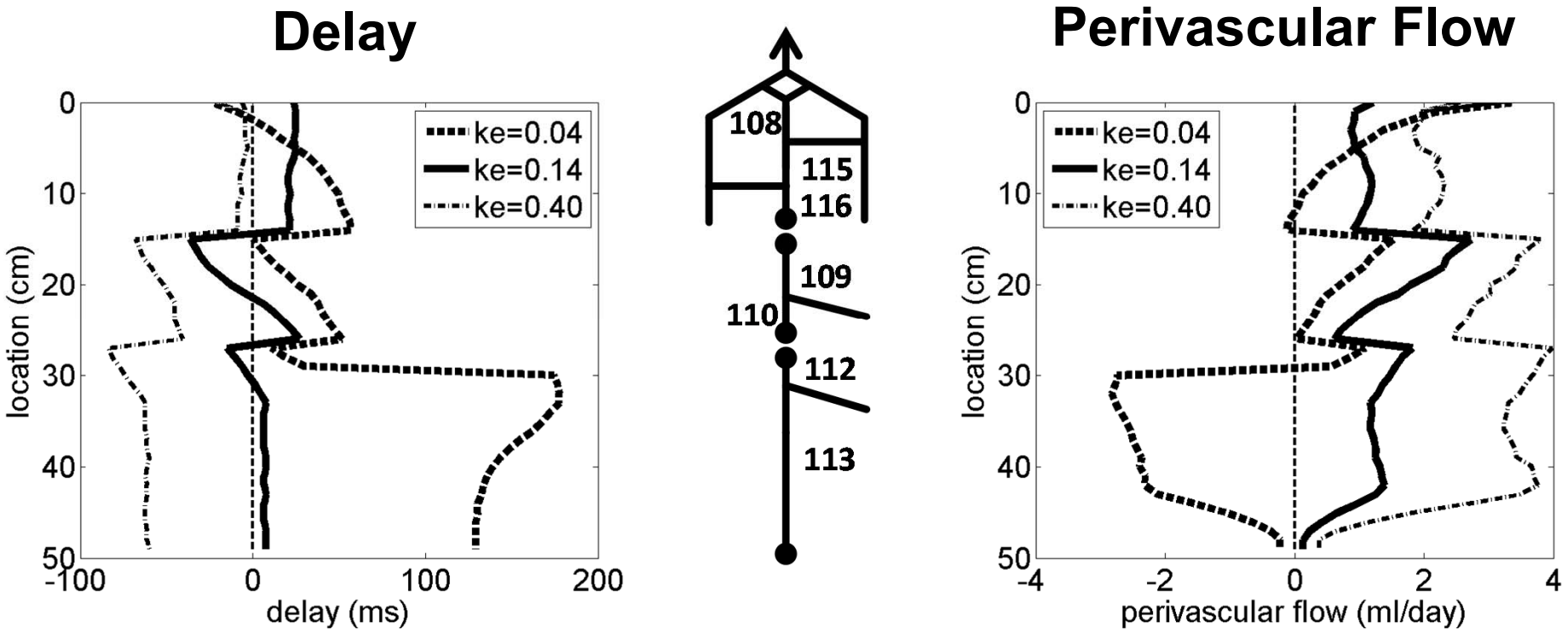

Perivascular flow, PWV & compliance

- PV flow changed direction depending on compliance
- Total PV flow could be significant with respect to CSF produced daily (500ml)

Elastance coeff. K_e (ml^{-1})	CSF PWV (m/s)	Average perivascular flow (ml/day)
0.04	2.3	-16
0.14	4.4	61
0.40	7.8	135

Conclusions

- Coupling between cardiovascular/CSF system was accomplished with a simple model
- Made predictions about SC blood flow, CSF PWV and PV fluid movement
- Need in vivo measurements to improve model

Work submitted: A coupled hydrodynamic model of the cardiovascular and cerebrospinal fluid system
Bryn A. Martin[1], Philippe Reymond[1], Jan Novy[2], Olivier Balédent[3], Nikolaos Stergiopulos[1]
[1]Ecole Polytechnique Federale de Lausanne, School of Engineering, Interfaculty institute of Bioengineering, Laboratory of Hemodynamics and Cardiovascular Technology, Lausanne, Switzerland
[2]Department of Neurology, Centre Hospitalier Universitaire Vaudois, Lausanne, Switzerland
[3]Department of Magnetic Resonance Image Processing, University Hospital of Amiens, Amiens, France

Craniospinal disorders: Hydrocephalus

Is craniospinal compliance a missing link in **hydrocephalus** assessment?

Hydrocephalus types

- Obstructive (no aqueduct)
  - Provide aqueduct with shunt
- Communicating (↑prod. or ↓absorption CSF)
  - Increase absorption with shunt
- Normal pressure (insufficient craniospinal compliance?)
  - Normal pressure, but larger ICP osc. amplitude?
  - (Eide, Czosnyka)

Eide, P. K. and A. Brean (2006). "Intracranial pulse pressure amplitude levels determined during preoperative assessment of subjects with possible idiopathic normal pressure hydrocephalus." Acta Neurochir (Wien) **148**(11): 1151-6; discussion 1156.
Eide, P. K. and W. Sorteberg (2008). "Changes in intracranial pulse pressure amplitudes after shunt implantation and adjustment of shunt valve opening pressure in normal pressure hydrocephalus." Acta Neurochir (Wien) **150**(11): 1141-7; discussion 1147.
Czosnyka, Z., N. Keong, et al. (2008). "Pulse amplitude of intracranial pressure waveform in hydrocephalus." Acta Neurochir Suppl **102**: 137-40.

Is the spine a “notch” filter to dampen CSF pressure oscillations?

- CBF → CSF
- CSF → spinal canal
- Spinal canal dampens CSF oscillations
- “cerebral Windkessel”
- (madsen, luciano)

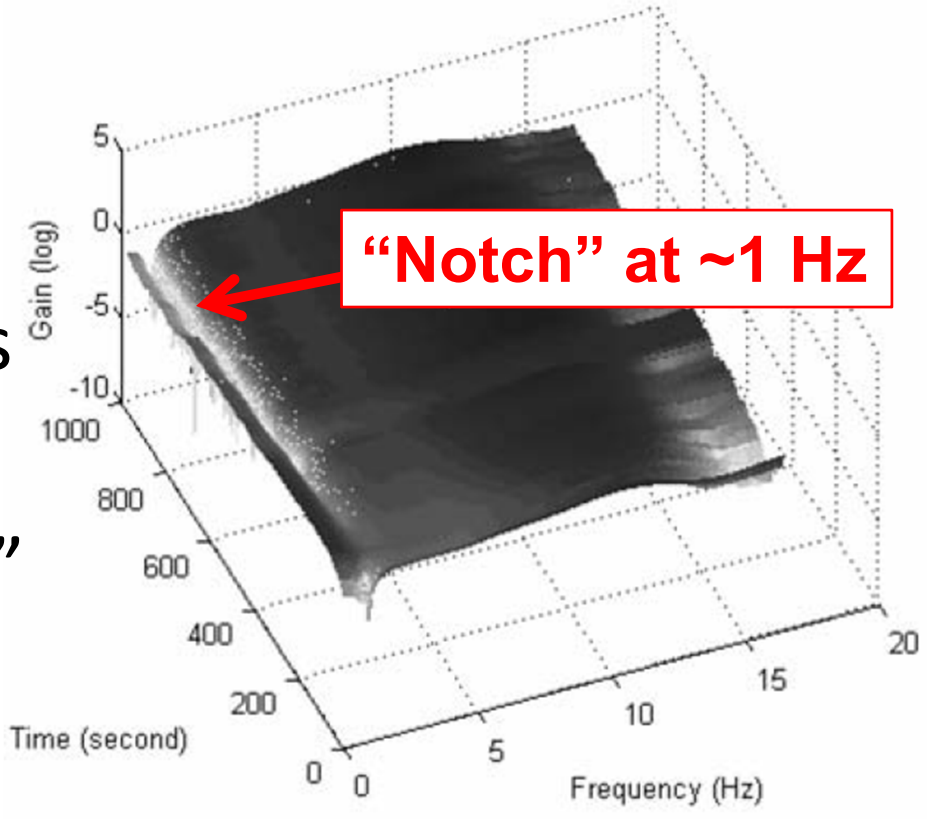

Madsen, J. R., M. Egnor, et al. (2006). "Cerebrospinal fluid pulsatility and hydrocephalus: the fourth circulation." Clin Neurosurg **53**: 48-52.

Luciano, M. and S. Dombrowski (2007). "Hydrocephalus and the heart: interactions of the first and third circulations." Cleve Clin J Med **74 Suppl 1**: S128-31.

In vitro models of the spinal subarachnoid space

Bryn A. Martin[1,6] Richard Labuda[2] Thomas J. Royston[3] John N. Oshinski[4] Bermans Iskandar[5] Francis Loth[1]

[1]University of Akron, Departments of Mechanical and Biomedical Engineering, Akron, OH, 44325, USA

[2]Chiari and Syringomyelia Patient Education Foundation, Wexford, PA, 15090, USA

[3] University of Illinois at Chicago, Department of Mechanical and Industrial Engineering, Chicago, IL, 60607, USA

[4] Emory University, Department of Radiology and Biomedical Engineering, Atlanta, GA, 30322, USA

[5] University of Wisconsin Medical School, Department of Neurological Surgery, Madison, WI, 53792, USA

[6]École Polytechnique Fédérale de Lausanne, Integrative Bioscience Institute, Laboratory of Hemodynamics and Cardiovascular Technology, Lausanne 1015, Switzerland

Chiari malformation (CM) & Syringomyelia (SM)

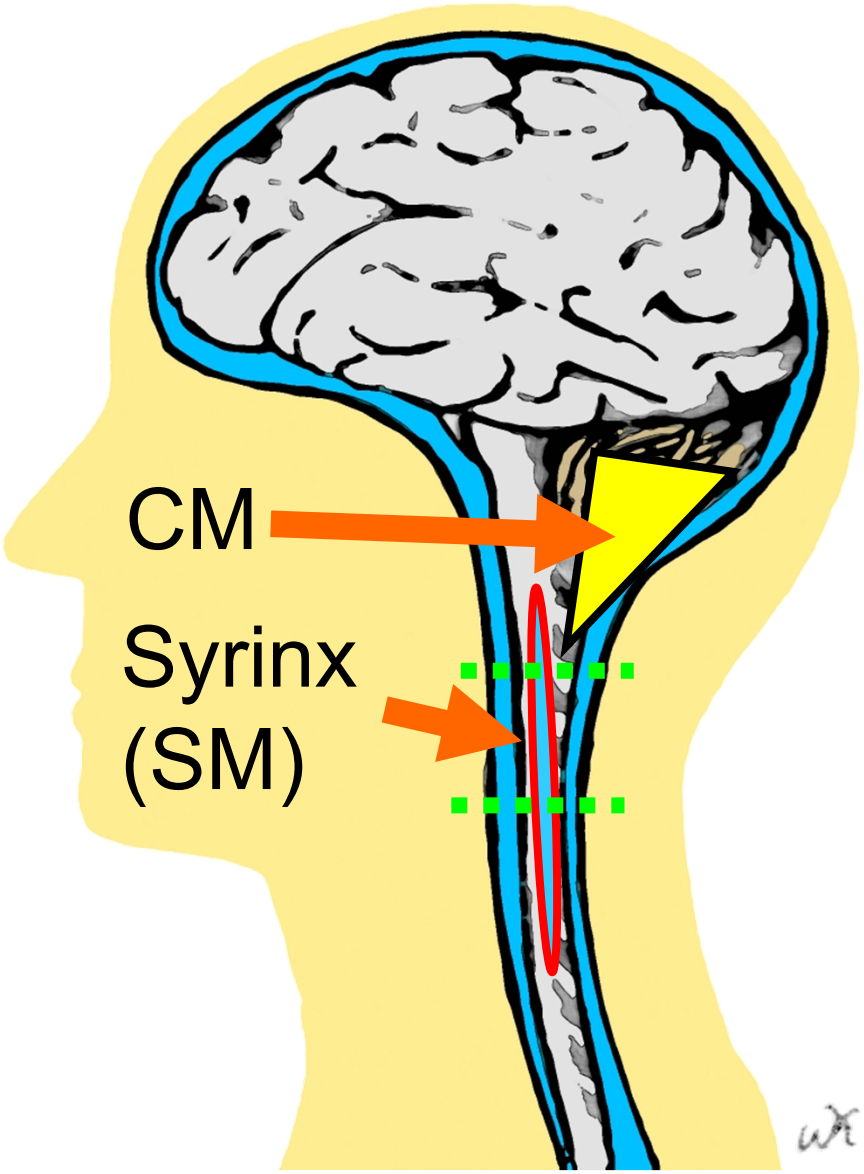

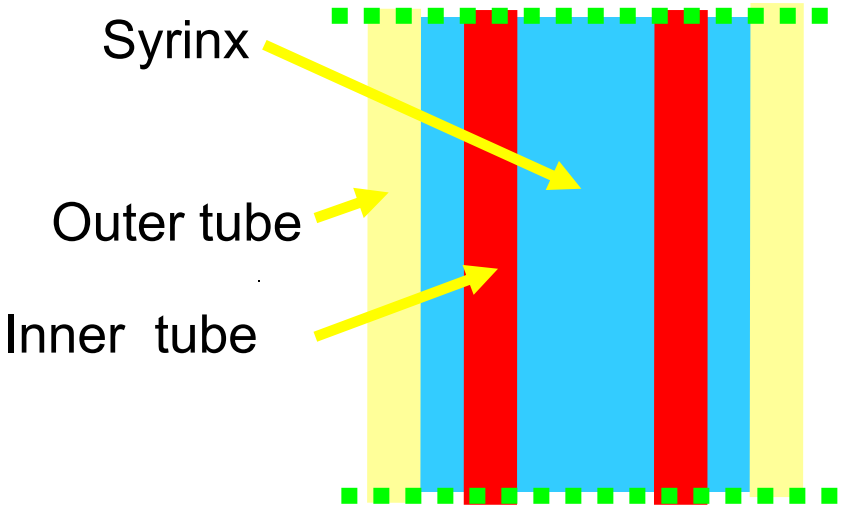

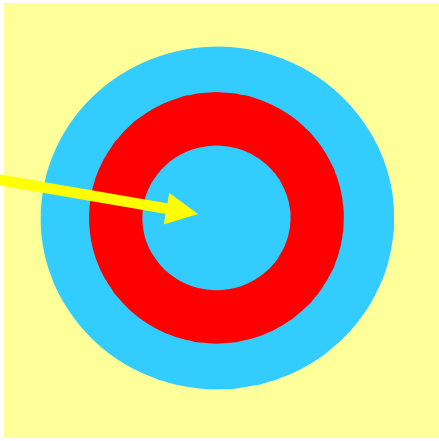

Motivation

Most theories claim that irregular hydrodynamic conditions caused by CSF flow blockage are a major factor in craniospinal disorder pathogenesis

Problem

- Theories lack experimental evidence

→Difficult to access CSF system *in vivo*

Methodology, in vitro measurement of:

- Pressure
- Flow
- Structural motion

Experimental set-up

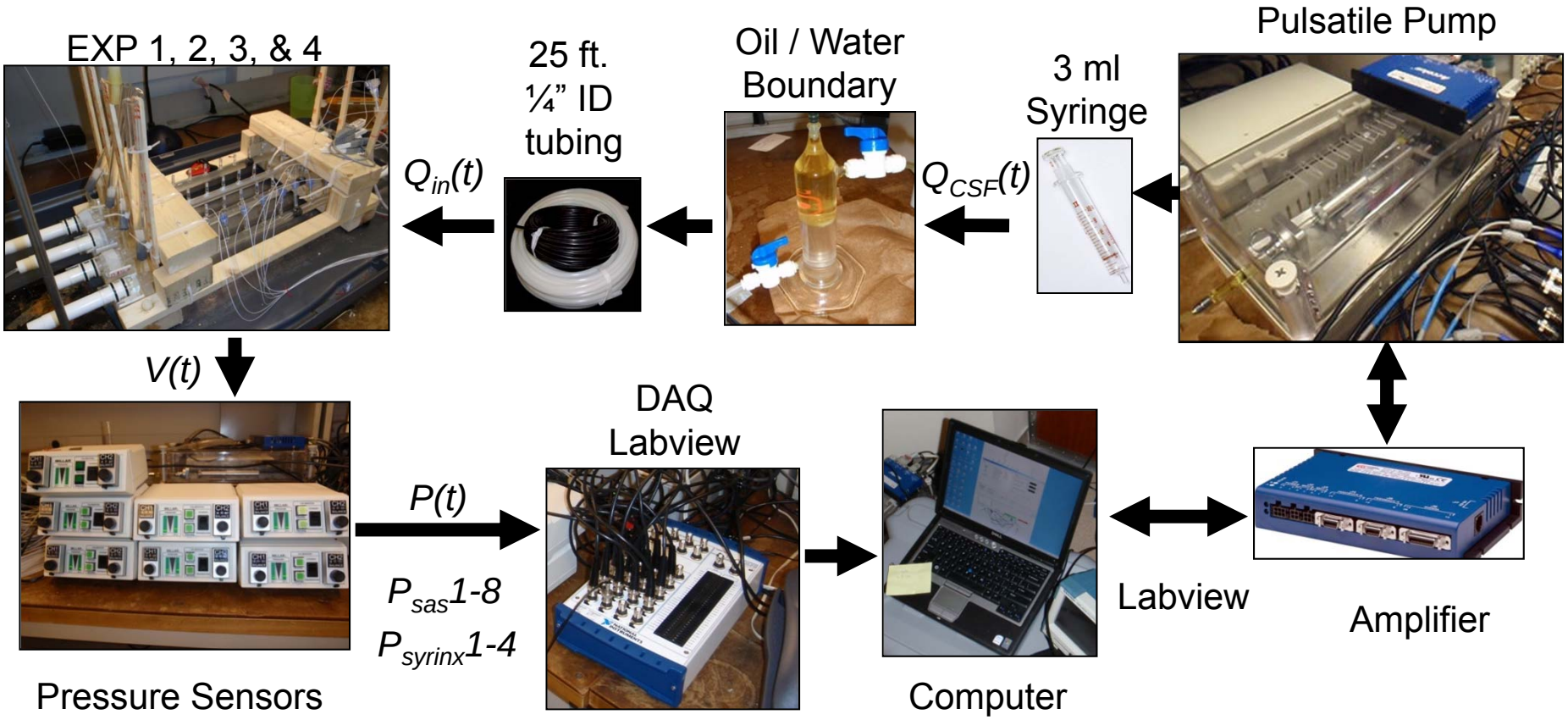

Model construction

Sylgard 184
25:1 base/hardner

Degass

Injection
Mold

Flexible spinal cord

Rigid/flexible spinal column

Model 1: no blockage + syrinx

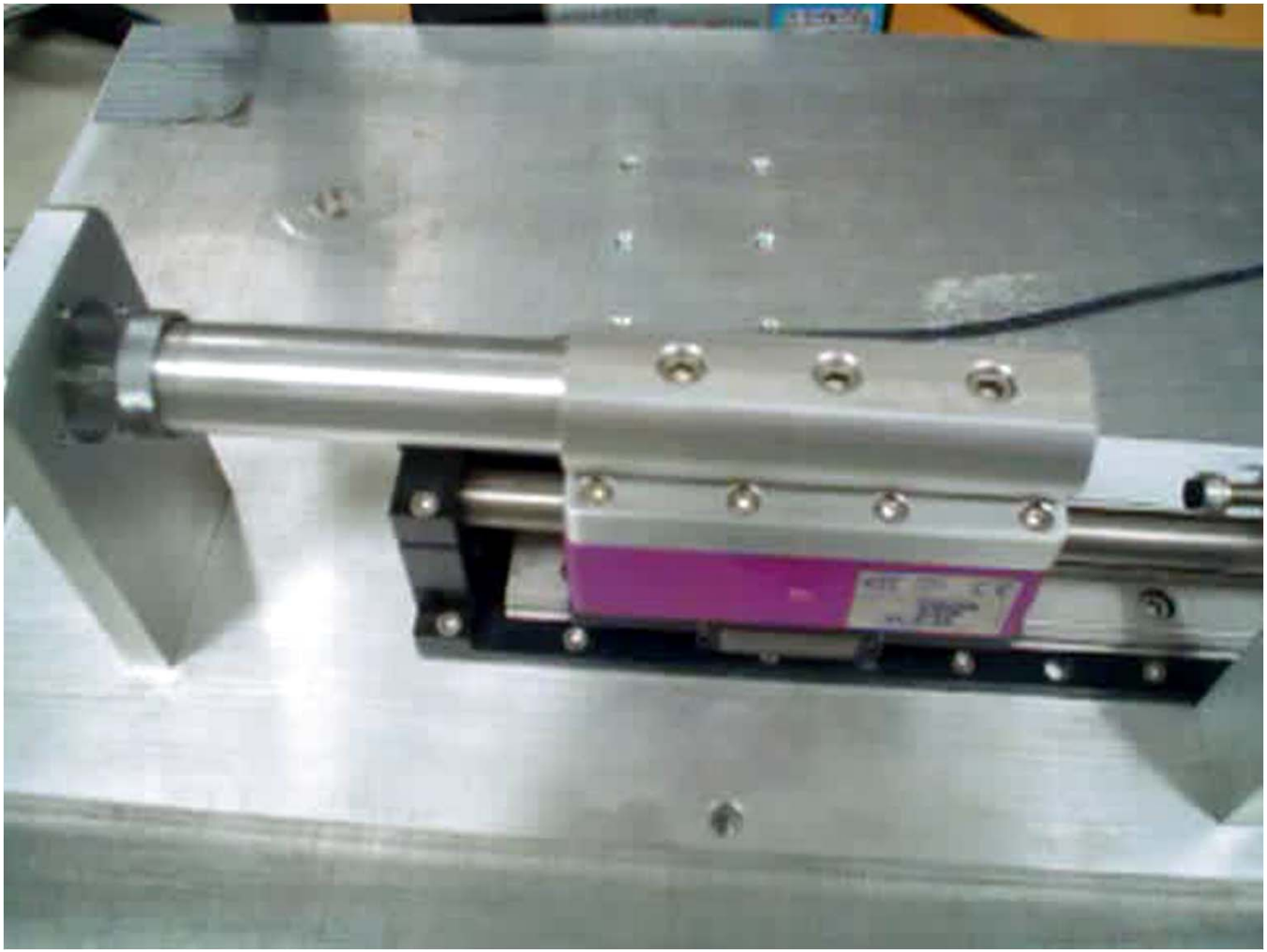

Martin, B. A., W. Kalata, et al. (2005). "Syringomyelia hydrodynamics: an in vitro study based on in vivo measurements." J Biomech Eng **127**(7): 1110-20.

Results (CSF no blockage + syrinx)

- CSF flow was similar to in vivo
- No transmural P to move fluid into syrinx
- Spinal cord motion was asymmetric (even with very symmetric model)

Model 2: syrinx + stenosis model

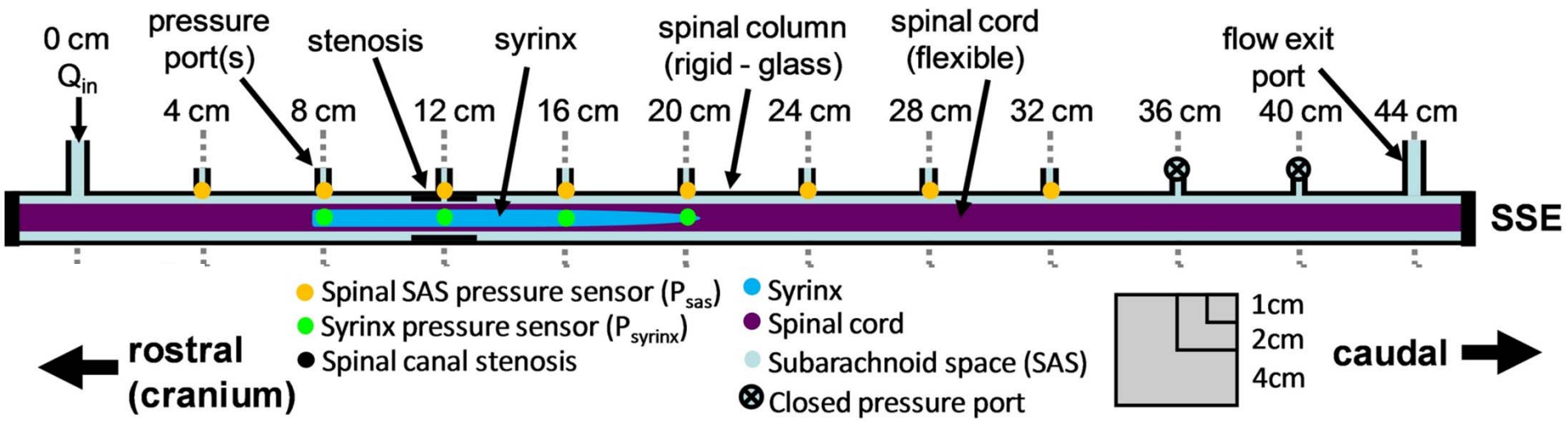

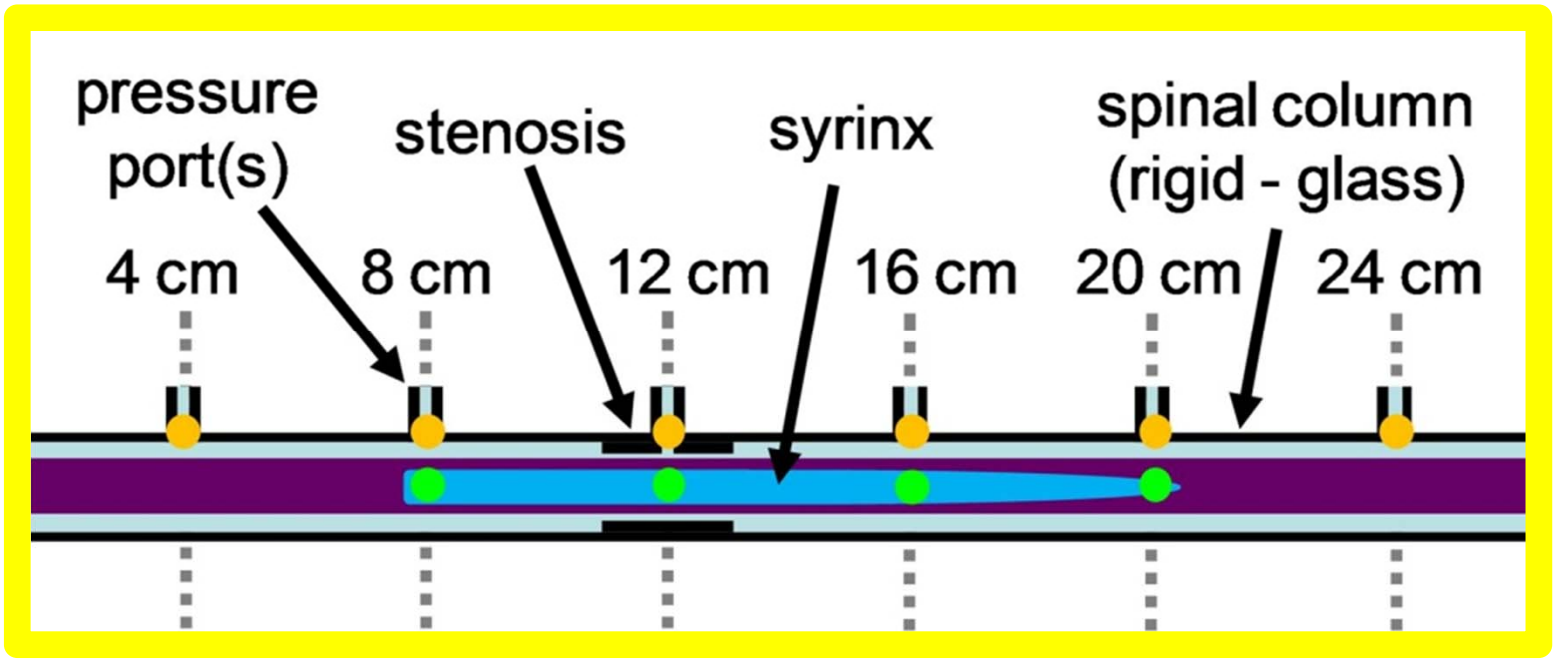

Spinal cord movement (syrinx + stenosis + normal CSF flow)

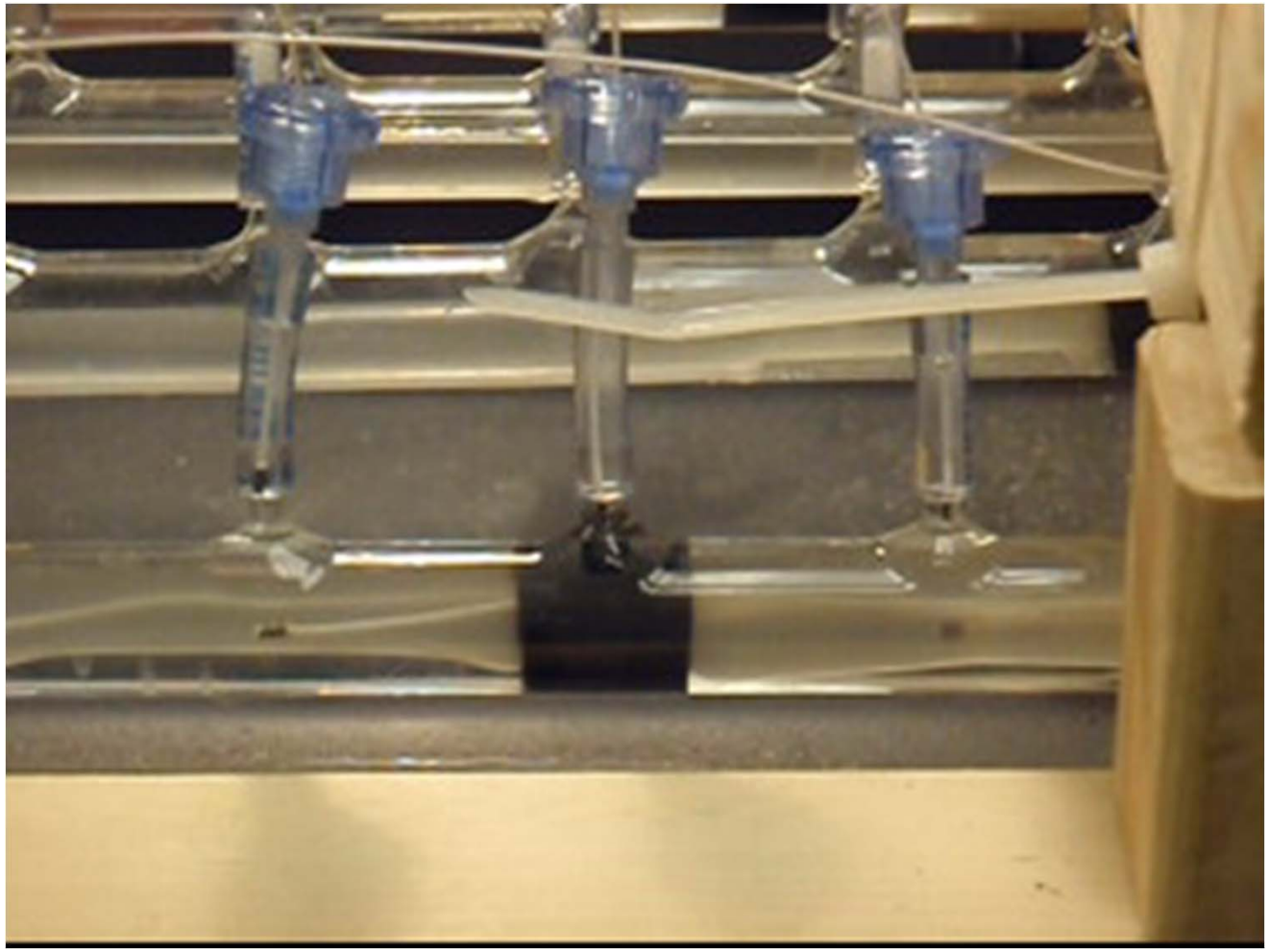

Martin BA, Labuda R, Royston TJ, Oshinski JN, Iskandar B, and Loth F. Spinal Canal Pressure Measurements in an In Vitro Spinal Stenosis Model: Implications on Syringomyelia Theories. *J Biomech Eng* In Press: 2009.

Diastolic valve mechanism

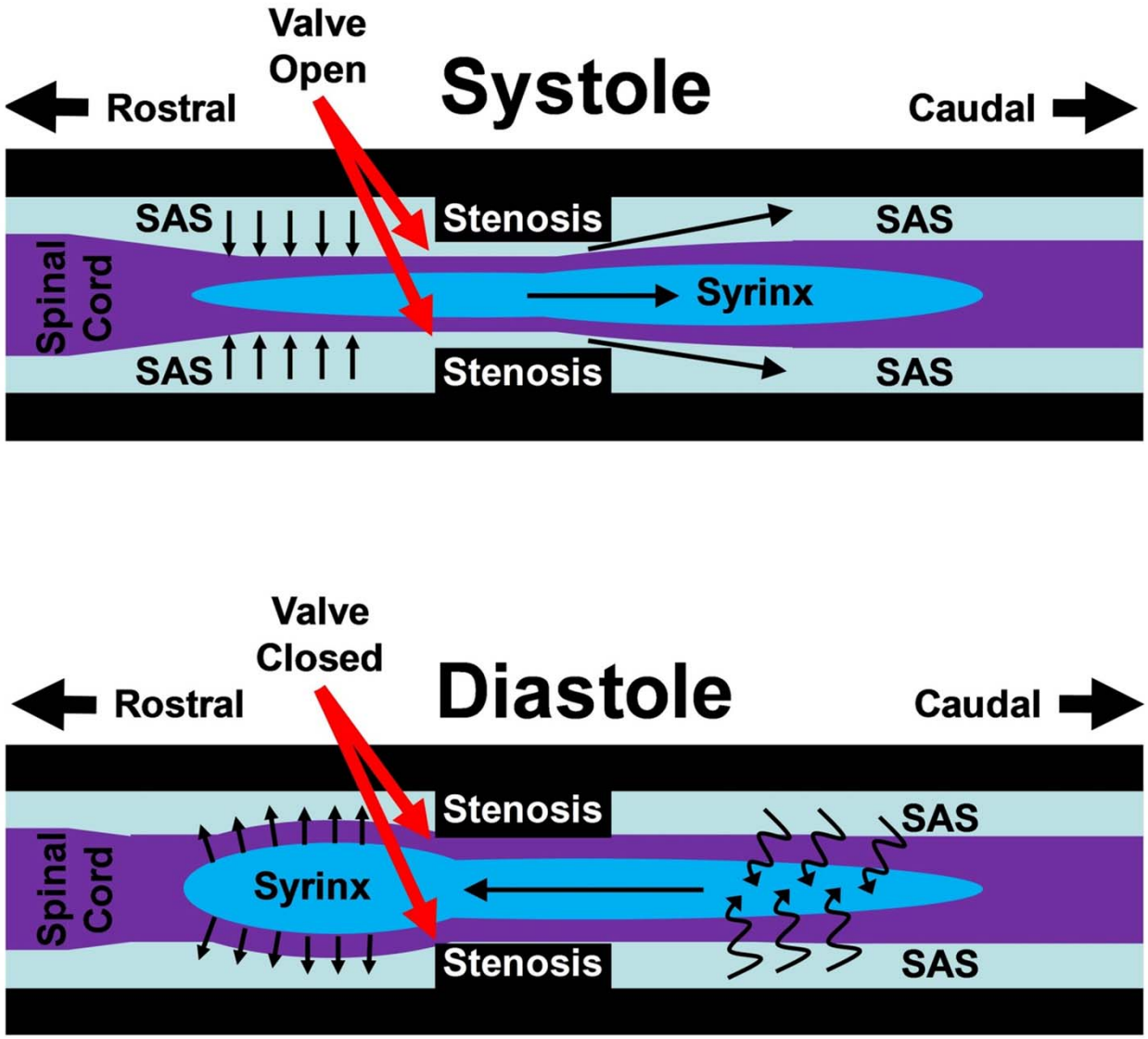

Martin BA, Labuda R, Royston TJ, Oshinski JN, Iskandar B, and Loth F. Spinal Canal Pressure Measurements in an In Vitro Spinal Stenosis Model: Implications on Syringomyelia Theories. *J Biomech Eng* In Press: 2009.

Model 3: syrinx + stenosis + cough pulse

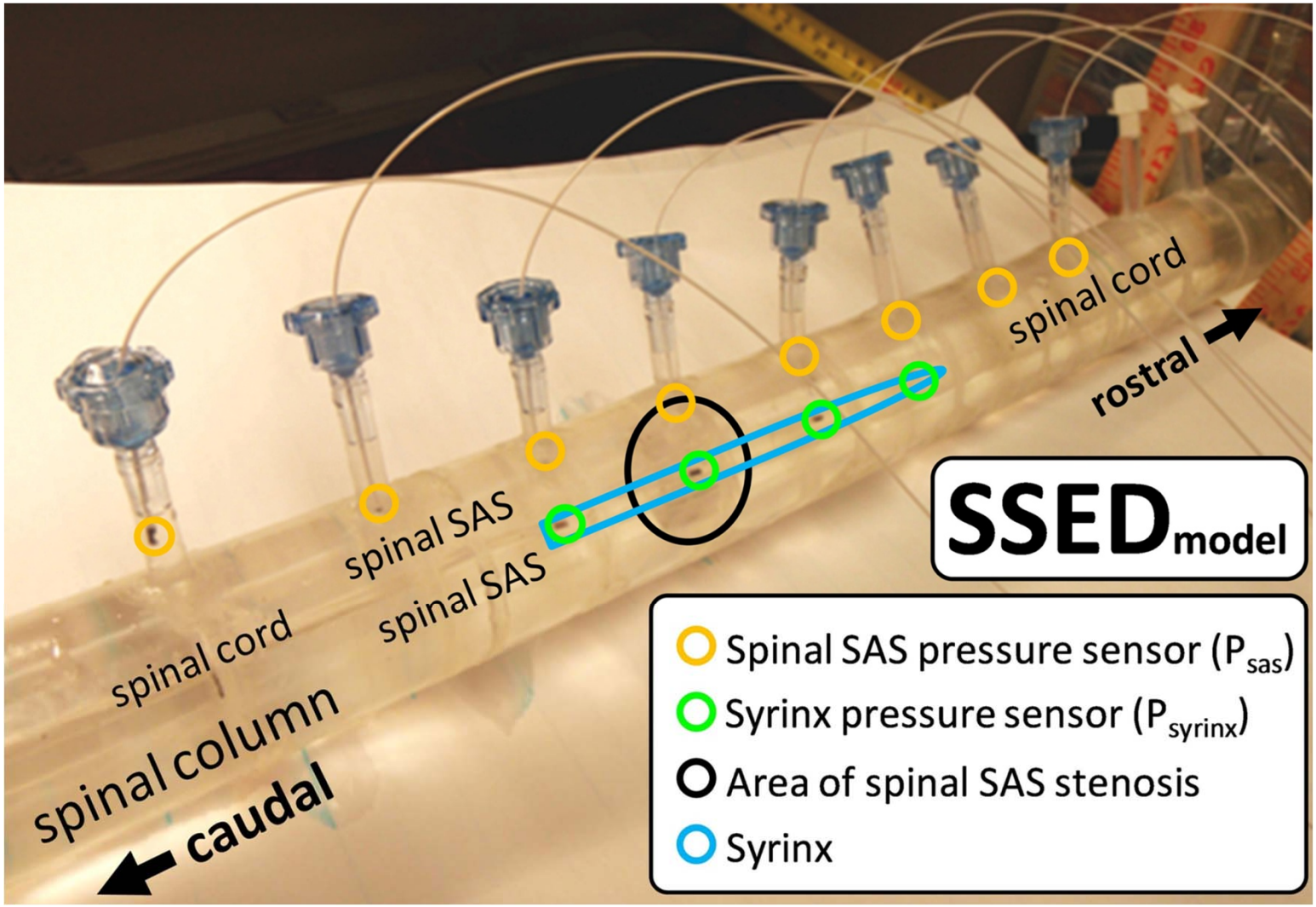

Martin, B. A. and F. Loth (2009). "The influence of coughing on cerebrospinal fluid pressure in an in vitro syringomyelia model with spinal subarachnoid space stenosis." Cerebrospinal Fluid Res 6(1): 17.

CSF PWV

- Similar to Kalata
- Modified by compliance, syrinx and stenosis
- Complex FSI

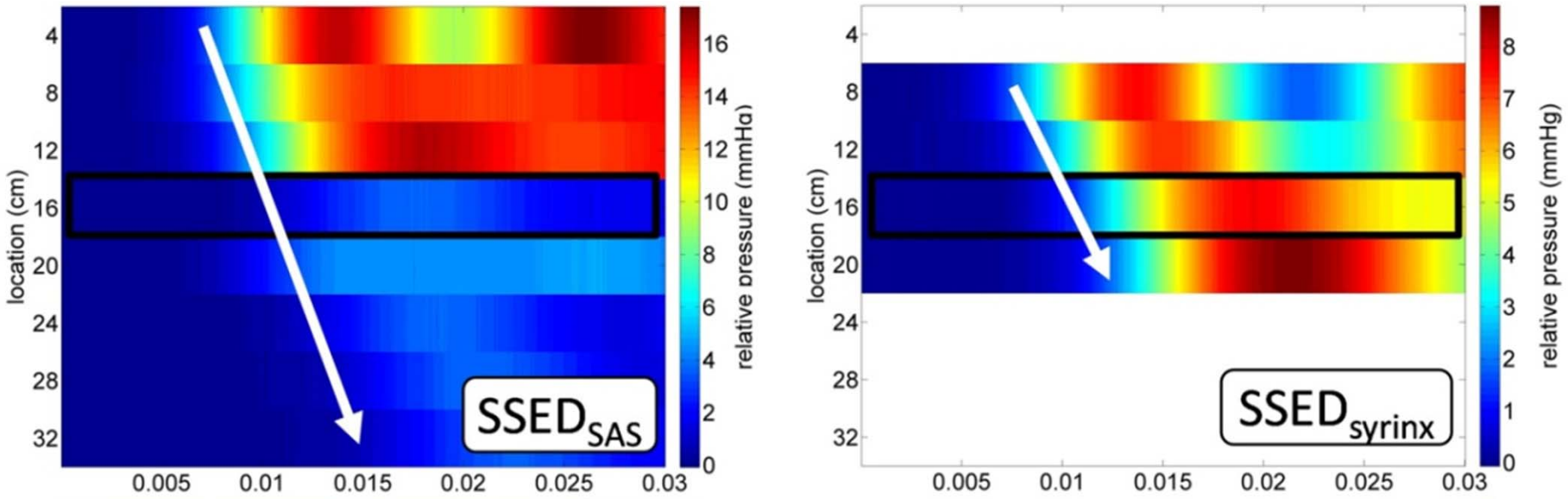

Kalata, W., B. A. Martin, et al. (2009). "MR measurement of cerebrospinal fluid velocity wave speed in the spinal canal." IEEE Trans Biomed Eng **56**(6): 1765-8.

In vitro model conclusions

- FSI was an important factor in disease states! (Bertram et al.)
- Removal of stenosis was needed to reduce pressure gradients acting on the SC
- Mechanical properties of tissue were important

Bertram CD. Evaluation by Fluid/Structure-Interaction Spinal-Cord Simulation of the Effects of Subarachnoid-Space Stenosis on an Adjacent Syrinx. *J Biomech Eng* 132: -, 2010.
Bertram CD, Bilston LE, and Stoodley MA. Tensile radial stress in the spinal cord related to arachnoiditis or tethering: a numerical model. *Med Biol Eng Comput* 46: 701-707, 2008.
Bertram CD, Brodbelt AR, and Stoodley MA. The origins of syringomyelia: numerical models of fluid/structure interactions in the spinal cord. *J Biomech Eng* 127: 1099-1109, 2005.

Craniospinal disorders: tethered spinal cord

- Controversy surrounding treatment of Chiari malformation (SM) by section of filum terminale (Royo-Salvador)

Royo-Salvador, M. B., Sole-Llenas, J., Domenech, J. M., and Gonzalez-Adrio, R., 2005, "Results of the section of the filum terminale in 20 patients with syringomyelia, scoliosis and Chiari malformation," Acta Neurochir (Wien), 147, pp. 515-523.

Craniospinal disorder: pseudotumor cerebri

- To be added soon

Intrathecal drug delivery

- Drugs that enter the blood stream can not penetrate and function in the brain, but instead must be administered into the cerebrospinal fluid (Guyton)

Direct drug delivery to brain (epilepsy)

- To be added

Cerebral venous innsuficiency

Alzheimer's disease

Multiple sclerosis

Current diagnostic and imaging trends in neurohydrodynamics

Quantitative comparison of 4D MRI and CFD (rigid) in the 3rd ventricle and aqueduct of Sylvius

Aurelie Picquot[1], Sérge Metailler, Francesco Santini, Jelena Block, Philippe Reymond,
Elenora Fonari, Nicolaos Stergiopulos

ISMRM abstract: An in vivo MRI and computational fluid dynamic simulation of cerebrospinal fluid hydrodynamics in the third ventricle

Motivation

- No quantitative comparison of 4DMRI and CFD has been made…

Qualitative CSF flow study by Santini et al.

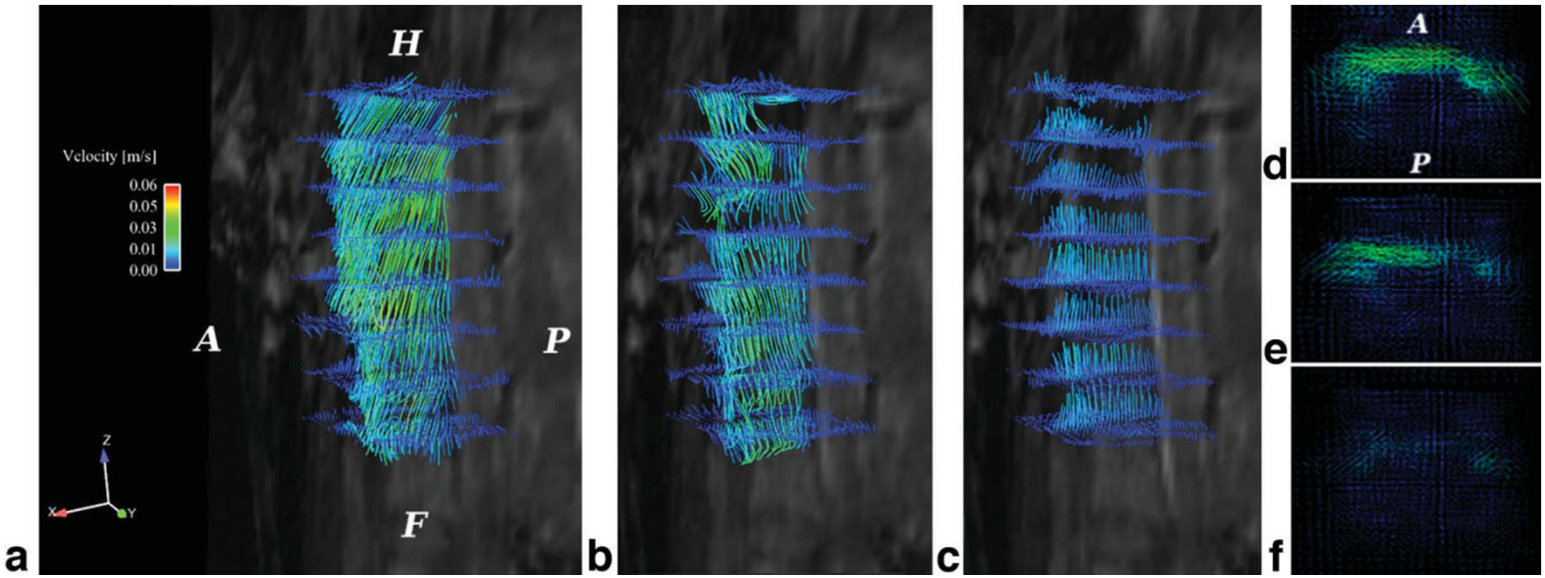

Santini F, Wetzel SG, Bock J, Markl M, and Scheffler K. Time-resolved three-dimensional (3D) phase-contrast (PC) balanced steady-state free precession (bSSFP). *Magn Reson Med* 2009.

5 geometries from same person

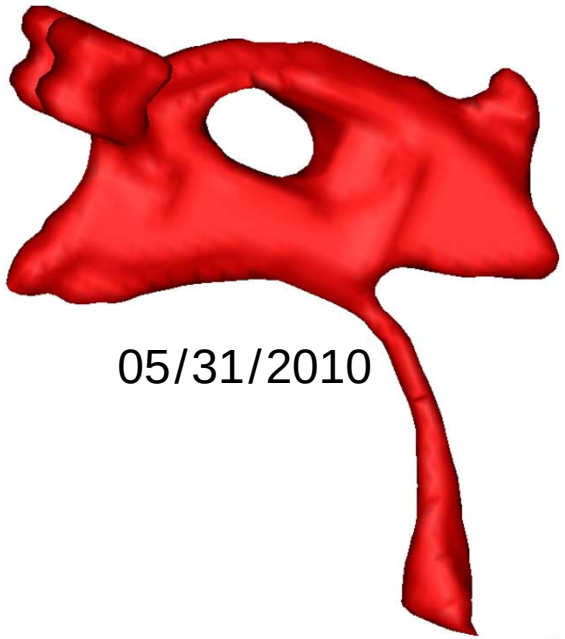

05/31/2010

04/27/2010

03/22/2010

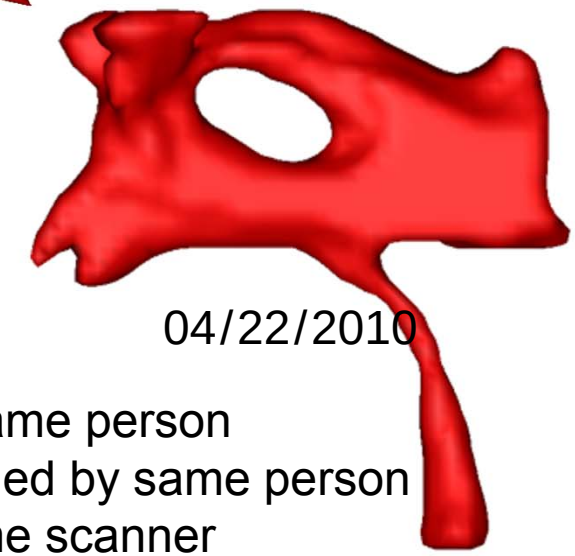

04/22/2010

03/10/2010

All geometries from same person
Segmentation performed by same person
Scan obtained on same scanner

A. Sylvius diameter for 5 cases

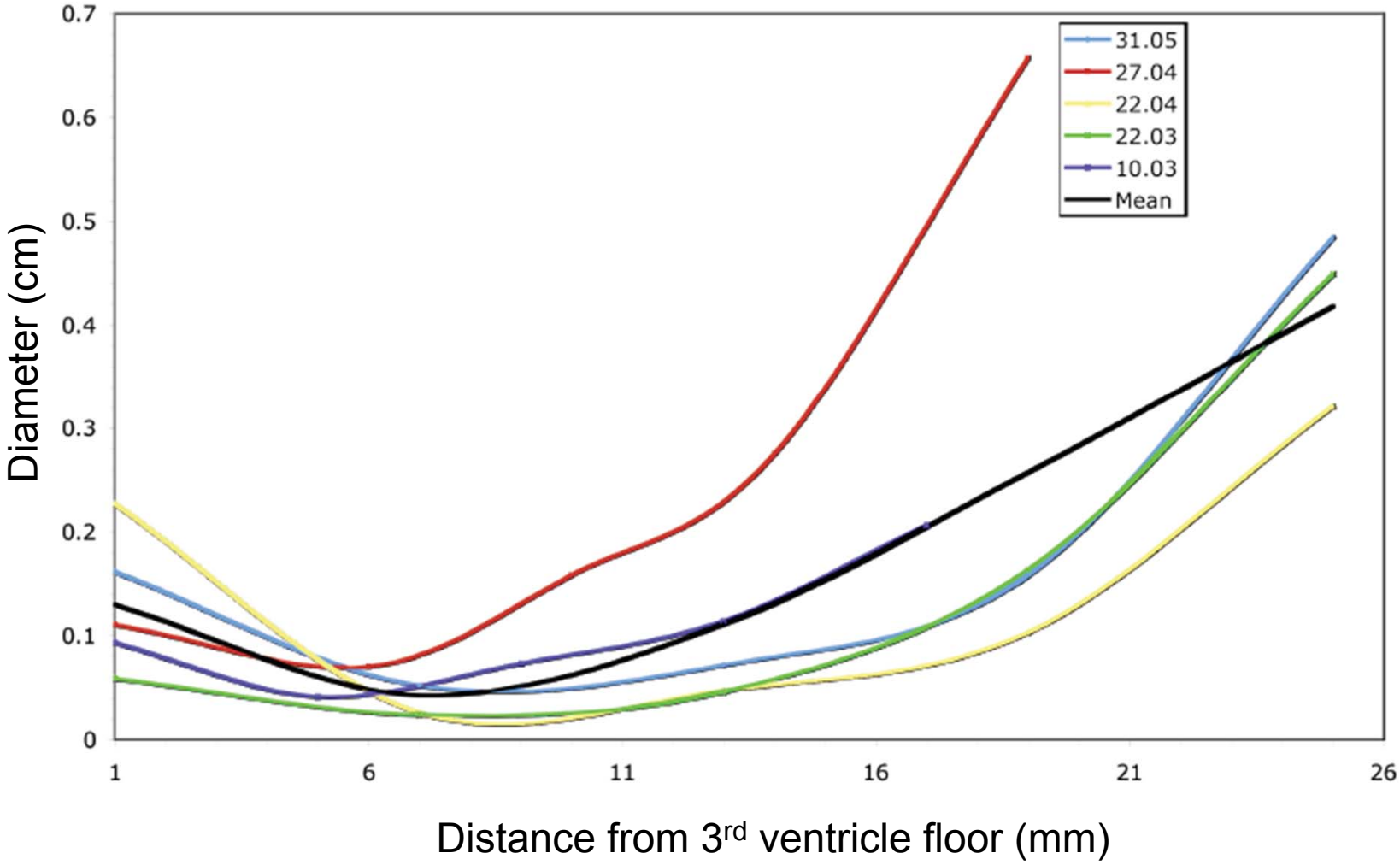

4D velocity peak (03/10/2010)

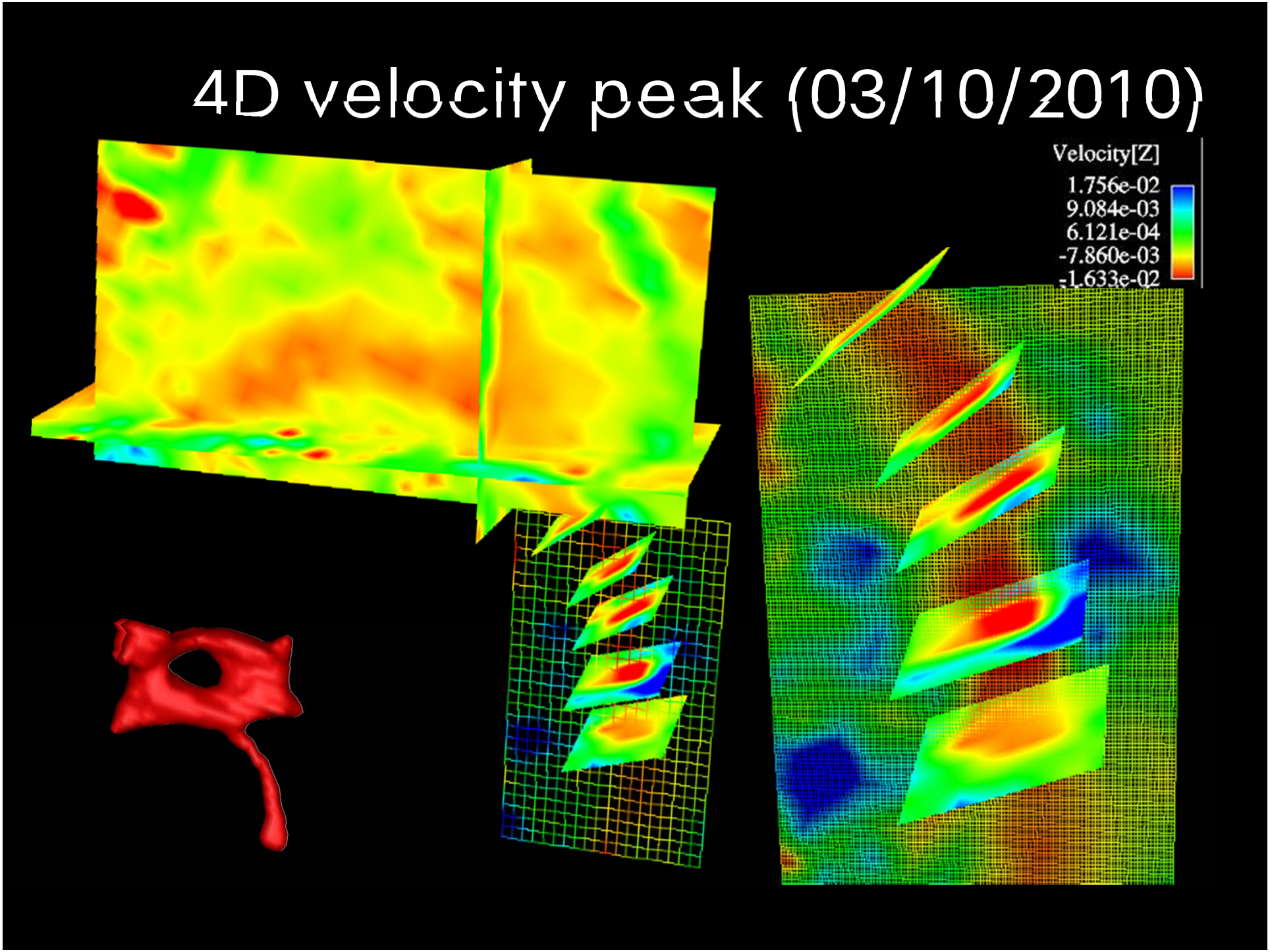

Animation (03/10/2010)

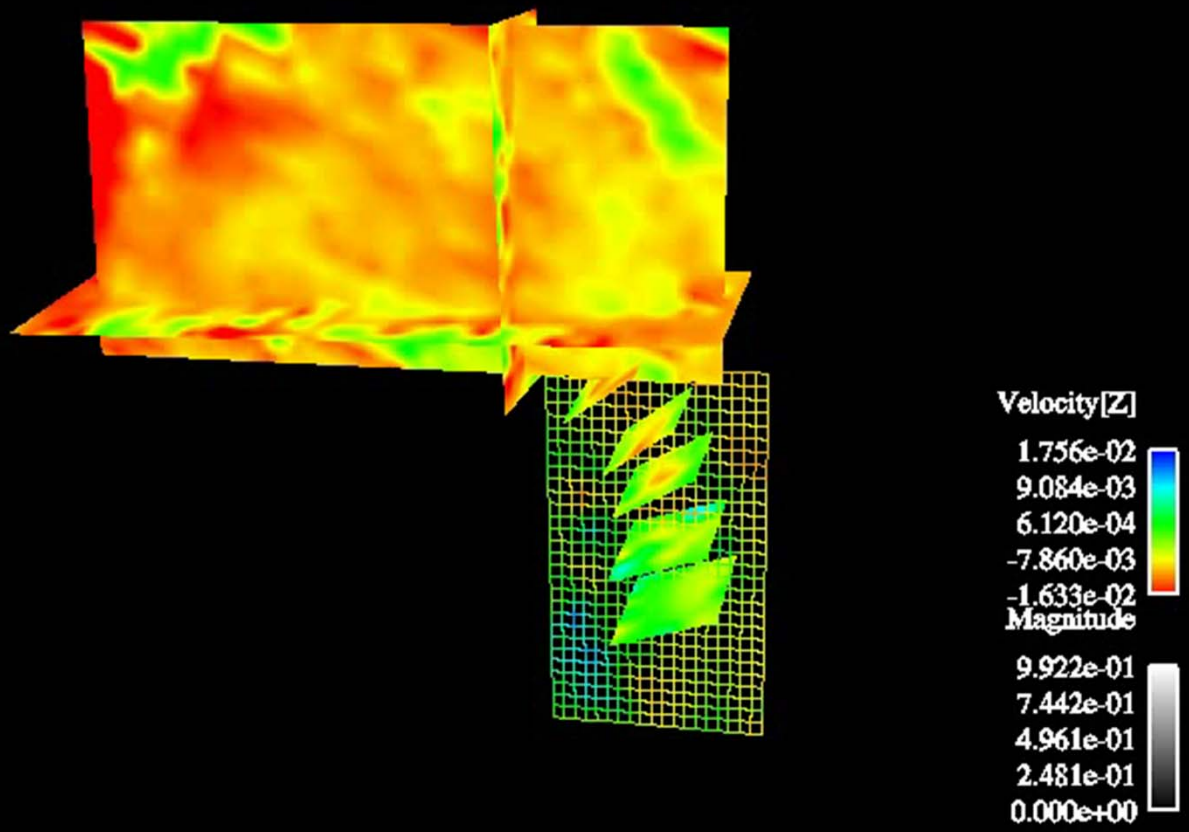

Results (31/5)

- Comparison O.K. in a. Sylvius
  - Poor elsewhere

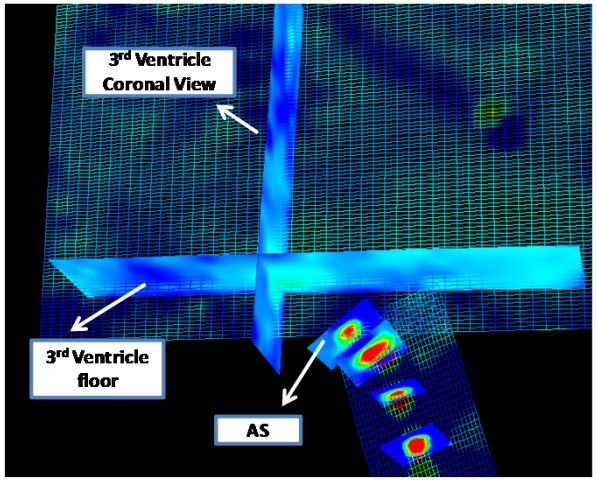

Aqueduct of Sylvius (AS)

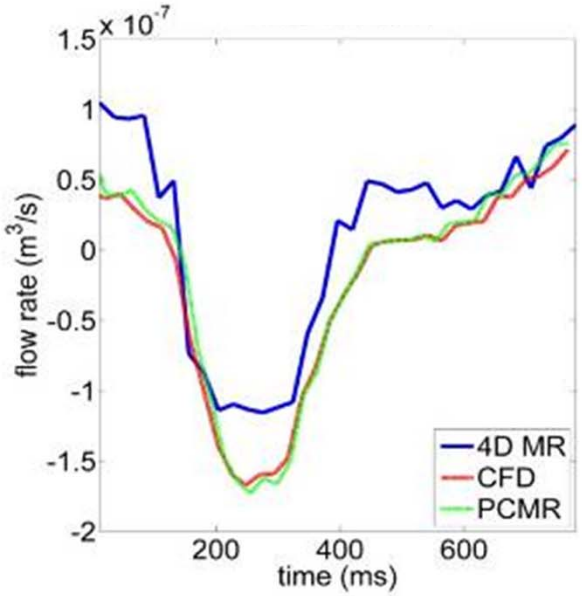

3rd Ventricle floor

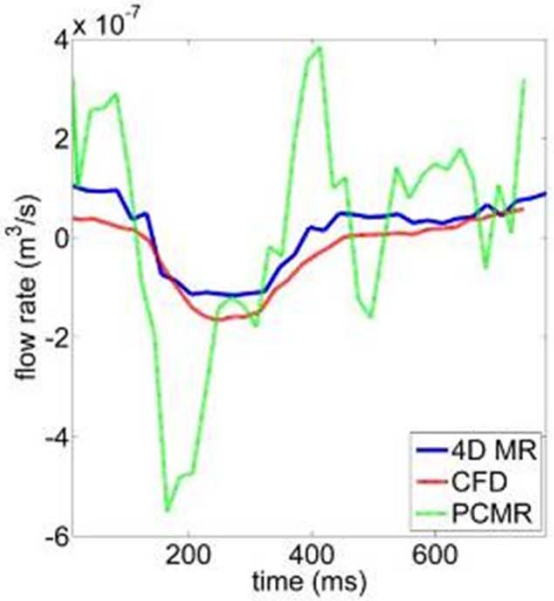

3rd Ventricle Coronal

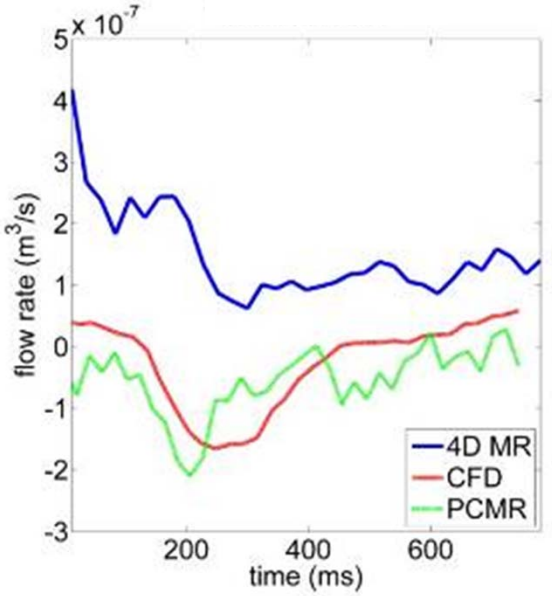

Quantitative comparison of 4D MRI in Chiari and syringomyelia patients

Leonie Asboth1, Bryn A. Martin[1], J.-R. Kroeger[2], Maintz D[2], N. Stergiopulos[1], A.C. Bunck[2]

[1] *Laboratory of Hemodynamics and Cardiovascular Technology, EPFL Switzerland*

[2]*University of Muenster Department of Radiology, Germany*

4DMRI videos

Healthy 4

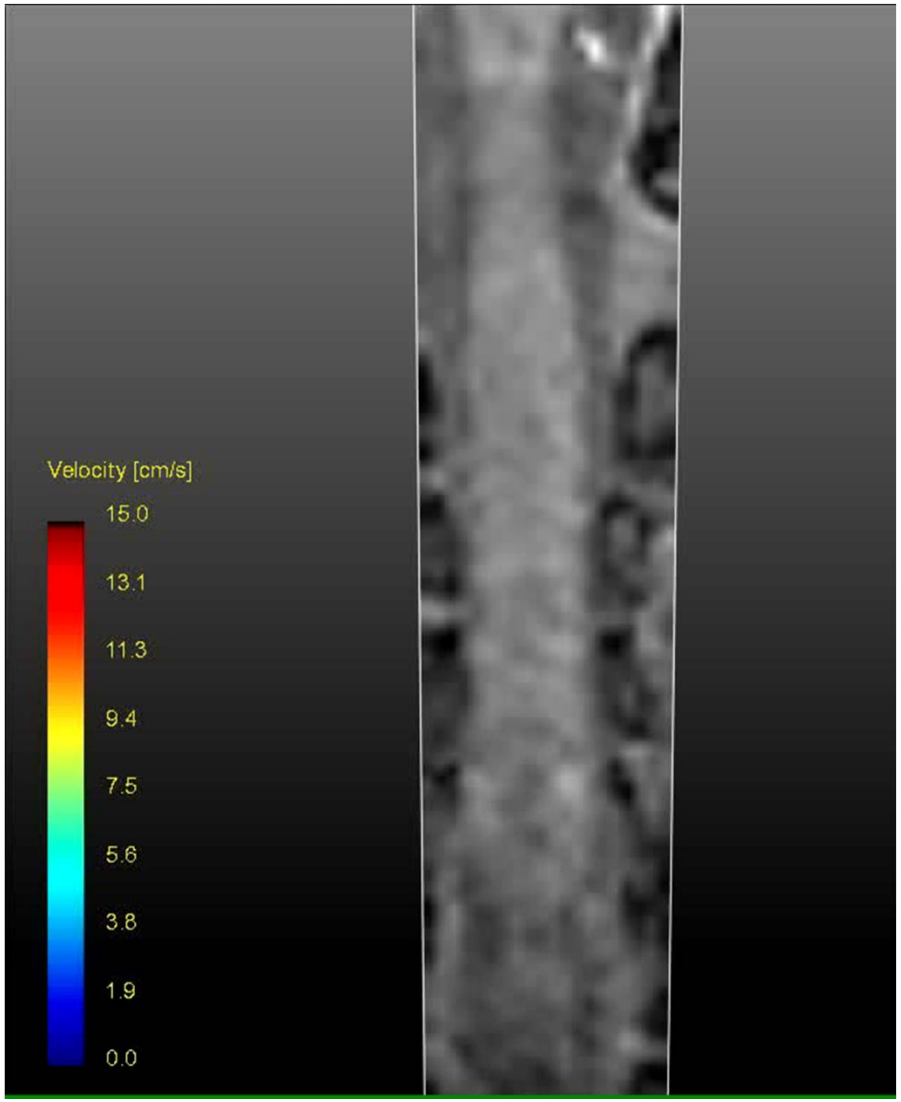

Patient (MRG / Chiari)

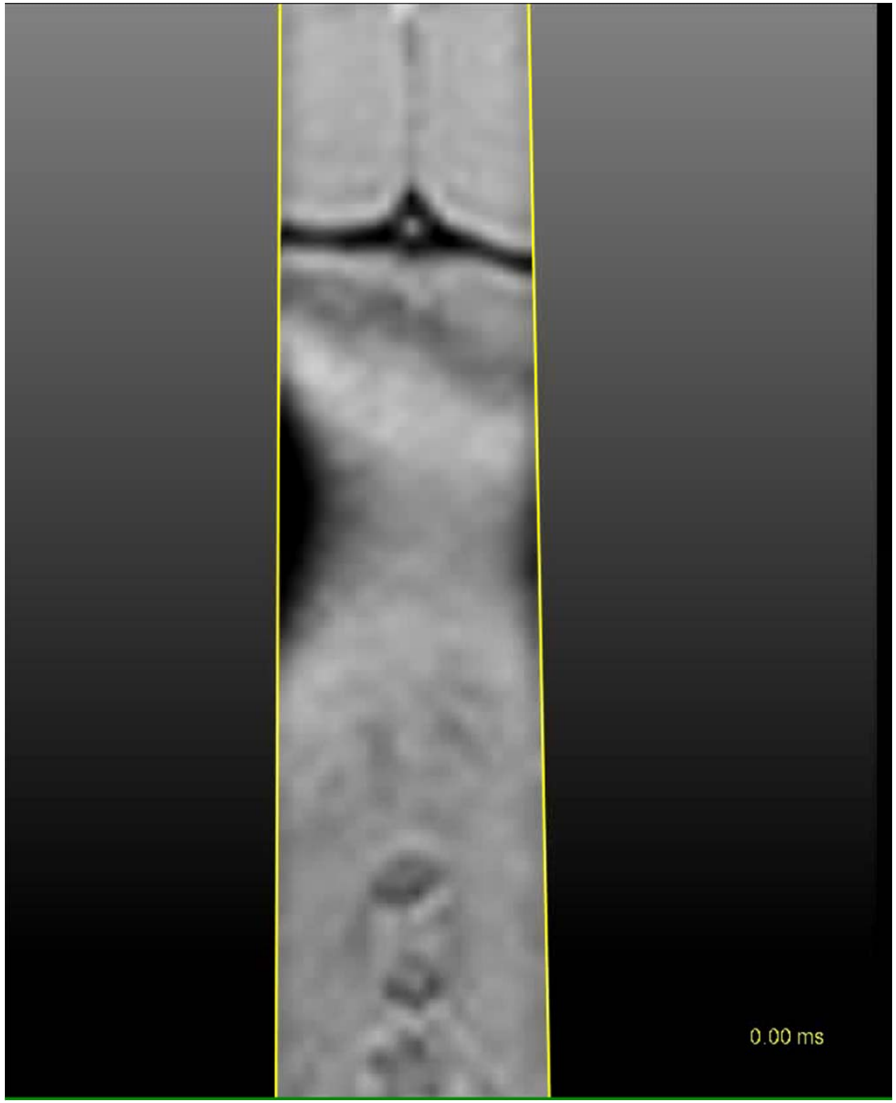

Post processing and visualization by GTFlow 1.3.11 (GyroTools, Zurich, Switzerland

Locations of velocity comparison

Healthy 4

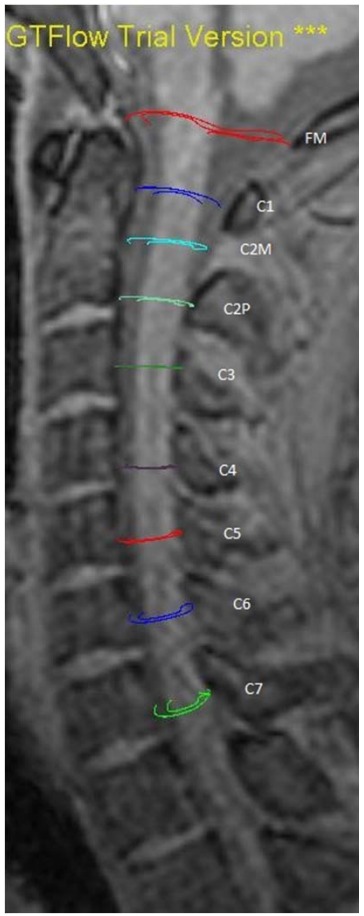

Chiari Patient

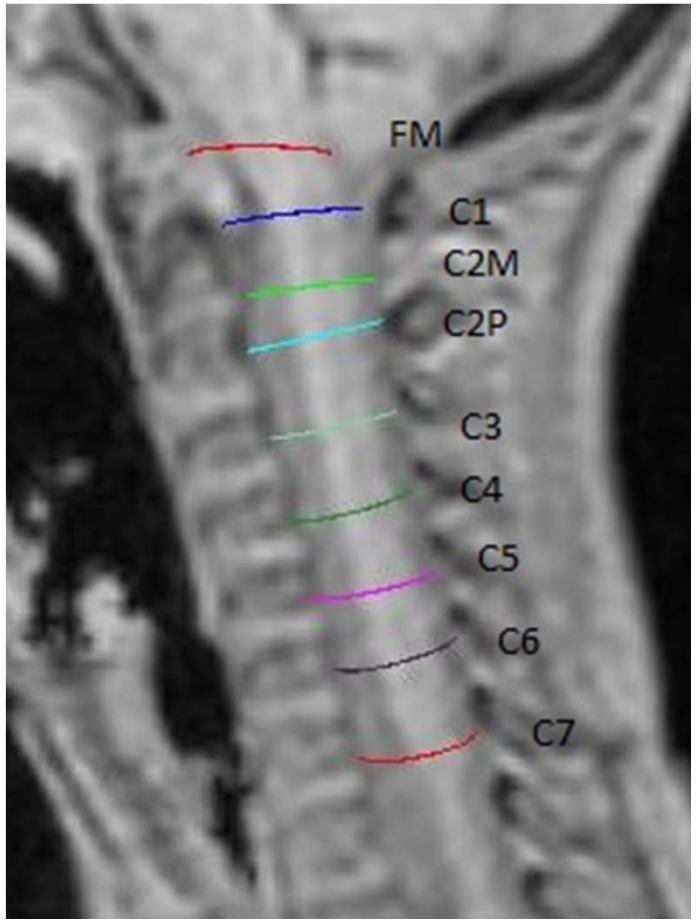

Comparison of 4DMRI and CFD

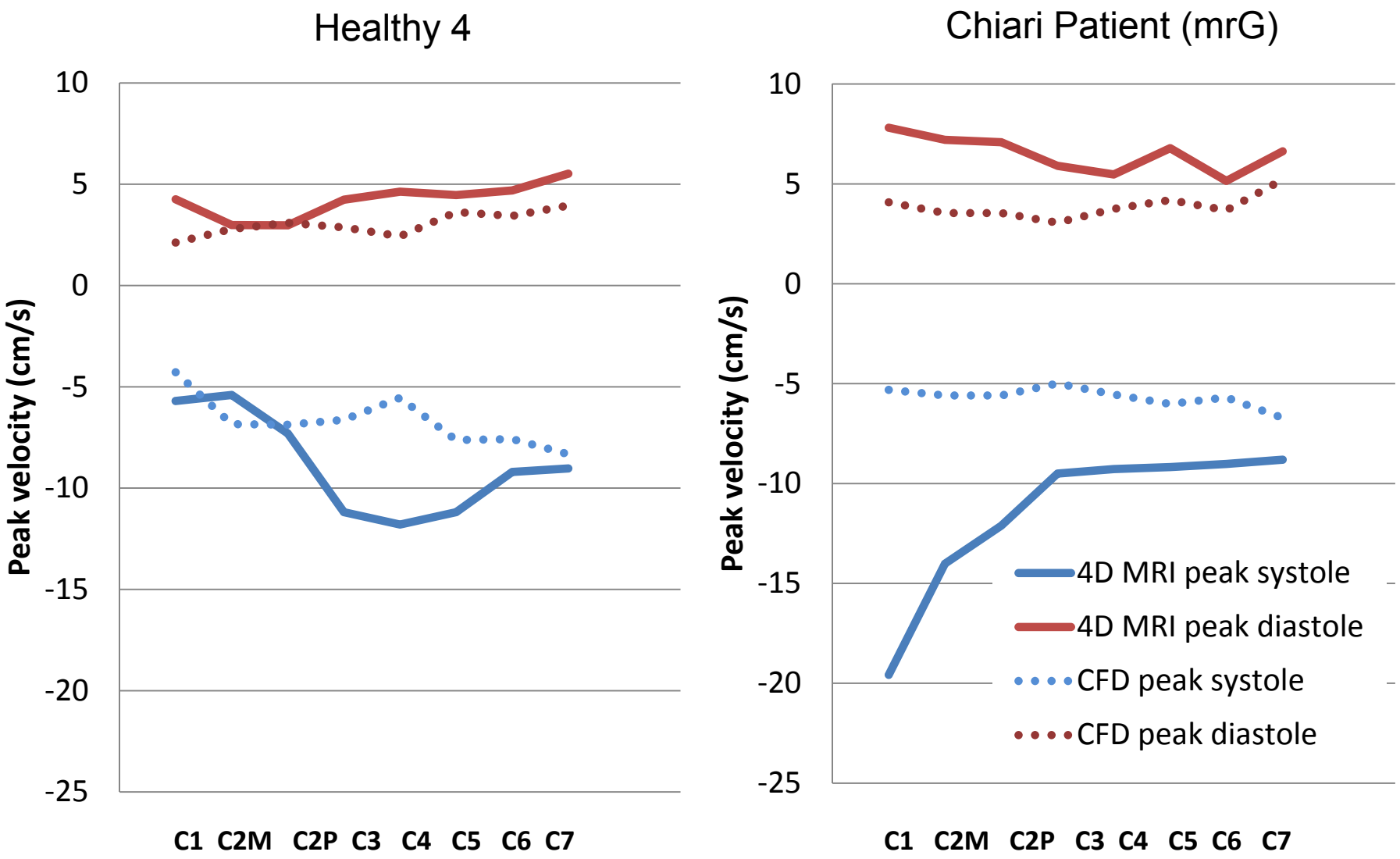

Conclusion

- CSF flow assessment by 4DMRI appears to be quantitatively similar to CFD (rigid) for healthy subjects.

Hypothesis

- We hypothesize that piston action of the cerebral tonsils in Chiari patients is responsible for the difference in CFD and 4D MRI flow velocities

MRI pulse wave velocity

- Craniospinal compliance might be reduced in patients with hydrocephalus…would a reduction in compliance change PWV in the spine?
- PWV in the spine was measured to be 4.6 m/s in healthy subjects (Kalata et al.)

Kalata, W., Martin, B. A., Oshinski, J. N., Jerosch-Herold, M., Royston, T. J., and Loth, F., 2009, "MR measurement of cerebrospinal fluid velocity wave speed in the spinal canal," IEEE Trans Biomed Eng, 56(6), pp. 1765-1768.

PWV – Motivation

- The goal of this project is to give a lower bound value for Pulse Wave Velocity of CSF in patients with craniospinal disorders.
- There is only little known about wave propagation inside the subarachnoid space
- Information about PWV in subarachnoid space would fill a blank spot of the CSF – CBF puzzle

PWV – Method

We recieved MRI images of 32 patients (total of > 100 data sets)

Analysis of the data:

Cross-correlation

Foot Location

Half-Maximum

Maximum

Max Up-Slope

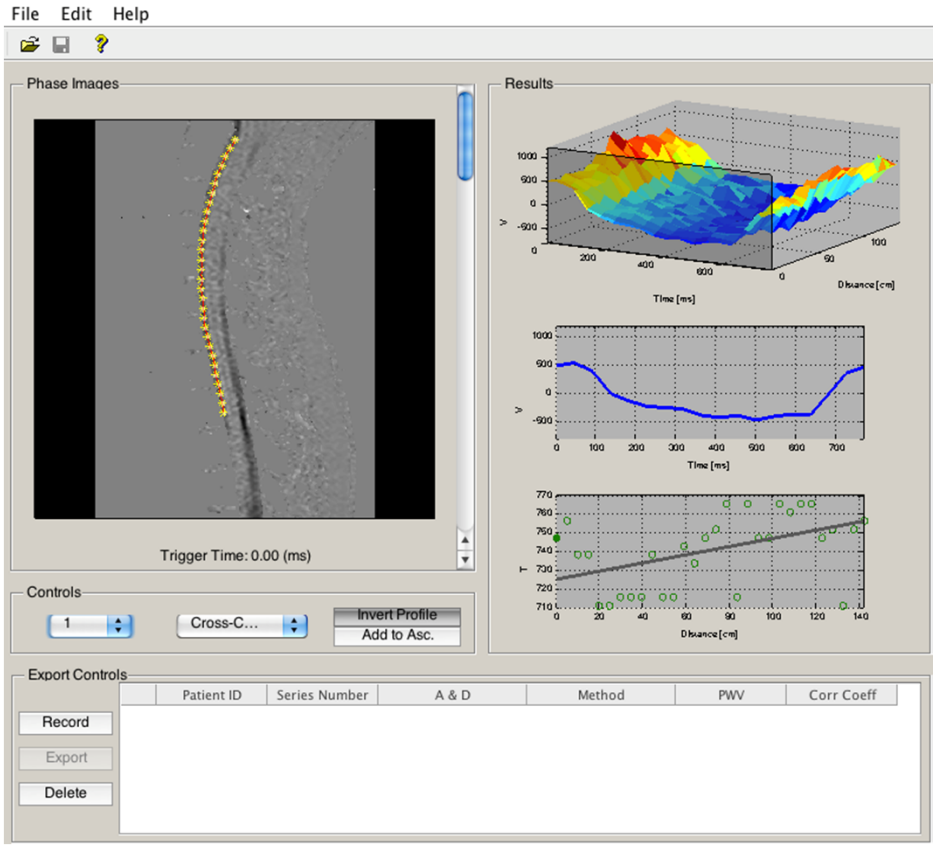

PWV – Results

What are the selection criteria:

Correlation Coefficient >0.3 or <-0.3

A PWV value which makes sense:

To avoid high errors, values over 8 m/s in absolute value are discard

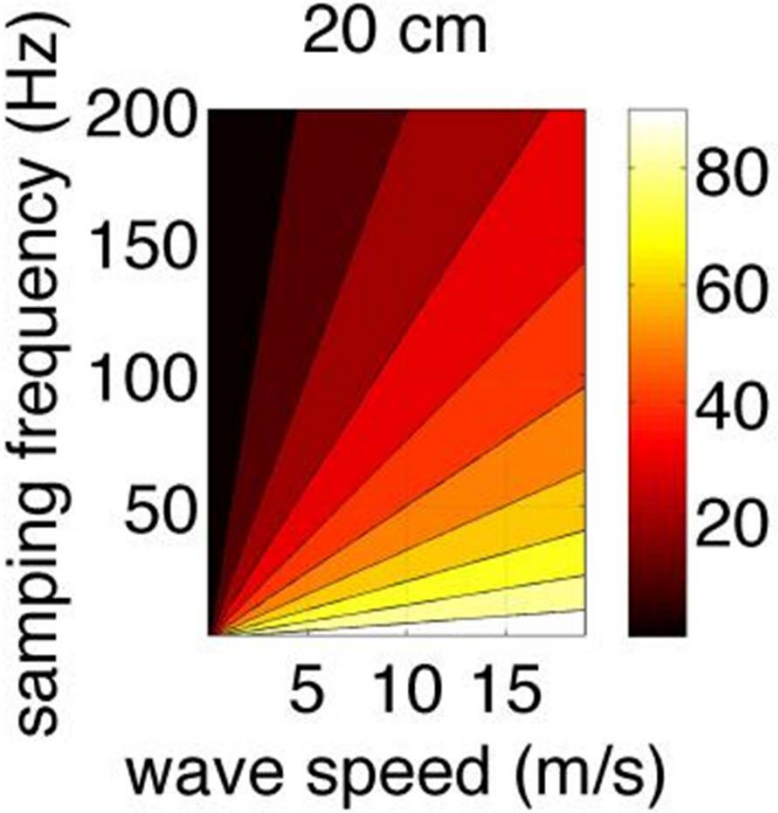

PWV – Results

104 measurements with a good correlation coefficient

Overall mean PWV value:	2.2	m/s
Standard deviation:	1.7	m/s

PWV – Results

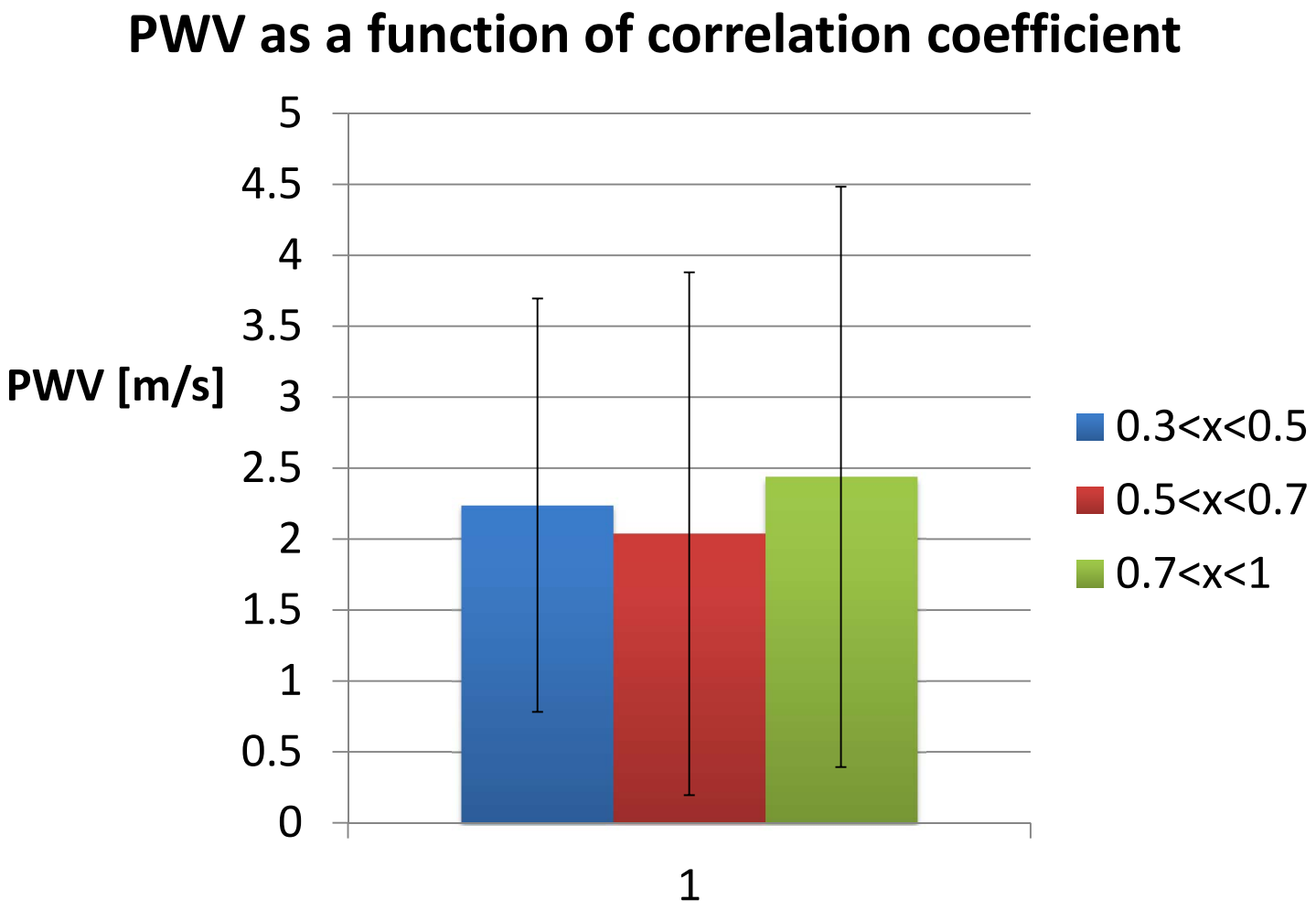
PWV as a function of correlation coefficient
PWV [m/s]
5
4.5
4
3.5
3
2.5
2
1.5
1
0.5
0
1
0.3<x<0.5
0.5<x<0.7
0.7<x<1

Thin arachnoid membrane can collapse and perturb CSF flow in pathologies

- 39 years old patient with thoracic syringomyelia and blockades of the CSF pulsation caused by thoracic arachnoid membranes

CSF flow study 5 cm/s

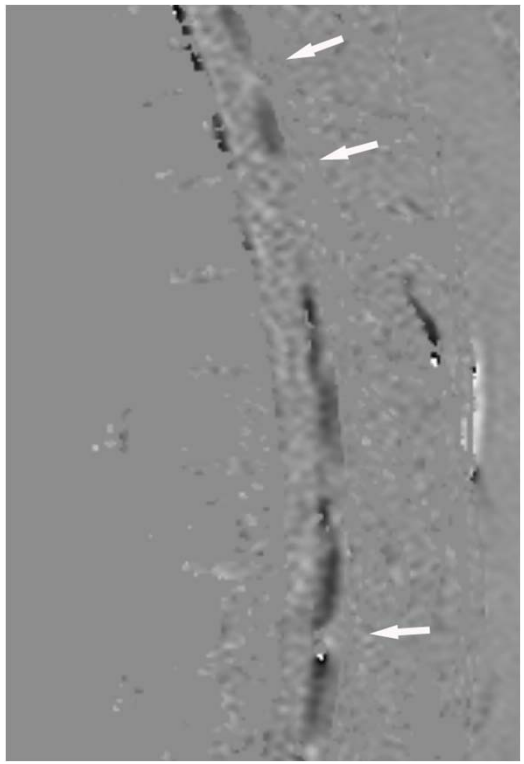

sag cine BFFE

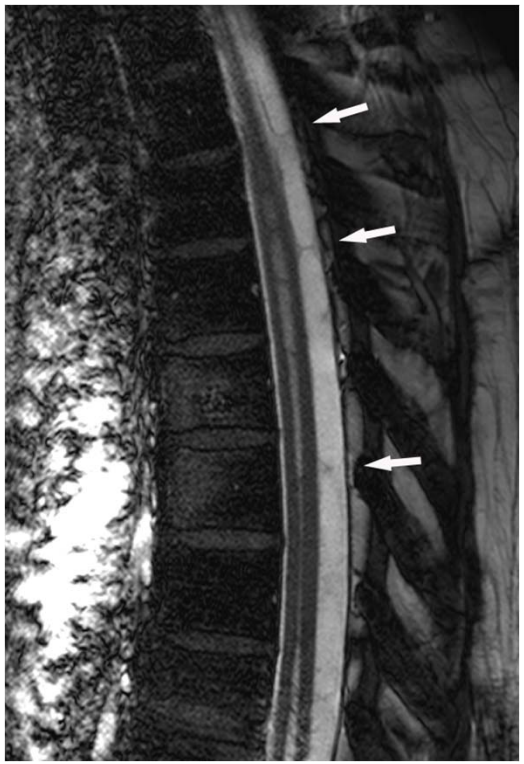

arachnoid membrane at T2/3

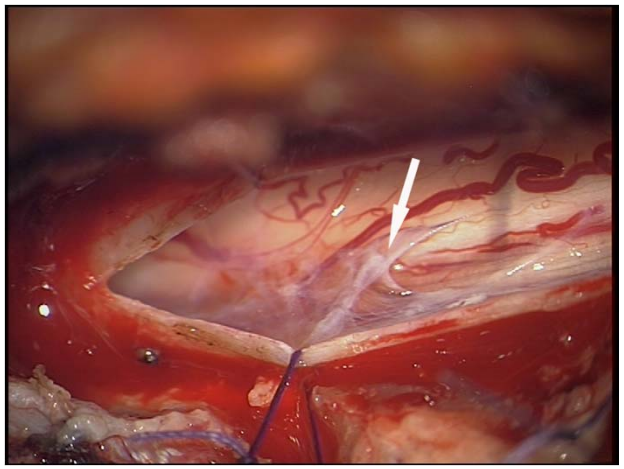

Gottschalk A, Schmitz B, Mauer UM, Bornstedt A, Steinhoff S, Danz B, Schlötzer W, Rasche V. Dynamic visualization of arachnoid adhesions in a patient with idiopathic syringomyelia using high-resolution cine MR imaging at 3T. JMRI 2010, 32(1): 218-222

Magnetic resonance elastography for material properties of brain

Shear moduli parallel (left) and perpendicular (right) to fiber tracts

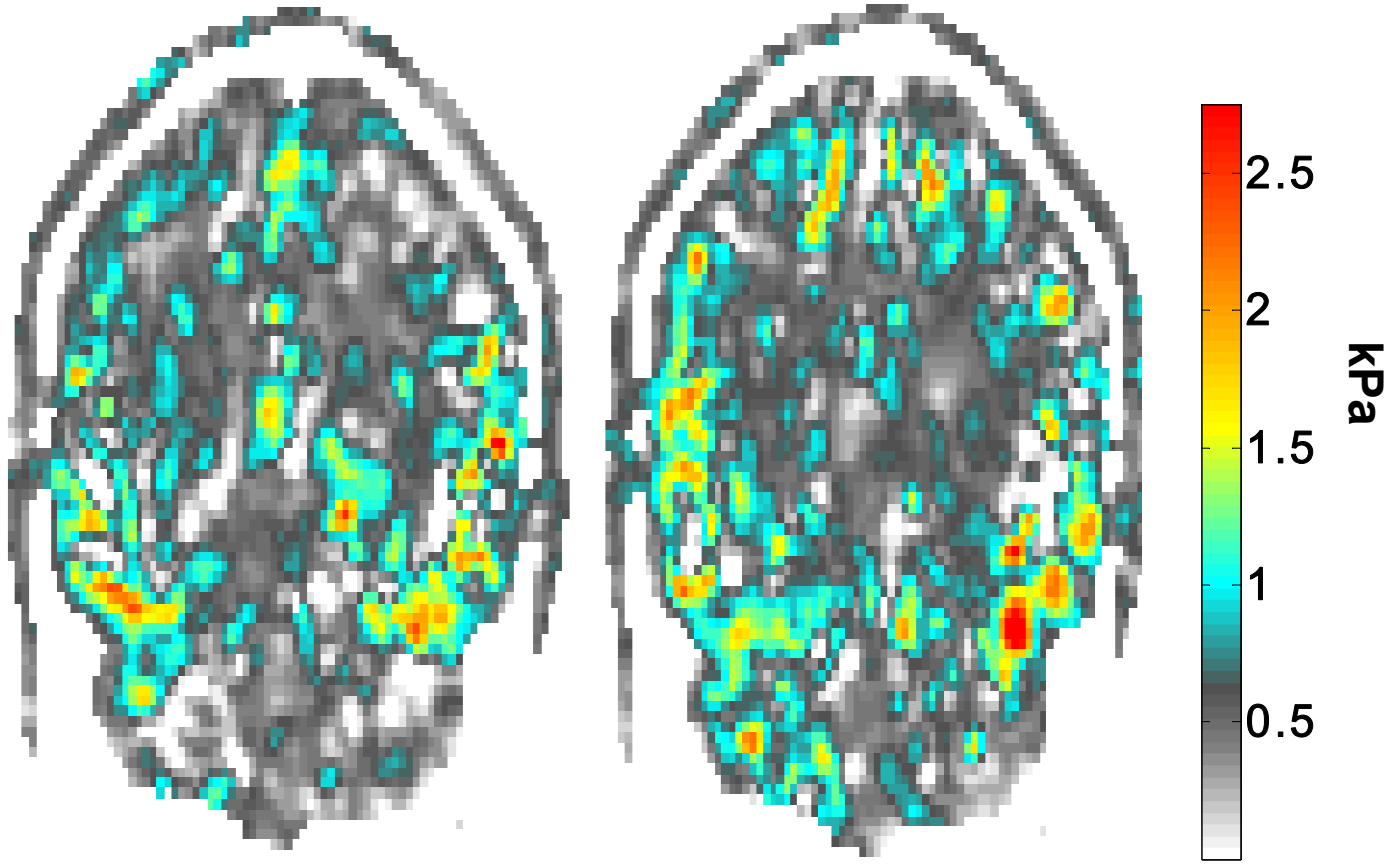

Green, M. A., L. E. Bilston, et al. (2008). "In vivo brain viscoelastic properties measured by magnetic resonance elastography." NMR in Biomedicine 21(7): 755-764.

MRI diffusion tensor imaging

MRI spectroscopy

Neurohydrodynamics research outlook

- At present, healthy state macro scale hydrodynamics can be modeled relatively well.
- Pathological states need more complex modeling (FSI).
- Transition from health to disease remains largely unknown, to understand the transition we need to build macro to micro scale coupled models.

From a patient / medical perspective

- Many new tools are available to help quantify disease states.
- We need to explore and further develop these tools working closely with doctors to reach clinical use.

EPFL CSF team

- **Thiresia Yiallourou, EPFL, Ph.D. student**
- Shahim Kamal, EPFL LSMX, Ph.D. student
- Serge Metarailler, EPFL, B.S. student
- Leonie Asboth, EPFL, M.S. student
- Christian Meuli, EPFL M.S. student
- Aurélie Picquot, EPFL masters student
- Adrien DeMuralt, EPFL masters student
- Navid Borhani, Ph.D.

Medical collaborators

- Jan Novy, M.D. CHUV neurology
- Lorenz Hirt, M.D., CHUV neurology
- Celine Odier, M.D. CHUV neurology
- Raphael Heinzer, M.D. CHUV sleep disorders
- Jose Haba-Rubio, M.D. CHUV sleep disorders
- Andreas Gottaschalk, M.D., Germany
- Alexander Bunck, M.D. Muenster, G.
- Shahan Momjain, M.D., HUG, Switzerland
- Bermans Iskandar, M.D. Univ. Wisc.

Engineering Collaborators

- Francis Loth, Ph.D. U. Akron
- Francesco Santini, Ph.D., Uni. Basel
- Matthias Stuber, Ph.D., CHUV CIBM
- John N. Oshinski, Ph.D., Emory Univ.
- Rick Labuda, Conquer Chiari
- Jean-Marie Drezet, Ph.D., EPFL
- Jelena Bock, Ph.D., Uni. Freiburg
- Eleonora Fonari, Ph.D., CHUV CIBM
- Novak Elliott, Ph.D. Univ. Warwick

Project advise

- John D. Heiss, M.D. NIH USA
- Christopher Bertram, Ph.D.
- Lynne Bilston, Ph.D.

Work funded by:
NSF Swiss
American Syringomyelia Alliance Project
Conquer Chiari

Thanks!

More information

Neurohydrodynamics wiki research site of Dr. Bryn Martin:

- www.neurohydrodynamics.com
- Please direct questions on this presentation to: mail@neurohydrodynamics.com